This is to certify that the
thesis entitled

QUANTITATIVE ANALYSIS OF AMINOPHOSPHOLIPIDS BY CHEMICAL DERIVATIZATION AND TANDEM MASS SPECTROMETRY

presented by

SICHANG LIU

has been accepted towards fulfillment
of the requirements for the

M.S. degree in Chemistry

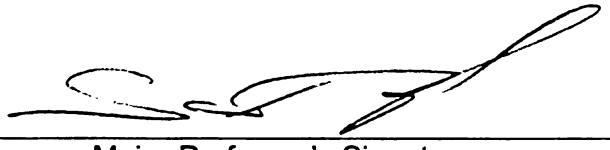

Major Professor's Signature

8/24/2010

Date

MSU is an Affirmative Action/Equal Opportunity Employer

QUANTITATIVE ANALYSIS OF AMINOPHOSPHOLIPIDS BY CHEMICAL DERIVATIZATION AND TANDEM MASS SPECTROMETRY

By

SICHANG LIU

A THESIS

Submitted to
Michigan State University
in partial fulfillment of the requirements
for the degree of

MASTER OF SCIENCE

Chemistry

2010

ABSTRACT

QUANTITATIVE ANALYSIS OF AMINOPHOSPHOLIPIDS BY CHEMICAL DERIVATIZATION AND TANDEM MASS SPECTROMETRY

By

SICHANG LIU

Aminophospholipid metabolism and cellular signaling are highly integrated processes that regulate various cellular functions. Abnormalities in lipid composition have established roles in human diseases, for example hepatocarcinogenesis- a kind of liver cancer. Thus, a comprehensive comparative analysis of changes in aminophospholipid profiles that occur between normal and diseased cells or tissues may enable the in-depth characterization of specific lipids that can serve as epigenetic factors and metabolomic biomarkers. In an effort to gain a precise and accurate relative quantification of aminophospholipids, one-step isotopic derivatization assay coupled with tandem mass spectrometry analysis was carried out. Heavy and light isotopic forms of a DMBNHS reagents which contain a positively charged sulfonium ion, were synthesized to efficiently and specifically derivatized amine-containing lipids. Aminophospholipids were subjected to such chemical derivatization in order to enhance ionization efficiency, assist structure elucidation and improved the precision of relative quantification by minimizing or negating errors associated with run-to-run irreproducibility. By mixing heavy- and light- labeled control and diseased mouse liver lipid extracts in 1 to 1 ratio's and performing a series of single-run neutral loss and precursor ion scan mode MS/MS experiments, we demonstrate significant alteration of aminophospholipid distributions of double mutant mice liver compared that of control mice.

AKNOWLEDGEMENT

It is a real pleasure to thank those who made this thesis possible. I am heartily thankful to my advisor, Professor Gavin Reid who has the attitude and the substance of a genius: he continually and convincingly conveyed a spirit of adventure in regard to research and science. His guidance and persistent help was invaluable to my whole life.

I would also like express my sincere thank the members of my committee, Dr. Daniel Jones, Dr. Gary Blanchard, and Dr. Dana Spence for their friendly encouragement, understanding, and meaningful suggestion. I would like to thank the members of the Reid Research Group, both past and present, for been a warm family for me here at MSU. I would especially like to thank Xiao Zhou and Yali Lu for their creative synthesis work which is the foundation of this project. I am grateful to have Salih Abduselam as my first African friend and as my energy resource through all those difficult times. In addition, thank you is never enough for my parents, Jian Liu and Xiurui Si. Without their praying, believing and constant support, I could not be the same person as who I am today.

I also want to appreciate Todd Lydic and Prof. Julia Busik from Physiology Department, without their enthusiasm and interdisciplinary knowledge, our collaborated project won't be so productive. I wish to acknowledge Prof. Rheal Towner from Oklahoma Medical Research Foundation for offering all the liver lipid samples. Last but not least, I would like to thank all my friends for accompanying me no matter where I am and where they are.

TABLE OF CONTENTS

LIST OF TABLES

TABLE **PAGE**

LIST OF FIGURES

LIST OF SCHEMES

SCHEME **PAGE**

CHAPTER ONE

INTRODUCTION

1.1 Lipids and Phospholipids

1.1.1 Overview of the Biological Function of Lipids

Lipids are defined as hydrophobic or amphipathic small molecules that may originate entirely or in part from carbanion-based condensations of thioesters and/or from carbocation-based condensations of isoprene units.[1] More specifically, lipids are a large and diverse group of naturally occurring organic compounds such as fats, waxes, sterols, fat-soluble vitamins, monoglycerides, diglycerides, phospholipids, etc. Literally there are hundreds of thousands of potential species of lipids. Why is there such diversity? The principle biological maxim that 'structure serves function' indicates that the complexity of lipids corresponds to their different biological functions.

Lipids fulfill three general functions. First, lipids serve as high density food and energy resources. Triacylglycerols and sterols are major forms of energy storage in animals. For example, the complete oxidation of fatty acids from triglycerides can provide more than twice the energy of the same mass of carbohydrates or proteins.[2]

Second, lipids, especially polar lipids, are major structural components of cell membranes. The membrane, which is a 30Å hydrophobic film, is essentially a form of lipid bilayer. The formation of lipid bilayers is an energetically favored process in aqueous environments. The general structure of polar lipids is a combination of

hydrophobic and hydrophilic moieties. The hydrophobic portions prefer to self-associate while the hydrophilic moieties favor interaction with aqueous environments. Such unique membrane structures help cells to separate their internal constituents from the outside environment. These membranes have the potential for budding, fission and fusion and are essential for cell division, reproduction and trafficking.[3] The composition and structure of membranes, which includes lipid asymmetry across the bilayer and lipid domains, are closely correlated with the phase behaviors of lipids, serve as a platform to interact with membrane proteins and realize multiple biological functions. Since lipids are necessary protein anchors. Palmitoylation (C16), laurylation (C12), prenylation (C15) are a series of protein modification process that are critical for proper protein functions. [4]Lipids also work as protein co-factors and targeting molecules. [5] As co-factors, lipid matrices offer adequate membrane orientation and activity for protein folding and subunit assembly. [6]

Third, lipids serve as signaling molecules. [5] A variety of lipids such as phosphatidylserine, prostaglandins, leukotrienes, inositol lipids and sphingolipids are involved in diverse biological pathways. As targeting molecules, their interactions with proteins can modulate their signaling and activity. The interactions of different membranes are crucial to vesicle trafficking or endocytosis. [7]

1.1.2 Lipid Structure and Classification

Carbanion-based condensations of thioesters generate 6 categories of lipids: fatty acyls, glycerolipids, glycerophospholipids, sphingolipids, saccharolipids, and polyketides. Carbocation-based condensations of isoprene units generate 2 additional categories of

lipids: prenol and sterol. In the following studies we are more interested in thioester-derived lipids, especially glycerophospholipids.[1]

Table 1.1 Distribution of lipid categories in a lipid database.

Category	Abbreviation	Structures in Database[8]
Fatty acyls	FA	2678
Glycerolipids	GL	3009
Glycerophospholipids	GP	1970
Sphingolipids	SP	620
Sterol Lipids	ST	1744
Prenol Lipids	PR	610
Saccharolipids	SL	11
Polyketides	PK	132

1.1.3 Fatty Acyls

The structure of fatty acyls is the most fundamental building block of complex lipids. The nomenclature of this class of lipids indicates the structure of a repeating series of methylene groups that impart hydrophobic character to this category. The most abundant subclass of this group is fatty acids which contain a terminal carboxylic acid. The simplest fatty acids are saturated fatty acids which have a straight carboxylic chain and have no double bonds. Variants of this structure have one or more double bonds and are named unsaturated and polyunsaturated fatty acids. Most naturally occurring fatty

acids have chains of 4 to 28 carbons and the number of carbon atoms is usually even. The balance and differences in geometry among the various types of unsaturated fatty acids, as well as between saturated and unsaturated fatty acids play an important role in biological processes, and in the construction of biological structures. Fatty acids and other lipids are in a state of dynamic flux. Fatty acids are readily released from triacylglycerols to provide a source of energy or structural components for cells. These free fatty acids are in an appropriate form that can be mobilized quickly when required for transport to different tissues where they can be oxidized.[9]

Other subclasses of more complex fatty acids with multiple functional groups are categorized by the total number of carbon atoms found in the critical biosynthetic precursor. For example, eicosanoids derived from arachidonic acid include prostaglandins, leukotrienes and other derivatives. [10]

1.1.4 Neutral Lipids

Neutral lipids, including simple glycerolipids and sterols (Figure 1.1), refer to lipids that do not carry charged or zwitterionic groups. The glycerolipid category is dominated by mono-, di- and tri-substituted glycerols. [11] In chemical terms, these consist of hydric alcohols esterified with one, two or three long-chain fatty acids. The stereochemistry of glycerol lipids is described by the "stereospecific numbering" (sn) system (Figure 1.2).

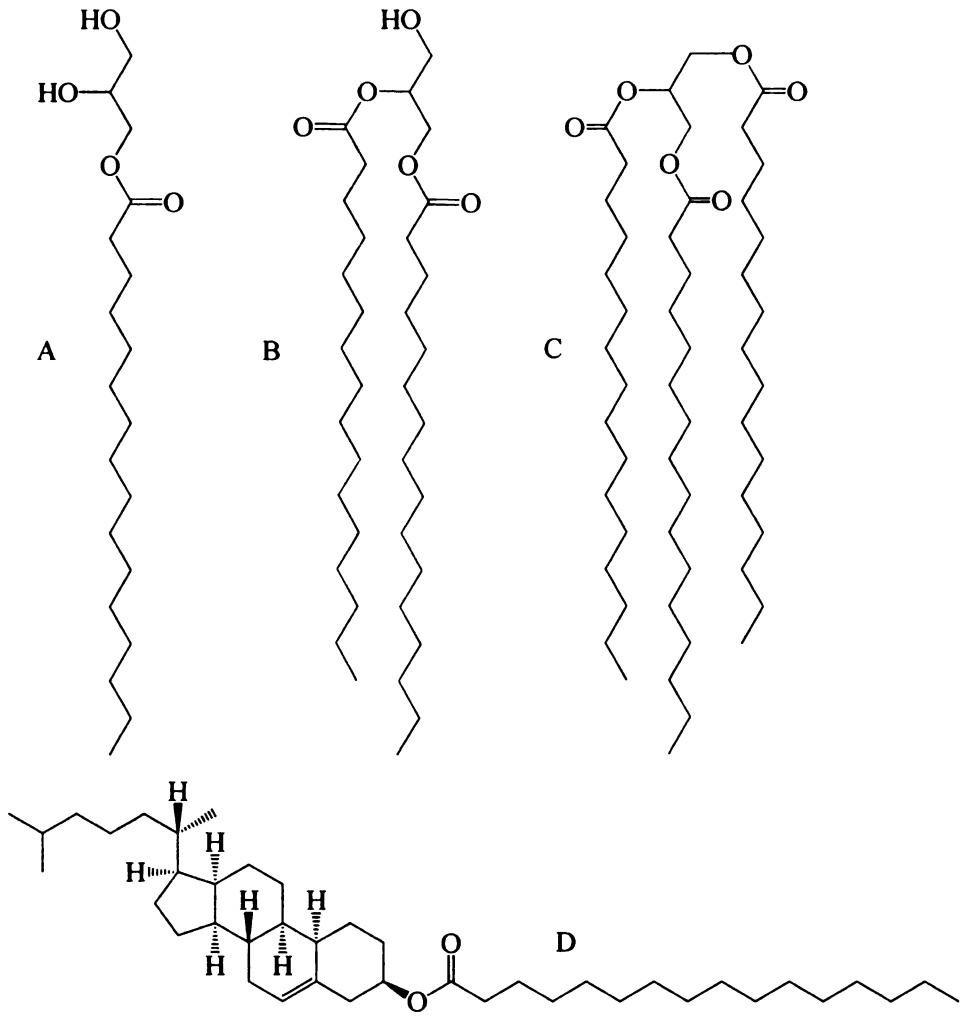

Figure 1.1 Neutral lipids. (A) monoacylglycerol, (B) diacylglycerol, (C) triacylglycerol, (D) Cholesterol ester. All lipids are of variable fatty acid chain length and unsaturation.

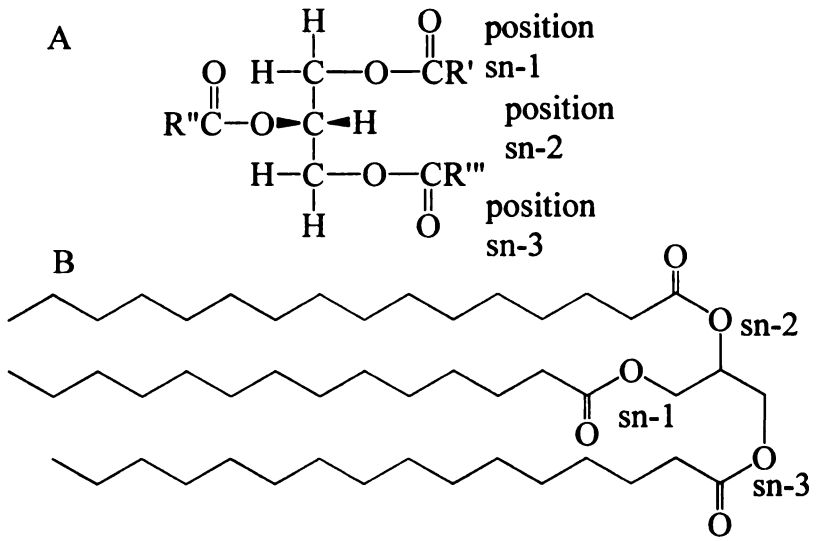

Figure 1.2 Fischer projection of L-glycerol (A) and its triacyl derivative (B).

1.1.5 Sphingolipids

Sphingolipids comprise a range of lipids in which fatty acids are linked via amide bonds to a long-chain base (Figure 1.3). Sphingosine for example, is the simplest functional sphingolipid. [12] Its derivatives – ceramides which contain a fatty acid linked by an amide bond are important precursors of phospholipids and glycolipids with a large range of functions in tissues. [13] The properties of more complex oligoglycosylceramides and gangliosides are quite distinct from that of the complex glycerolipids. [13] Sphingolipids are not only an important component of cellular membranes but also when combined with cholesterols to generate unique structures called membrane rafts that are recently been found to play a crucial role in signaling and especially as docking sites of proteins. [14]

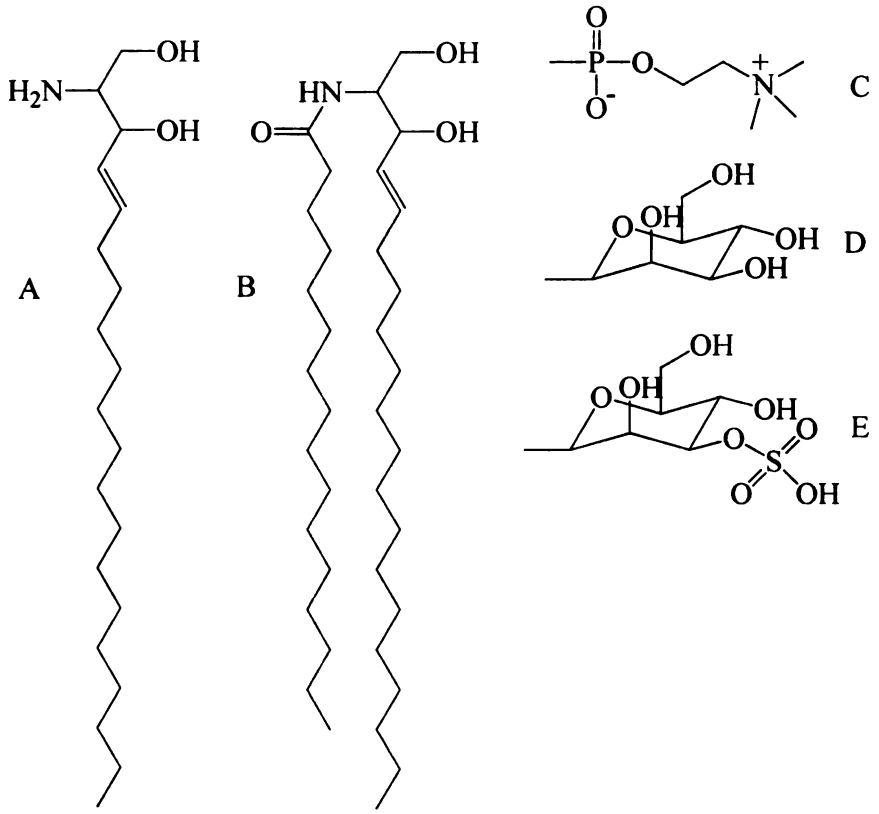

Figure 1.3 Sphingolipids. (A) sphingosine, (B) ceramide, (C) sphingomyelin, (D) galactosylceramide (cerebroside), (E) sulfatide. (A) and (B) contain variable fatty acid chains and (C), (D) and (E) are derivatives of (B) with different head group structures.

1.1.6 Glycerophospholipids

Glycerophospholipids are ubiquitous in nature and are key structural components of the cell membrane bilayer.[2-3] Glycerophospholipids are derived mainly from sn-1,2-diacylglycerols that consist of two long hydrophobic chains with a phosphate residue in the sn-3 position linked to a small polar head group (Figure 1.4). Recently two-letter generic abbreviations (PC, PE, PS etc.) have been used to define glycerophospholipids in shorthand form regarding the differences of head groups.[1] The physical properties of

glycerophospholipids are important for their functions. Lipids such as PC, PI, PA and CL have cylindrical shape because their head groups and hydrophobic tails are of equal sizes. The cylindrical molecular shape prefers to generate a monolayer with zero to positive curvature. Alternatively, the cone-shaped PE with a smaller head group and larger hydrophobic tail prefers to assemble into a monolayer with negative curvature. Such discontinuity between bilayer lipids is important for protein insertion into membranes.[15] Previous studies have shown that different membranes contain different lipids, however PC, PE, PI, PS and sphingomyelin are the five most abundant membrane lipids in almost all membranes. [16]

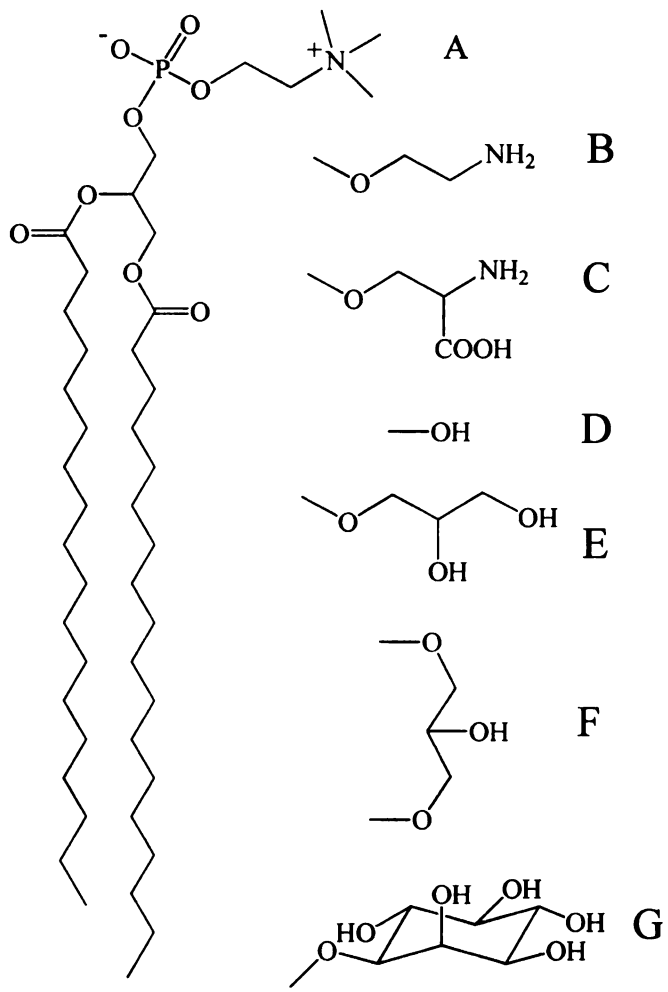

Figure 1.4 Glycerophospholipid species. (A) phosphatidylcholine (PC), (B) phosphatidylethanolamine (PE), (C) phosphatidylserine (PS), (D) phosphatidic acid (PA), (E) phosphatidyl glycerol (PG), (F) Cardiolipin (CL), (G) phosphatidylinositol (PI).

1.1.7 Aminophospholipids

Aminophospholipids are a subclass of glycerolphospholipids that contain primary amino groups. Within this subclass, the two most common lipid types are phosphatidylethanolamine (PE) and phosphatidylserine (PS) (Figure 1.5). As described above, the polar head group is attached at the sn3 position of the glycerol backbone,

while long carbon side chains are attached at the sn1 and sn2 positions. Typically, sn1 fatty acids are saturated or monounsaturated and sn2 fatty acids are either mono- or polyunsaturated. The positions of double bonds are defined by counting from the terminal end carbon to the glycerol moiety. (e.g., n3, n6 or omega 3, omega 6). Cis conformations are defined by using "c" or "z". Alkyl ether and 1Z-alkenyl ether (Plasmalogen) species are represented by an "O-" or "P-" identifier. For example, the abbreviated name of the lipid in Figure 1.5 panel C is PE (P-16:0/18:5(9Z)). Mon-or-adyl-glycerophospholipids or lysophospholipids may be specified with a letter "L" in the abbreviation, for example, LPE (16:0) in Figure 1.5 panel A. [8]

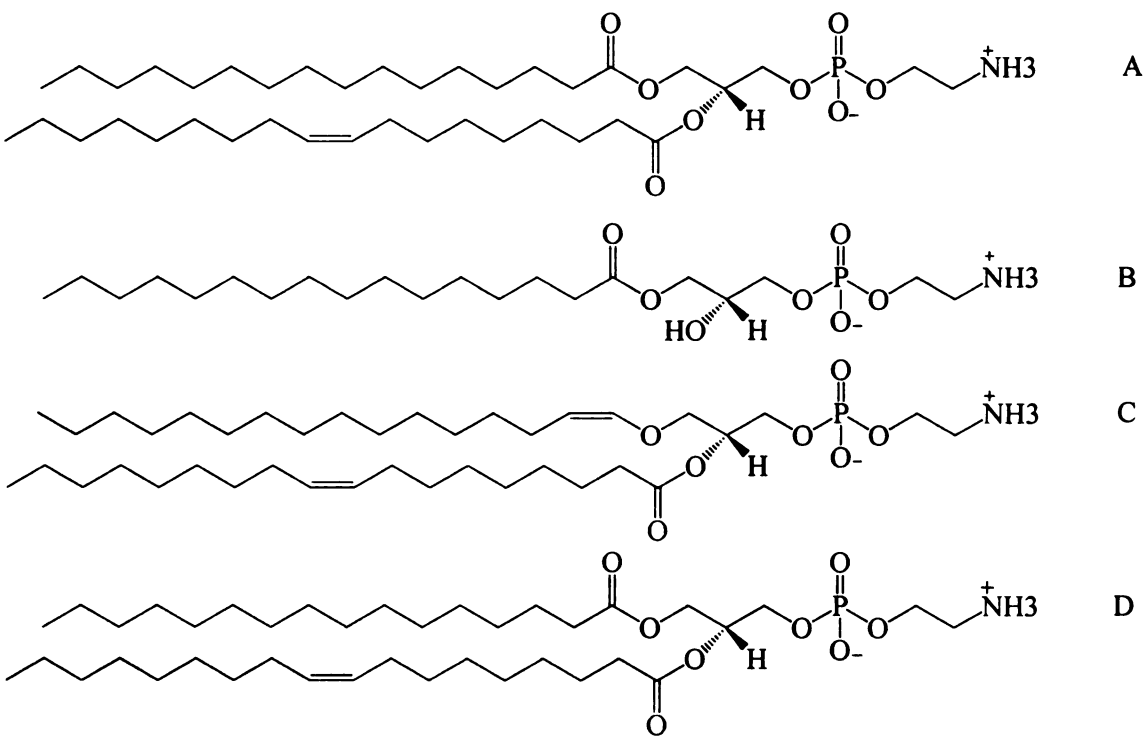

Figure 1.5 Aminophospholipid species. (A) PE $_{(16:0/18:1)}$, (B) lysoPE $_{(16:0)}$, (C) PE $_{(16:0p/18:1)}$, (D) PS $_{(16:0/18:1)}$.

1.1.8 Aminophospholipid Membrane Asymmetry and Disease

Prior studies have confirmed that there is asymmetry in the distribution of lipids between the inner and outer leaflets of bilayers (Figure 1.6).[17,18] Normally in the plasma membranes of normal eukaryotic cells, phosphatidylcholine (PC) and sphingomyelin (SM) are predominantly present in the outer leaflet. Phosphatidylethanolamine (PE) and phosphatidylinositol (PI) reside mainly in the inner leaflet, while phosphatidylserine (PS) is located almost exclusively in the inner leaflet.[19]

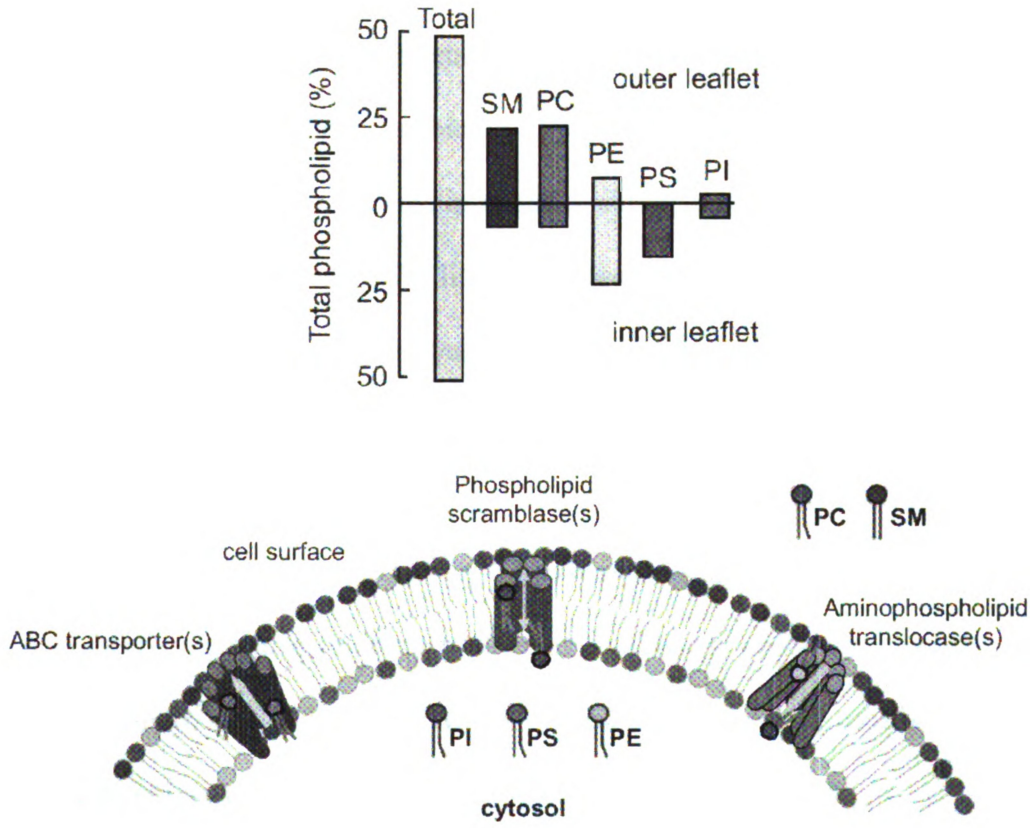

Figure 1.6 Phospholipid asymmetry in plasma membranes.[19]

Multiple factors contribute to lipid asymmetry in membranes. Not only do lipids carry different biophysical properties as described above (head group size, charge state and fatty acyl chain length, double bond numbers and positions), but also the presence of transporters (enzymes) can assist the translocation of particular lipid species across the bilayer. [20, 21] The bi-directional transport (flip-flop) of lipids between leaflets is controlled by ATP-binding cassette (ABC) transporters, aminophospholipid translocases, and phospholipid scramblases.[22]

In a biophysical aspect, the cross-membrane asymmetric distribution of lipids is the result of a non-zero transmembrane potential in the absence of ions. This intrinsic membrane potential is generated by the condensation of zwitterionic lipids and anionic lipids (PE and PS) in opposite leaflets of the membrane. The loss of membrane lipid asymmetry is crucial for integrated biological processes such as cellular signaling and metabolism. For example, an increase in negative charge on the surface of apoptotic cells resulting from externalization of PS lipids has been shown to activate endothelial cell membrane hyperpolarization and cytoskeleton reorganization processes involved in angiogenesis and vascular remodeling.[23] Negatively charged PS also contributes to the recruitment of cationic proteins such as the c-Src tyrosine kinase.[24]

The appearance of anionic phospholipids such as PS and PE on the cell surface have also been implicated in numerous other biological processes, including blood coagulation, microtube formation, vesicle fusion, cell division, sperm capacitation, phagocytic recognition and clearance of apoptotic cell corpses.[25, 26]

Abnormalities in aminophospholipid composition and distribution have established roles in human diseases including diabetes, cancer, obesity and

neurodegenerative diseases.[27] For example, vascular endothelial cells in tumors, but not in normal tissues, externalize PS as a result of tumor-associated oxidative stress and activating cytokines. [28] Scientists are currently working on using PS as an accessible marker of tumor vasculature to generate tumor imaging and therapy. [29] Also, inhibiting the activation of PE externalization triggered by PE-binding proteins appears to promote cellular resistance to tumor necrosis factor (TNF)-induced apoptosis. [30] Recent advances in aminophospholipid analysis provide an opportunity to define new roles for lipids in drug delivery. Anionic, pH-sensitive liposomes which contain specific PE and PS lipids allow efficient release and delivery of anti-cancer drugs such as antisense oligonucleotides.[31] In the post-genomic era, epigenetic factors and biomarkers such as aminophospholipids can be utilized to provide a better understanding of the mechanisms of diseases and realize the benefits of personalized medicine.

1.2 Mass Spectrometry-Based Strategies for Lipid Analysis

State-of-the-art mass spectrometry (MS) based techniques for profiling and quantification of lipids provide powerful tools to determine the roles of lipids in cell function and disease. Before the development of the modern mass spectrometer, thin-layer-chromatography (TLC) was used to separate different classes of lipids while phosphorus analysis was applied to quantify the total amount of phospholipids. [32, 33] For a simple and purified lipid profile, nuclear magnetic resonance (NMR) has also been used to achieve identification, while structure details of low mass range lipids are elucidated by gas chromatography mass spectrometry (GC-MS).[34] Subsequent progress

in mass spectrometric ionization methods showed that lipids could be analyzed using 'soft' ionization techniques such as field desorption[35] or fast atom bombardment (FAB)[36, 37]. However, poor reproducibility and moderate sensitivity prevent the widespread application of these methods for lipid analysis.

1.2.1 Electrospray Ionization (ESI)

Among the softest of ionization methods developed for the analysis of biomolecules, electrospray ionization (ESI) was a major breakthrough because it made possible the determination of both the molecular weight and the nature and structure composition of a variety of lipids of different classes. Furthermore, such analysis requires low quantities of samples ranging from pg to ng of total lipids.[38]

To reach the goal of comprehensive lipid profiling by ESI, solvent systems should be optimized. Typically, a solvent system contains methanol and chloroform with a volume ratio of 1:2 (sometimes 2-propanol/methanol/chloroform system is used). To balance the solubility and ionization efficiency of lipids, ammonium acetate (or other salts like ammonium hydroxide, methylamine) with mM level concentrations are added to the solvent.[39] More recently, nano-electrospray (nESI) is employed instead of normal ESI to further improve the sensitivity and overall performance of the analysis.

Another advantage of ESI is its capability to introduce molecules to the mass spectrometer by either direct infusion or by coupling with high performance liquid chromatography (HPLC). A comparison of the advantages/disadvantages of HPLC separation and direct infusion will be discussed later on.

After ionization, different mass analyzers can perform various experiments to provide m/z information from ionized lipid molecules, or to provide structural information via gas-phase fragmentation reactions. Quadrupole time-of-flight (qTOF) mass analyzers reach the requirement of a wide dynamic range with outstanding mass accuracy (e.g., 1-2 ppm), while triple stage quadrupole (TSQ) and ion trap mass analyzers can perform fast cycle MS/MS experiments with high sensitivity.[40, 41]

1.2.2 Tandem Mass Spectrometry Fragmentation Reactions

Because of their molecular composition and ionization characteristics, most lipids present in cell membranes have molecular masses in the range between m/z 600 and 1500. In complex lipid mixtures, a common phenomenon is the presence of two different lipids with isobaric masses in the MS spectrum. Moreover, the presence of various cationic or anionic adducts of lipids further complicate analysis of the spectra. Therefore, simply matching the m/z of an MS ion with the theoretical mass of a possible lipid may result in ambiguity. [41] On the other hand, in a tandem mass spectrometry (MS/MS) experiment, mass selected lipid ions undergo dissociation to generate structure-specific fragments corresponding to their different headgroups and fatty acyl chains. Therefore, MS/MS is a more reliable tool for lipid identification. By monitoring and scanning representative fragments (either as a product ion or as a neutral loss) for a given lipid class, it is possible to 'pull out' a specific lipid class of interest from within a complex lipid mixture so that the detection of these lipids is of improved sensitivity and accuracy. Figure 1.7 shows the typical gas phase bond fragmentation positions of aminophospholipids while Table 1.2

summarizes the typically used MS/MS scan information provided from each subclass of aminophospholipid.[41]

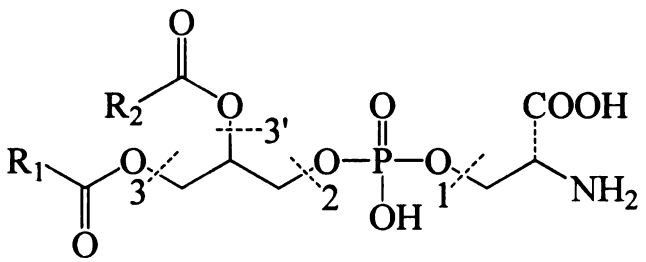

Figure 1.7 Typical aminophospholipid gas-phase fragmentation cleavage sites.

Table 1.2 Summary of class specific aminophospholipid fragmentation scan modes available in positive and negative ion modes of analysis.[42, 43, 44]

Lipid type	Positive ion mode	MS/MS	Bond cleavage	Negative ion mode	MS/MS	Bond cleavage
PE	$[M+H]^+$	NL 141	2	$[M-H]^-$	PI $RCOO^-$ NL RCOOH NL 196	3 3 +3'-H_2O
lysoPE	$[M+Na/K]^+$	NL 43	2	$[M-H]^-$	$RCOO^-$ NL RCOOH	 3
pPE	$[M+H]^+$ $[M+Na/K]^+$	NL 18	2	$[M-H]^-$	$RCOO^-$ NL RCOOH	 3
PS	$[M+H]^+$	NL 185	2	$[M-H]^-$	NL 87	1

1.2.3 Challenges of Mass Spectrometry-Based Lipid Analysis

1.2.3.1 Sample Complexity

MS/MS experiments can help resolve isobaric peaks from complex lipid mixtures. However, ionization bias of lipids due to differences in their structure and functional groups and the natural wide range of abundances of the different lipid classes can limit the efficient profiling of lipids with low concentrations, such as aminophospholipids. Although aminophospholipids are minor components of membrane lipid profiles, they serve important roles in various biological processes, so tracing these classes of lipid has more potential for the discovery of biomarkers.

HPLC coupled with mass spectrometry can provide primary separation of aminophospholipids, but the limitations of HPLC should also been taken into consideration. Factors such variety of exogenous and endogenous chemical species in biological samples may yield matrix ionization effects of lipid analysis and require additional strategies for evaluation.[45] This will decrease the reproducibility of lipid analyses.

1.2.3.2 Quantitative Analysis

Currently, the use of synthesized (not naturally occurring) lipid standards is not able to fulfill the requirement of quantitative analysis which typically requires multiple internal standard lipids to be spiked into the profile.[39] For example, the fatty acyl chain length, as well as the number of double bond numbers and their positions is known to affect peak intensities resulting in a non-linear correlation and preventing the ability to rely on a single internal standard to accurately calculate an unknown lipids concentration.

[46] In addition, sample preparation differences (differences in tissue homogenization or extraction efficiency from batch to batch) and mass spectrometry system errors (e.g., variation in spray stability) from run to run all add to inefficiency to quantitative analysis. As a result, real biological variances between normal and diseased state lipid profiles may appear to be statistically insignificant compared to these variances. These issues amplify the challenge of dependable quantitative analysis of aminophospholipids.

1.3 Chemical Derivatization Strategies for Aminophospholipids Analysis

Chemical derivatization applied to lipid analysis was first employed to adjust the physical properties of biological molecules for ease of GC-MS analysis. [34] Confronted with the challenge of ESI mass spectrometry analysis, scientists began to search for practical solutions in the field of chemical derivatization. By modifying biological molecules with a functional tag, chemical derivatization helps to increase the polarity of the compound to further enhanced ionization efficiency. [47] The attached functional group may also change the gas-phase fragmentation patterns and create new detection channels. [48] In general, chemical derivatization aids in superior selectivity, sensitivity and structure elucidation for mass spectrometry based lipidomics.

1.3.1 Trinitrobenzenesulfonic Acid (TNBSA) Derivatization

The earliest approach for aminophospholipid derivatization was described by Francise Hullin *et. al.* [49] Trinitrobenzene sulfonic acid (TNBSA) (Figure 1.8) reacts

with primary amino groups in aqueous solution at pH 8 to form yellow adducts. Conventional TLC followed by HPLC UV detection was then used to quantify TNBSA-derivitized PE lipids. The colored derivatives were monitored at 335-345 nm and have extinction coefficients in the range of 10,000-15,000. Based on this reaction, TNBSA has been used as a hydrophilic modifying reagent for the detection of primary amines in samples containing amino acids, peptides or lipids.

1.3.2 Fluorenylmethoxylcarbonyl Chloride (Fmoc-Cl) Derivatization

More recently Han and coworkers presented a novel MS based methodology for the analysis of PE and lysoPE lipids through fluorenylmethoxylcarbonyl (Fmoc) chloride modification (Figure 1.9). [50] This one-step *in situ* derivatization process achieved significant improvement in the detection of PE and lysoPE species in negative ion mode MS analysis.

1.3.3 Isotope-Tagged Reagent Derivatization

Multiplexed sets of differentially isotopically enriched N-ethylpiperazine acetic acid N-hydroxysuccinimide ester reagents (Figure 1.10) have also been used for MS analysis of changes in PE aminophospholipid abundances that result from different biological stimuli.[51, 52] Here, the derivatized PE lipids were isobaric and chromatographically indistinguishable, but yielded characteristic reporter ions (m/z 114

or 117) after collision induced dissociation (CID)-MS/MS in positive ion mode that could be used to quantify individual members of the multiplexed set.

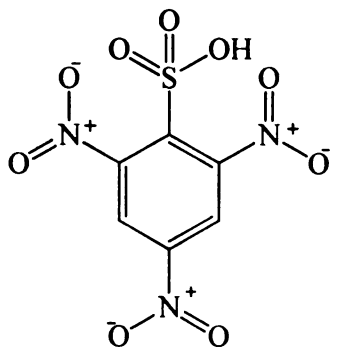

Figure 1.8 Structure of TNBSA.

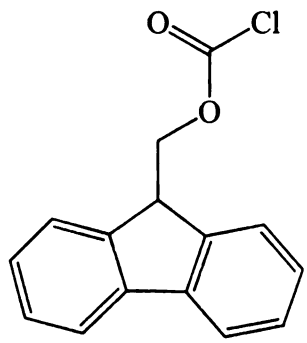

Figure 1.9 Structure of Fmoc-Cl.

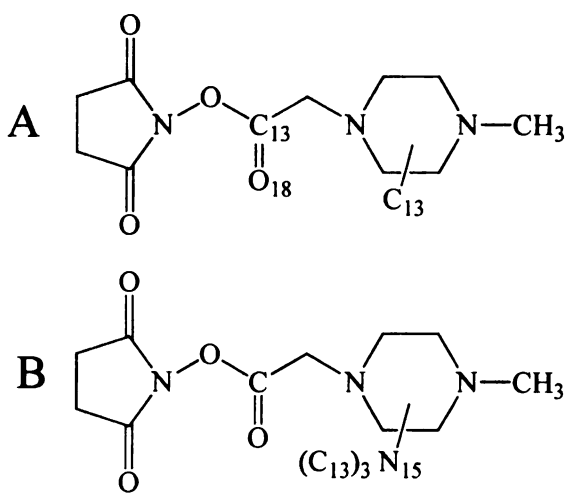

Figure 1.10 Structure of two versions of isotope-tagged NHS reagents.

1.4 Aims of This Thesis

The hypothesis for the research described in this thesis is that the development and application of chemical derivatization reagents and MS/MS analysis strategies for lipid identification, and for the quantitative analysis of changes in aminophospholipid profiles that occur between control and diseased tissues, will provide enhanced sensitivity and specificity for the identification of effective biomarker signatures for diagnosis and prognosis. We propose to examine this hypothesis by developing and using chemical derivatization and mass spectrometric methods as described in following specific aims.

Aim 1: Establish a novel sulfonium ion chemical derivatization and mass spectrometry based analysis methodology for the identification, structure elucidation and quantitative analysis of PE and PS aminophospholipids.

Aim 2: Application of the mass spectrometry based chemical derivatization strategy toward quantitative analysis of changes in liver aminophospholipid profiles in a mouse model of hepatocellular carcinoma.

CHAPTER TWO

EXPERIMENTAL

2.1 Materials

Methanol (HPLC grade), sodium methanethiolate, β-butyrolactone, D_6-γ-butyrolactone, 4-bromobutyric acid, thiourea, trinitrobenzenesulfonic acid (TNBSA), fluorenylmethoxylcarbonyl chloride (Fmoc-Cl), fluorenylmethoxylcarbonyl N-hydroxysuccinimide (Fmoc-NHS), and D_3-iodomethane were purchased from Sigma-Aldrich (St. Louis, MO). Dimethylsulfoxide (DMSO), N-hydroxysuccinimide, methylthiobutyric acid and N,N'-dicyclohexylcarbodiimide were from Fluka (Switzerland). Ethanol was purchased from the AAPER Alcohol and Chemical Co. (Shelbyville, KY). Isopropanol, triethanolamine and diethyl ether were from Jade Scientific (Canton, MI). Ammonium acetate, glacial acetic acid, acetonitrile, chloroform (ACS and HPLC grades) and CH_2Cl_2 were obtained from Mallinckrodt Baker (Phillipsburg, NJ). Ammonium hydroxide (28.0-30.0%), potassium hydroxide, anhydrous magnesium sulfate and hydrochloric acid were from Columbus Chemical Industries (Columbus, WI). Methylthiobutyric hydroxysuccinimide ester and iodomethane were purchased from EMD Chemicals (San Diego, CA, USA).

Synthetic lipid standards, $PE_{(14:0/14:0)}$, $PE_{(18:0/18:0)}$, $PE_{(18:0/18:1)}$, $PE_{(18:0/20:4)}$, $PE_{(22:6/22,6)}$, $PS_{(14:0/14:0)}$ and $PS_{(18:0/18:1)}$, were purchased from Avanti Polar Lipids Inc.

(Alabaster, AL). The lipid nomenclature the follows the system recommended by the LIPIDMAPS consortium in 2009.[1]

2.2 Synthesis of Sulfonium Ion Reagents

2.2.1 Synthesis of S, S'- dimethyl thiobutynolhydroxysuccinimide Ester Sulfonium Iodide (DMBNHS)

A sulfonium ion containing modification reagent with a three carbon alkyl chain was synthesized by Zhou *et al.* using the three-step process as shown in Scheme 2.1 below. [53] Based on the method of Musker et al.[54], 99.5 mmol sodium methanethiolate and 74.63 mmol of β-butyrolactone were dissolved in 90 mL of dry DMSO. Then, the solution was stirred under an N_2 atmosphere at room temperature for 6 days. 166 mL of 1M HCl was added to the resulting slurry and the aqueous solution was extracted with 6 x 104 mL of diethyl ether. The solvent was evaporated under reduced pressure. The resulting viscous liquid was purified by silica gel column chromatography (100% ethyl acetate). The eluent containing the product was collected and concentrated under reduced pressure giving 5.97 g (60%) methylthiobutyric acid **(1)** as a colorless oil. ^{1}H NMR (500 MHz, $CDCl_3$): δ1.90 (m, 2H), 2.07 (s, 3H), 2.47 (t, 2H), 2.52 (t, 2H), 11.15 (s, 1H).

(1) was then esterified by reaction with N-hydroxysuccinimide (NHS) to yield methylthiobutyric hydroxysuccinimide ester **(2)**. Under a N_2 atmosphere, 33 mmol of NHS and 30 mmol of **(1)** were dissolved in a mixture of 60 mL of $CHCl_3$ and 30 mL of

CH_2Cl_2. The mixture was stirred for 5 minutes at room temperature. Then 33 mmol of N,N'-dicyclohexylcarbodiimide (DCC) was added and a precipitate formed immediately. The resulting slurry was stirred in a N_2 atmosphere. After 24 hrs, the mixture was filtered and the solution was collected and concentrated under reduced pressure. Then 5 mL of acetonitrile was added to the liquid and the precipitate was filtered out. The resultant solution was dried under vacuum, after which 6.08g (88%) product **(2)** was obtained as a white solid. ^{1}H NMR (500MHz, $CDCl_3$): δ2.02 (m, 2H), 2.09 (s, 3H), 2.59 (t, 2H), 2.75 (t, 2H), 2.82 (s, 4H).

Finally, **(2)** was reacted with methyl iodide to yield S, S'- dimethyl thiobutynolhydroxysuccinimide ester sulfonium iodide (DMBNHS) **(3)**. 1 mmol of methylthiobutyric hydroxysuccinimide ester **(2)** and 5 mmol of iodomethane were dissolved in 2 mL of CH_3CN then stirred in the dark at room temperature for 2 days. The resulting solution was then concentrated under reduced pressure. The resultant yellow solid was washed with 10 mL of dichloromethane then dried under vacuum over night to give 0.28 g (76%) product **(3)** as yellow crystals. The product was stored in the dark. ^{1}H NMR (500MHz, CD_3CN): δ2.16 (m, 2H), 2.77 (s, 4H), 2.81 (s, 6H), 2.85 (t, 2H), 3.29 (t, 3H).

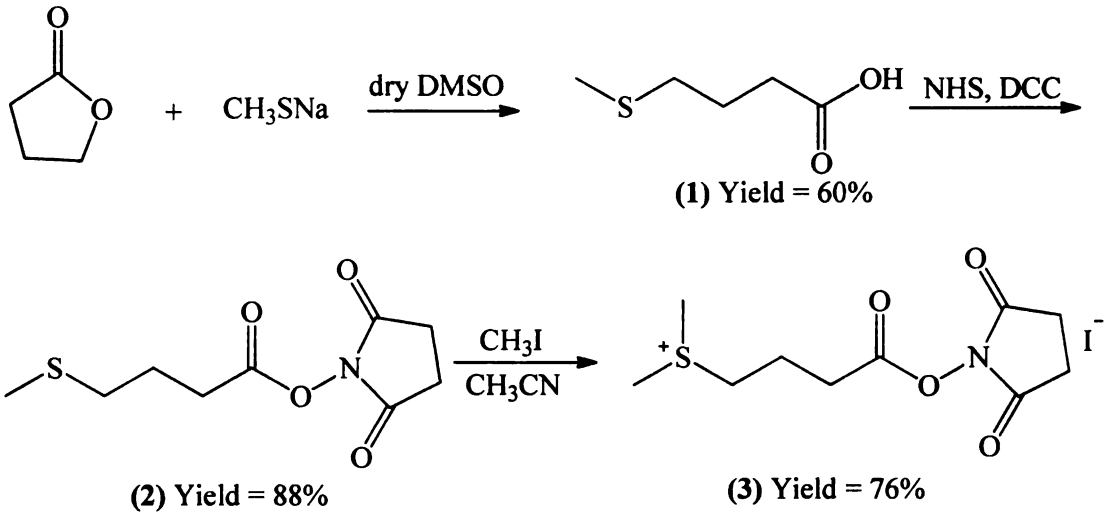

Scheme 2.1 Synthetic route for the preparation of the sulfonium ion containing DMBNHS reagent (**3**).[53]

2.2.2 Synthesis of S, S'- d_6-dimethyl Thiobutynolhydroxysuccinimide Ester Sulfonium Iodide (D_6-DMBNHS)

Based on the method of Jessing *et. al* [55], 4-bromobutyric acid (8.35 g, 50.0 mmol) and thiourea (5.70 g, 75.0 mmol) were dissolved in 100 mL of ethanol and refluxed overnight (Scheme 2.2). The solvent was then evaporated under reduced pressure and 65 mL of 7.5 M NaOH (aq) was added. The mixture was refluxed at 90 °C under a N_2 atmosphere. After a 16 h reaction, 2M H_2SO_4 was added slowly while stirring in an ice bath until the pH = 1. The resulting mixture was extracted 4 times with 60 mL of CH_2Cl_2, dried over anhydrous $MgSO_4$, and concentrated *in vacuo* to give 5.27 g (88%) of thiobutyric acid (**4**) as a colorless oil. ^{1}H NMR (500MHz, $CDCl_3$): δ1.33 (t, 1H, J = 8), 1.93 (m, 2H, J = 7), 2.50 (t, 2H, J = 7), 2.59 (q, 2H, J = 7), 11.28 (s, 1H)

Adapted from the method of Crouch *et. al* [56], potassium hydroxide (1.31 g, 23.4 mmol) in 2 mL of methanol was added dropwise to **(4)** (1.08 g, 9 mmol) dissolved in 10 mL of methanol in an ice bath and stirred for 10 min. D_3-iodomethane (672.4 μL, 10.8 mmol) was added slowly over 10 min and the solution was stirred at room temperature overnight. After evaporating the solvent under reduced pressure, 12 mL of H_2O was added followed by 2M HCl until the pH equals 1. The solution was extracted with 4 × 18 mL of diethyl ether. The organic extracts were combined and dried over anhydrous $MgSO_4$. The solvent was removed *in vacuo* and 858.2 mg (70%) of d_3-methylmercaptobutyric acid (**5**) was obtained as brown oil. ^{1}H NMR (500MHz, $CDCl_3$): δ1.92 (m, 2H, J = 7.5), 2.49 (t, 2H, J = 7.5), 2.53 (t, 2H, J = 7.5).

Under a N_2 atmosphere, N-hydroxysuccinimide (792.4 mg, 6.89 mmol) and (**5**) (858.2 mg, 6.26 mmol) were dissolved in a mixture of $CHCl_3$ (15 mL) and CH_2Cl_2 (10 mL). The mixture was stirred for 5 minutes at room temperature, then N,N'-dicyclohexylcarbodiimide (1419.5 mg, 6.89 mmol) was added and a precipitate formed immediately. The resulting slurry was stirred in a N_2 atmosphere. After 18 hrs, the mixture was filtered and the filtrate was collected and concentrated under reduced pressure. Then acetonitrile (3 mL) was added and the precipitate was filtered out. The solvent was removed *in vacuo* to yield d_3-methylmercaptobutyric hydroxysuccinimide ester (**6**) as a yellow solid with a quantitative yield. ^{1}H NMR (500MHz, $CDCl_3$): δ 2.02 (m, 2H, J = 7.5), 2.58 (t, 2H, J = 7.5), 2.74 (t, 2H, J = 7), 2.82 (s, 4H).

Finally, (**6**) (933.6 mg, 3.99 mmol) and d_3-iodomethane (1.16 g, 7.98 mmol) were dissolved in CH_3CN (8 mL) and stirred in the dark at room temperature for 2 days. The resulting solution was concentrated under reduced pressure. The resultant yellow solid

was washed with dichloromethane and then dried *in vacuo* over night to yield 1.19 g (79%) of d_6-dimethylmercaptobutyric hydroxysuccinimide ester sulfonium iodide (**7**) as a white solid. The product was stored in the dark. ^{1}H NMR (500MHz, CD_3CN): δ 2.16 (m, 2H, J = 7.5), 2.77 (s, 4H), 2.85 (t, 2H, J = 7.5), 3.30 (m, 2H).

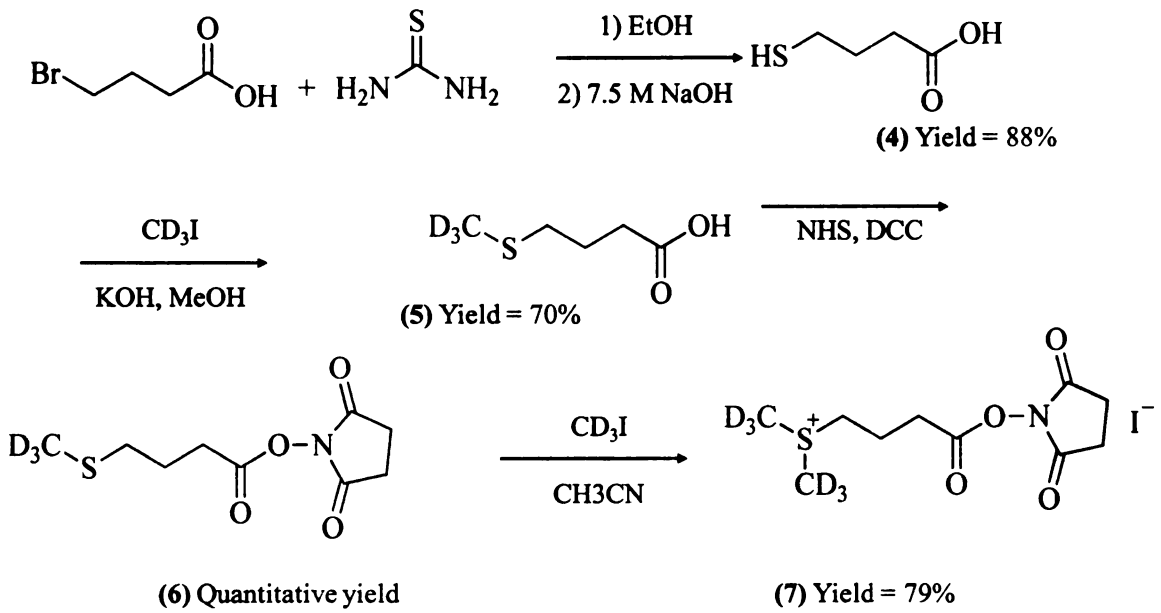

Scheme 2.2 Synthetic route for the preparation of the isotope labeled sulfonium ion containing reagent, D_6-DMBNHS (**7**).

2.3 Chemical Derivatization of Standard Aminophospholipids

The derivatization of aminophospholipids is performed to covalently attach a specific moiety to the amino group. Normally, such categories of reaction are achieved under neutral to basic conditions. To optimize the reaction conditions and examine the effects of pH conditions on derivatization, addition of a small amount of base in equal molar ratio to the labeling reagent was used. Different bases such as triethylamine (TEA),

triethylamonium bicarbonate ($TEAHCO_3$) and dimethylaminopyridine (DMAP) were tested. The most efficient base for each kind of derivatization reaction is reported in the following description.

The general derivatization strategy was to keep the ratio of aminophospholipids, labeling reagent and weak base about 1:10:11 and to monitor the modification process by quenching the reaction within a 10 min to 2 hour time scale. More specifically, 10μl of premixed chloroform stock solution containing 1.6 nM each of $PE_{(14:0/14:0)}$, $PE_{(18:0/18:0)}$, $PE_{(18:0/18:1)}$, $PE_{(18:0/20:4)}$, and $PE_{(22:6/226)}$, and 1 nM each of $PS_{(14:0/14:0)}$ and $PS_{(18:0/18:1)}$ were dried under a stream of nitrogen. The dried aminophospholipids were resuspended in either (i) 39:1.1 (v/v) Methanol/0.1M weak base (total of 40μl) (organic solvent reaction conditions) (ii) 39:1.1 (v/v) water/0.1M weak base (aqueous solvent reaction conditions). 1 μl of the derivatizaton reagent solution (0.1M in adequate solvent) was then added and the solution was vortexed and incubated at room temperature for 10 min to 2 hours. In both organic and aqueous environments, the reaction process was monitored every 10 min. At each time point, the derivatization reaction was quenched by quickly taking the mixture to dryness under a stream of nitrogen. The samples were then stored under nitrogen in glass vials in the dark at -80°C until further use. Immediately prior to mass spectrometry analysis, the lipid mixtures were resuspended in 800μl 4:2:1(v/v/v) isopropanol-methanol-chloroform containing 20mM NH_4Ac or NH_4OH. The final concentration of each derivatized PE was 2μM and of each PS was 1.25μM, to mimic the biological sample lipid profile composition. These solutions were then directly infused to the mass spectrometer for analysis, as previously described.[57]

2.3.1 Trinitrobenzenesulfonic Acid (TNBSA)

The labeling reaction by TNBSA was performed by following the procedure of Hullin *et. al.*[49] The process was essentially identical to that described above, but where $TEAHCO_3$ served as the weak base.

2.3.2 Fluorenylmethoxylcarbonyl Chloride (Fmoc-Cl)

Fmoc-Cl derivatization followed the same method as for the TNBSA reaction, except that TEA was used as the weak base due to its improvement of reaction efficiency. Also since the Fmoc-derivatized aminophospholipids are preferably detected in negative ion mode, 5 mM NH_4OH and 0.2 mM CH_2NH_2 was added to the 800µl 4:2:1(v/v/v) isopropanol-methanol-chloroform diluted lipid solution prior to MS analysis.

2.3.3 Fluorenylmethoxylcarbonyl Hydroxysuccinimide Ester (Fmoc-NHS)

The method for Fmoc-NHS derivatization was the same as that for Fmoc-Cl except that 0.1M Fmoc-NHS chloroform solution was used instead of 0.1M Fmoc-Cl.

2.3.4 DMBNHS

The method for DMBNHS derivatization was the same as for Fmoc-Cl except that the lipid mixture was finally resuspended in 800μl 4:2:1(v/v/v) isopropanol-methanol-chloroform with 20 mM NH_4Ac.

2.4 Mouse Liver Lipid Sample Extraction and Derivatization

2.4.1 Animals and Induction of Hepatocarcinogenesis by Gene Mutation

Over expression of the c-myc proto-oncogene and transforming growth factor-alpha (TGF-α) has been frequently observed in human Hepatocarcinogenesis (HCC), suggestive of a pivotal role for these proto-oncogenes in liver oncogenesis [58]. A double transgenic mouse model involving co-expression of c-myc and TGFα has been developed, that results in >90% incidence of spontaneous liver cancer within 6-8 months. [59] Importantly, the TGF-α/c-myc transgenic mouse hepatocarcinogenesis model represents genetic and molecular alterations also observed in human HCCs, suggesting that this mouse model can serve a useful platform to identify molecular changes that are prognostic of the onset and progression of human HCC. As part of an ongoing collaboration between Prof. Rheal Towner at the Oklahoma Medical Research Foundation and the Reid laboratory [60], multiple analytical and clinical data showed significant alterations in the fatty acid distributions in the c-myc and TGFα transgenic induced HCC liver tissue. ESI CID-MS/MS analysis indicated a significant increase in the abundance of specific 16:0 and 18:1 containing PC lipids in HCC mouse model liver sample compared with control sample. [60]

More recent data obtained by this group has demonstrated that non-mammalian omega-3 desaturase prevents neoplasia when introduced to this mouse hepatocarcinogenesis model. [61] These mice, crossed with mice expressing the *C. elegans fat-1* gene encoding an n-3 fatty acid desaturase that converts n-6 to n-3 fatty acids *in vivo* [62] (which is absent in mammals), generated mice with a triple mutation (TM). MRI analysis of triple mutant (TM) mice showed the absence of neoplasia at all time points for 92% of mice in the study. Pathological changes of TM (TGFα/c-myc/fat-1) mouse liver tissue was similar to control mouse liver tissue. This was also demonstrated by mass spectrometry analysis of PC and PE phospholipid profiles from control, DM and TM mice liver tissue and Chapter 4). The analysis indicated significantly decreased 16:0/20:4 and 18:1/20:4 and elevated 16:0/22:6 fatty acyl groups in both PC and PE lipids, and elevated 16:0/20:5, 18:0/18:2, 18:0/18:1 and 18:0/22:6 in PC lipids within TM mice compared to DM mice. Total fatty acid analysis indicated a significant decrease of 18:1 omega 9 fatty acid in TM mice compared to DM mice. [61]

2.4.2 Lipid Extraction and Concentration Normalization

Lipids from control, DM and TM mouse liver tissue samples (approx. 200 mg each) were extracted using a modified method of Folch [63], where a 2:1 chloroform:methanol mixture containing 0.01% butylated hydroxytoluene was used to extract the lipids after tissue homogenization, and a sodium sulfate filled funnel was used to remove excess water, followed by drying under a stream of N_2 [60]. Stock solutions of the lipid extracts were then prepared by resuspending the dried samples in 500μL

methanol: chloroform (1:1) in glass vials, and then were stored under nitrogen in the dark at -80°C until further use.

For quantitative mass spectrometry analysis (Chapter 4), the total phospholipid concentration for each sample was determined by phosphorus assay following the method of Chen [64]. Since the result showed that the sample-to-sample phosphorus concentration varied from 0.67 mM to 4.61 mM, lipid extracts from five individual control mice tissue samples, were pooled, where the volume of each sample was inversely proportional to its phosphorus concentration. By doing so, a homogeneous pooled solution of control mice liver tissue lipid extract was prepared. Similar pooled solutions were prepared for the DM and TM groups.

2.4.3 DMBNHS Derivatization of Aminophospholipids from Mouse Liver Extracts

The same procedure as described in Section 2.3 above was used to derivatize aminophospholipids from the mouse liver extracts, using either the DMBNHS (light version) or D_6-DMBNHS (heavy version) reagents. 10 μL of the stock solution from either an individual lipid extract solution or a pooled lipid extract was used for each derivatization reaction. For all samples, synthetic PE $_{(14:0/14:0)}$ and PS $_{(14:0/14:0)}$ lipid standards were spiked into each sample prior to derivatization. After the derivatization reaction, the DMBNHS derivatized lipid mixtures were dried under a stream of nitrogen, then resuspended in 1600 μL 4:2:1(v/v/v) isopropanol-methanol-chloroform with 20mM NH_4Ac for mass spectrometric analysis. The final concentration of the spiked in PE and PS lipid standards were 0.5 and 0.16 μM respectively. For quantitative analysis, after

individual derivatization of control, DM or TM mice liver pooled lipid extracts with light or heavy versions of the DMBNHS reagent, a simple 1:1 ratio combination step was used to generate a mixture of control/DM and control/TM samples.

2.5 Mass Spectrometry

2.5.1 Introduction

Mass spectrometry (Scheme 2.1) is an analytical technique that is used to identify compounds, elucidate the structure of molecules and to quantify their abundance. The general process includes ionization of the sample components to form gas-phase ions, separation of ions based on their mass-to-charge (m/z) ratios, detection of the ions and measurement of their abundances.

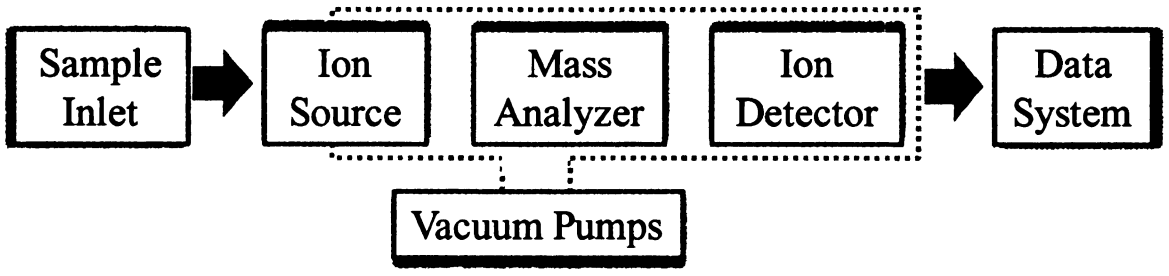

Figure 2.1 Components of a mass spectrometer (adapted from "What is mass spectrometry". www.asms.org).

2.5.2 Ionization Sources

Prior to the 1980s, traditional ionization sources for mass spectrometric analysis were electron ionization (EI) and chemical ionization (CI).[65] Nowadays new generation of ionization techniques, including matrix-assisted laser desorption/ionization (MALDI) and electrospray ionization (ESI) have revolutionized biomolecular analyses. Of these methods, ESI has clearly evolved to be the method of choice to perform fast, sensitive and quantitative lipid analysis.[66, 41]

2.5.2.1 Electrospray Ionization (ESI)

The application of electrospray ionization to the mass spectrometric analysis of biological macromolecules was introduced by John B. Fenn [67]. ESI produces gas-phase ionized molecules directly from a liquid solution. Such a 'soft' ionization method essentially eliminates fragmentation of the molecular ions that frequently result from using EI and CI, thereby providing molecular mass information which is an important character of biomolecules.

ESI involves the process of gas phase ion generation from a flowing liquid solution when exposed to an intense electric field. By applying a high potential (several kV) between the flowing capillary and a counter electrode, the electric field generated at the needle outlet will disperse the liquid into a fine spray of charged droplets. Then, a series of coulombic fission events occurs whereby the solvent is evaporated from the droplet. As the droplets get smaller and ions closer, one would reach the point where the Coulombic repulsion between these charges will be greater than the surface tension of the liquid that brings the droplets together (known as Rayleigh limit) so that the primary

droplets will break up into a batch of smaller droplets. Such offspring droplets of the first disruption will go through the same Rayleigh instability and break up into smaller droplets and so on. Nano-scale ultimate droplets are formed after repeated evaporation and gas-phase analyte ions are finally generated by releasing from the droplets.

One of the most disputed topics of ESI mechanisms is the gas-phase ion formation process. In the 1970s, Dole and co-workers proposed the Charge Residue Model (CRM)[68] assuming that droplets keep shrinking as the solvent evaporates, and that the droplets break up into smaller offspring droplets to maintain below the Rayleigh limit until close to dryness when each of the droplets contains only one analyte molecule. This molecule becomes a free gas phase ion by retaining some of the droplet's charge as the final solvent evaporates. An alternative theory, the Ion Evaporation Model (IEM) [69], described by Iribarne and Thomson, proposed that due to the high charge density on the droplet's surface, charged analytes can be directly ejected from the droplet surface at a stage prior to formation of the ultimate droplets. In either case, the emerging ions are directed into an orifice through electrostatic lenses leading to the vacuum of the mass analyzer. Because ESI involves the continuous introduction of solution, it is suitable for using as an interface with HPLC or capillary electrophoresis.

2.5.2.2 Nano-ESI

Nano-electrospray ionization (nESI) has considerably extended the usability of ESI in the analytical mass spectrometric laboratory. One of the remarkable characteristics of nESI is its extremely low sample consumption. However, nESI is not only

advantageous for reasons of sample consumption, but also for stable spraying of a variety of solvent as well as for its tolerance of elevated levels of salts or buffers.[70]

2.5.2.2.1 Triversa Nanomate System

A nESI chip-based infusion process performed by the Triversa Nanomate (Advion Biosystems, Ithaca, NY) system helps to achieve reproducible and automated lipid analysis. The Triversa Nanomate is an automated nano-electrospray ion source for mass spectrometers[71], with sampling from 96 or 384-well sample plates at user defined times. Automated sample analysis is achieved by loading a disposable, conductive pipette tip on a moveable sampling probe to engage against the back of the ESI Chip. The ESI Chip is a microarray of nESI nozzles etched in a silicon chip. The chip is fabricated from a monolithic silicon substrate using deep reactive ion etching and other standard microfabrication techniques. The inert coating on the surface allows a variety of acidic and organic compositions and concentrations to be used to promote ionization without degradation of the nozzle. NanoESI is initiated by applying gas pressure and voltage to a sample in the pipette tip. Each nozzle and tip is used only once in order to eliminate carryover and contamination typical to conventional autosamplers.

2.5.3 Mass Analyzers

With the previously described development of ionization sources that can vaporize and ionize biomolecules, it has become necessary to improve the performance

of mass analyzers, especially with respect to their speed, accuracy, and resolution. In order to be interfaced with ESI and MALDI, quadrupoles (Q), quadrupole ion traps (QIT), time-of-flight (TOF) and ion cyclotron resonance (ICR) mass analyzers have undergone numerous modifications over the past two decades. [72]

2.5.3.1 Tandem Mass Spectrometry (MS/MS or MS^n)

Besides accuracy, resolution, mass range and scan speed which are general performances of a mass analyzer that people typically focused on, MS/MS capabilities are also a crucial aspect that needs to be considered.

Typically, MS/MS experiments are performed by collision between a selected lipid ion and inert gas molecules such as argon or helium and the resulting fragments are then mass analyzed. MS/MS analysis is used to structurally elucidate lipids and other biomolecules. MS^n experiments (where $n>2$) are performed by adding additional ion isolation and reaction event steps following the initial MS/MS reaction so that sequential fragments can be analyzed.

2.5.3.2 Quadrupoles

Since ESI creates ions in a continuous stream from charged droplets under atmospheric pressure conditions, quadrupole mass analyzers are well-suited for ESI since they are both tolerant of relatively high pressure (10^{-5} torr) and they are capable of continuously scanning the ESI ion stream.

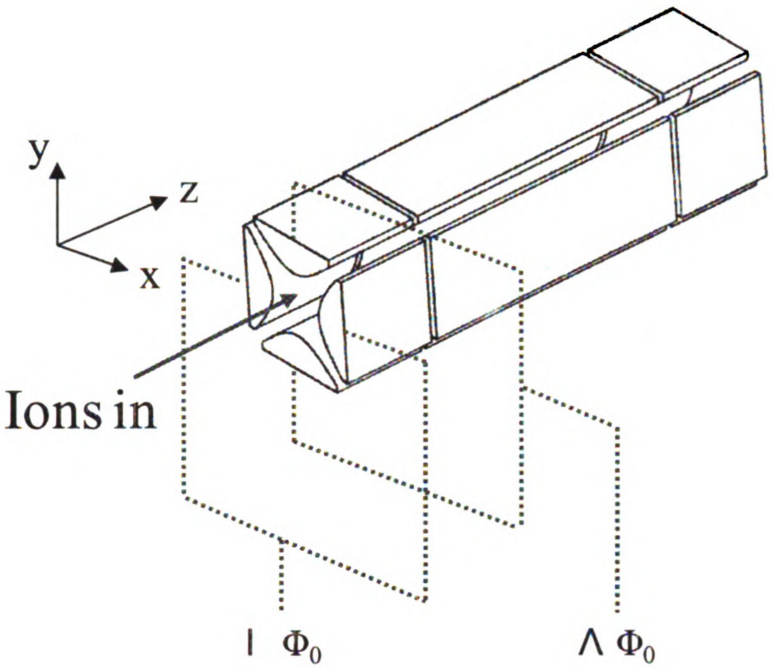

Figure 2.2 Scheme of a quadrupole mass spectrometer, showing applied potential Φ_0 as a combination of AC and DC.

The physical composition of a quadrupole mass analyzer is four hyperbolic-shaped rod electrodes assembled in parallel (Figure 2.6). The combination of an alternating current radiofrequency potential (RF) and a direct current potential (DC) are applied to the two pairs of opposite electrodes to form a quadrupole electric field. The combination of applied potentials follow equation (1) below, where U is the direct current potential, V is the maximum amplitude of the RP potential, ω is the angular frequency which can be derived from the frequency of the RF field, and t represents time.

$$\Phi_0 = +(U - V\cos\omega t) \quad \text{and} \quad -\Phi_0 = -(U - V\cos\omega t) \tag{1}$$

When ions travel through the mass analyzer along the z dimension, they experience a force induced by the electric field Φ_0 in the x and y dimensions. The x and y dimension forces are expressed in equations (2) and (3) respectively. [73]

$$Fx = m\frac{d^2x}{dt^2} = -ze\frac{\partial\Phi}{\partial x} \tag{2}$$

$$Fy = m\frac{d^2y}{dt^2} = -ze\frac{\partial\Phi}{\partial y} \tag{3}$$

Taking equation (1) into equations (2) and (3) and canceling out Φ and Φ_0 will generate equation (4) and (5).

$$\frac{d^2x}{dt^2} + \frac{2ze}{mr_0^2}(U - V\cos\omega t)x = 0 \tag{4}$$

$$\frac{d^2y}{dt^2} - \frac{2ze}{mr_0^2}(U - V\cos\omega t)y = 0 \tag{5}$$

Using u to represent either x or y in equations (4) and (5) respectively, using q_u and a_u as dimensionless parameters, and transforming these two equations into the form of the Mathieu equation, we can generate the working equations of ion motion in a quadrupole. The stability and movement of ions in the quadrupole electric field are described by the solutions of the Mathieu Equations as follows.[73]

$$a_u = a_x = -a_y = \frac{8zeU}{m\omega^2 r_0^2} \tag{7}$$

$$q_u = q_x = -q_y = \frac{4zeV}{m\omega^2 r_0^2} \tag{8}$$

Based on the solutions to these equations, an ion will only have a stable trajectory if its x and y dimension movement do not exceed r_0, the distance from the center of the quadrupole to the electrodes. Otherwise the ion will collide with an electrode and be discharged.

Equations (7) and (8) may also be rearranged as a function of RF and DC potentials.

$$U = a_u \frac{m\omega^2 r_0^2}{8ze} \tag{9}$$

$$V = q_u \frac{m\omega^2 r_0^2}{4ze} \tag{10}$$

In these equations, e is a constant, and r_0 and ω are fixed values for a given quadrupole, and U and V are experimental variables. Thus, the regions where ions of different masses have a stable trajectory through the quadrupole is obtained by plotting U as a function of V as shown in Figure 2.3 below for positively charged ions with increasing m/z values from m_1 to m_3.

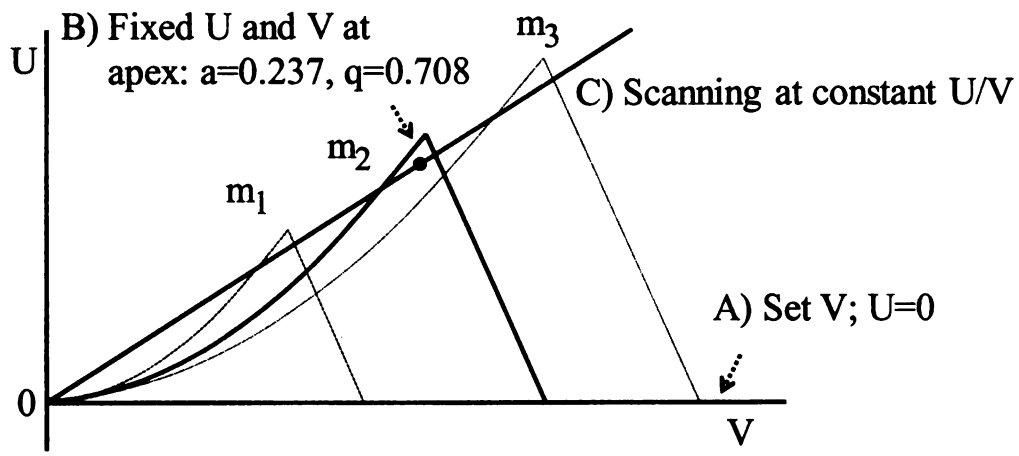

Figure 2.3 Stability diagram as a function of U and V for positively charged ions with different masses ($m_1 < m_2 < m_3$). Each ion can be observed successively by changing U linearly as a function of V while maintaining a constant ratio of U/V. (Reproduced and modified from reference [73].

Based on the stability diagram, the quadrupole can operate in three modes by applying different combinations of U and V values:

High Pass Filter

As a high pass filter for ion transmission, the quadrupole is operated by keeping V a constant value while setting U at zero. All ions with m/z higher than a value corresponding to the lowest applicable V are transmitted and ions with lower m/z become unstable and are lost.

Mass selective device

As a mass selective device, the quadrupole is operated by applying a fixed pair of U and V values which places the ion of interest at the apex of the stability diagram at a=0.237 and q=0.708. Under these conditions, only that specific ion with the desired m/z will be stably transmitted.

Mass analyzer

In this mode, the quadrupole is operated by scanning U and V while keeping the ratio of their amplitudes constant. For each pair of U and V, only one ion with a specific m/z will be stable and transmitted. By steadily scanning U and V, ions within a certain m/z range are sequentially transmitted and analyzed.

2.5.3.3 The Triple Quadrupole Mass Analyzer

The triple quadrupole mass analyzer consists of three quadrupoles (Q1, q2 and Q3) connected in series. Both Q1 and Q3 can function as mass selective devices, mass transmission devices or mass analyzers by apply different U and V voltage, while q2 has only a mass transmission function and serves as a reaction cell for the MS/MS experiment.

A simple MS experiment can be performed by setting Q1 in mass analyzer mode and transmitting ions through q2 and Q3. Different MS/MS experiments are achieved by setting Q1, q2 and Q3 at different combinations of operation modes as shown in Figure 2.4 and described below.

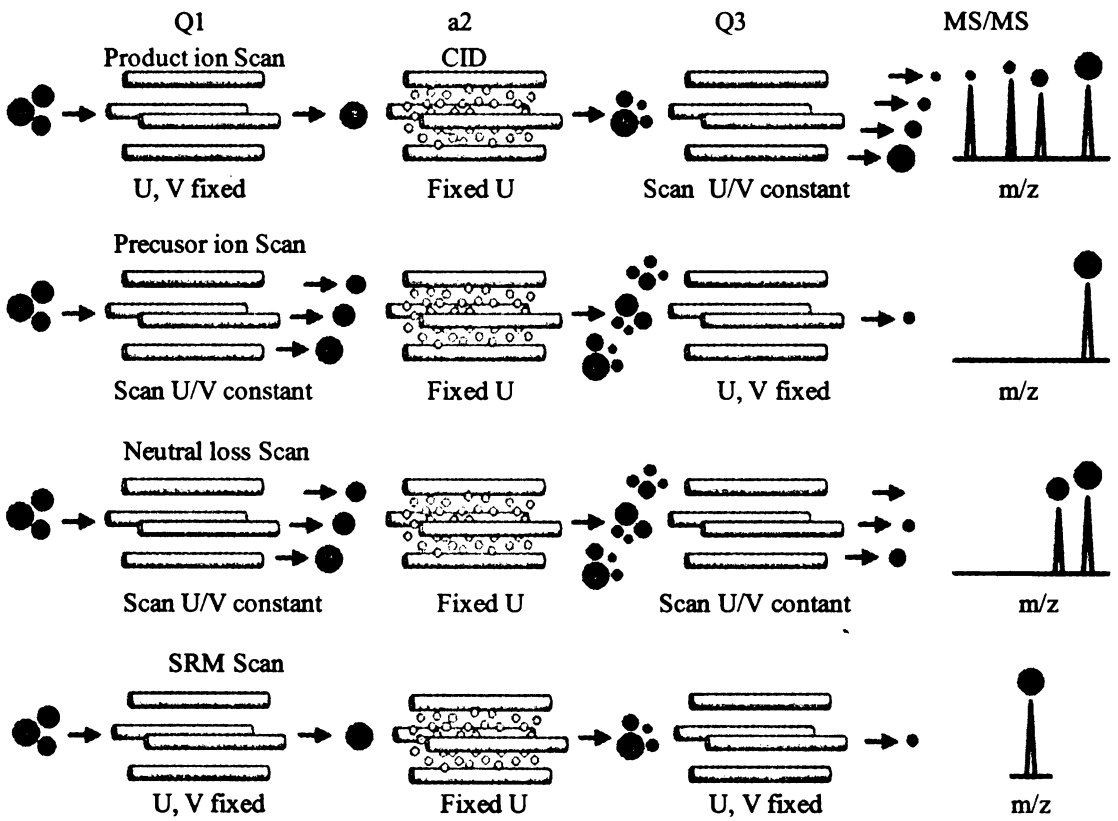

Figure 2.4 Four types of CID MS/MS scans typically applied in a triple quadrupole mass spectrometer: product ion scan, precursor ion scan , neutral loss scan and SRM scan.

The four types of MS/MS scans are product ion scan, precursor ion scan, and neutral loss scan and selected reaction monitoring. In product ion scan mode, Q1 serves as a mass selective device and a chosen U and V is applied to stabilize the specific precursor ion. This precursor ion is then been transmitted to q2 and undergoes collision-induced dissociation (CID) by colliding with Ar (typically present at 1-2 mTorr). All the fragments above a defined low mass cutoff are then transferred to Q3 which operates as a mass analyzer. By scanning U and V in Q3, all the fragment product ions are detected sequentially. In precursor ion scan mode, Q1 and Q3 perform the reverse role as for the

product ion scan. U and V in Q1 are proportionally scanned to transmit all the precursor ions while a fixed U value in Q3 allows only a specific product ion m/z to be detected. Only precursor ions that yield the defined product ion are detected. In neutral loss scan, both Q1 and Q3 act as mass analyzers and are scanned simultaneously, but with a constant difference of U and V values between them. Only precursor ions that undergo the defined neutral loss are detected. In a selected reaction monitoring (SRM) experiment, a single precursor ion is mass-selected by Q1. The selected precursor ion of interest then undergoes fragmentation in the collision cell generating product ions. A specific fragment ion of interest (normally of the highest intensity or representative of a specific structure) is then selectively transmitted by Q3.

2.5.3.4 The Quadrupole Ion Trap Mass Analyzer

The physics behind the operation of the quadrupole mass analyzer and the quadrupole ion trap mass analyzer are similar to that for the quadrupole [73]. The structure of a three-dimensional quadrupole ion trap mass analyzer is shown in Figure 2.5. The ion trap contains a hyperbolic ring electrode with an internal radius r_0 surrounding two hyperbolic end-cap electrodes each located with a distance z_0 from the center of the trap. A high voltage RF potential is applied to the ring electrode, while the end-cap electrodes are held at ground. Ions entering the trap via a small hole in the end-cap electrodes can be stably trapped, provided their initial kinetic energies are sufficiently low and their m/z is above a low mass cutoff value determined by the amplitude of the

applied RF. Introduction of helium bath gas into the system at approximately 1 mTorr can improve the overall trapping efficiency due to the effect of collisional cooling.

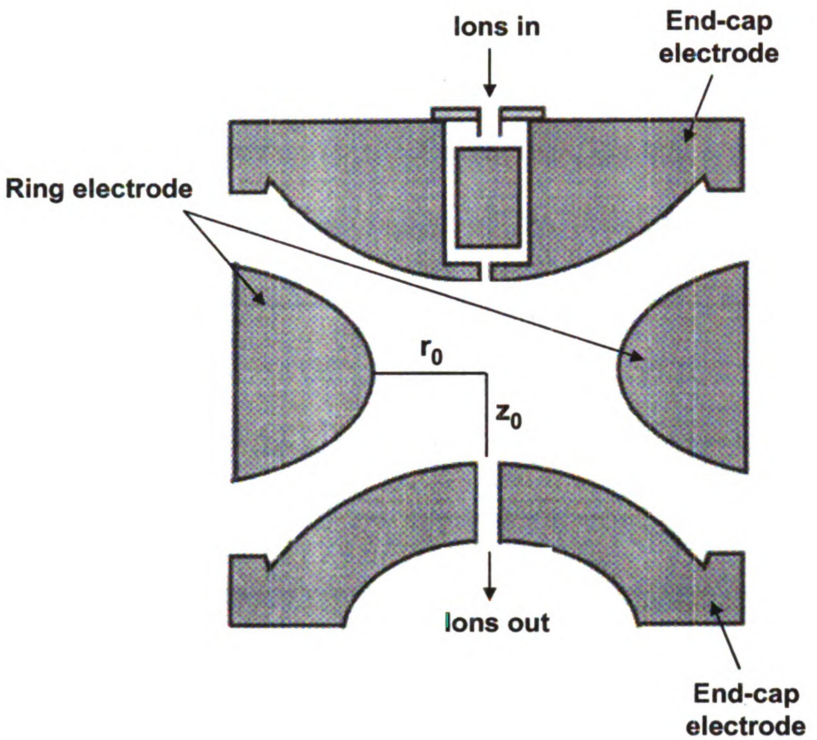

Figure 2.5 Cross-section of a three-dimensional quadrupole ion trap. (Reproduced and modified from reference [74]).

Similar to the quadrupole mass analyzer, the working equations of ion motion in the 3D quadrupole ion trap can also be expressed in the form of the Mathieu equation and are given by equations (11) and (12) below. [73] According to these equations, an ion will have a stable trajectory if the motion of the ion does not exceed z_0 and r_0 for a defined set of operating conditions (i.e., U, V and ω).

$$a_u = a_z = -2a_r = \frac{-16zeU}{m(r_0^2 + 2z_0^2)\omega^2} \tag{11}$$

$$q_u = q_z = -2q_r = \frac{8zeV}{m(r_0^2 + 2z_0^2)\omega^2} \tag{12}$$

The Mathieu stability diagram for a 3D quadrupole ion trap is presented in Figure 2.6. Ions located within the bounded region of the stability diagram have stable trajectories, while those lying outside of the bounded region have unstable trajectories. Typically a_z is equal to zero, since a DC potential (U) is not applied to the ring electrode so the ion trap is operated along the q_z axis. Based on equation (12), the m/z value of an ion is inversely proportional to q_z. Thus low m/z ions (represented by the smaller balls in Figure 2.6) have larger q_z values, while high m/z ions (represented by the larger balls) have smaller q_z values. In equation (12), the term *e* is a constant, and r_0, z_0 and ω are fixed values, therefore the q_z value of an ion with a particular m/z increases as the amplitude of the applied RF potential, V, increases. When q_z reaches a value of 0.908 (the stability limit), the ion is no longer stable and is ejected from the trap in the z_0 dimension for detection. A mass spectrum can therefore be acquired by linearly ramping V to progressively destabilize ions of increasing m/z value. This method of mass analysis is referred to as ion ejection at the stability limit.

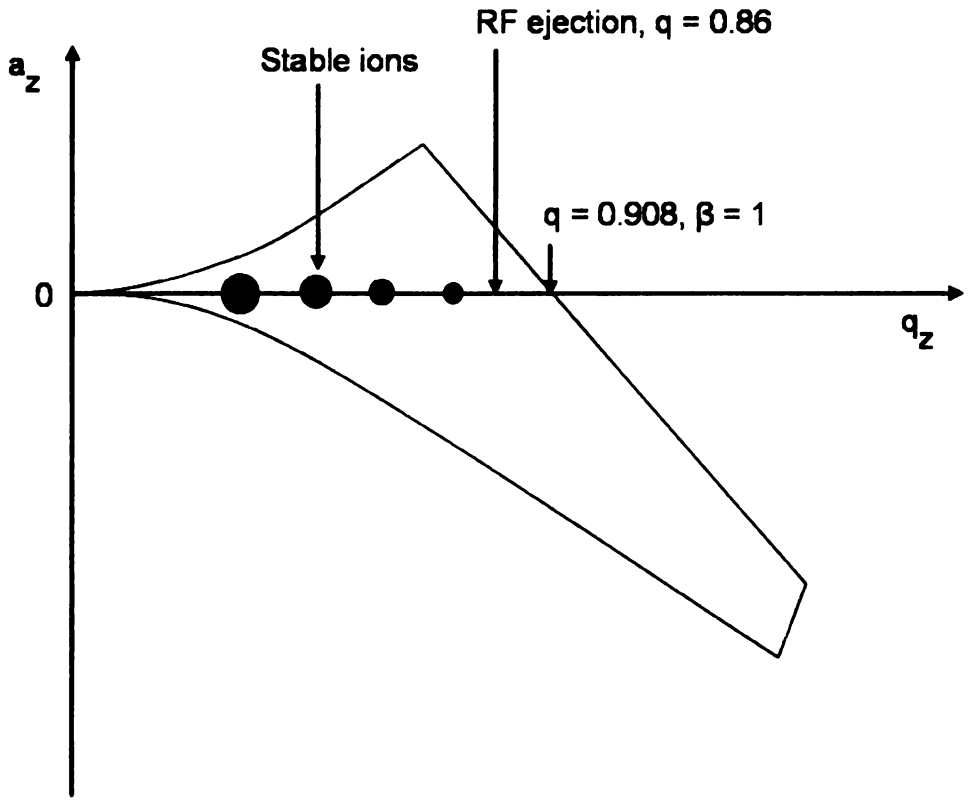

Figure 2.6 Typical Mathieu stability diagram for the quadrupole ion trap. The larger balls represent high mass ions whereas the smaller balls represent low mass ions. (Reproduced and modified from reference [74]).

However, mass analysis is typically is accomplished by resonance ejection. In this technique, a supplementary high amplitude RF potential is applied to the end-cap electrodes at a q_z lower than boundary ejection (normally 0.86 instead of 0.908). The amplitude of the RF voltage applied to the ring electrode is then linearly scanned, which causes the secular frequency at which an ion oscillates in the trap, f_z, to slowly increase. The secular frequency of an ion is not equal to the fundamental frequency, v, of the applied RF potential and, is expressed by equation (13)

$$f_z = \frac{\beta_z v}{2} \tag{13}$$

where β_z is a fundamental stability parameter and is approximated by equation (14) for q values less than 0.4.

$$\beta_z = \left[a_z + \left(\frac{q_z^2}{2} \right) \right]^{1/2} \tag{14}$$

When the secular frequency of an ion matches the frequency applied to the end-cap electrodes, the kinetic energy of the ion will increase rapidly to the point where the ion's trajectory becomes unstable and the ion is ejected. This results in higher mass resolution when compared to mass analysis via ion ejection at the stability limit.

Tandem mass spectrometry in the quadrupole ion trap is "tandem-in-time" such that more than two stages of mass selective dissociation experiment can be performed. For MS/MS, the RF voltage is adjusted and multi-frequency resonance ejection waveforms are applied to the trap to eliminate all but the desired m/z in preparation for subsequent fragmentation and mass analysis. The voltages applied to the ion trap are adjusted to stabilize the selected ions and to allow for collisional cooling in preparation for excitation. The kinetic energy of the ions is then increased by the application of a supplemental resonance excitation voltage applied to the ring electrode at the secular frequency of the ion. This increase in energy results in dissociation of the selected ions due to collisions

with the bath gas. Product ions formed above a low mass cutoff defined by the applied RF amplitude are retained in the trapping field.

Scanning the contents of the trap to produce a mass spectrum is accomplished by linearly increasing the RF voltage and utilizing a supplemental resonance ejection voltage as described above. The overall process (in terms of the applied RF potential and supplemental resonance voltage) is shown in Figure 2.7.

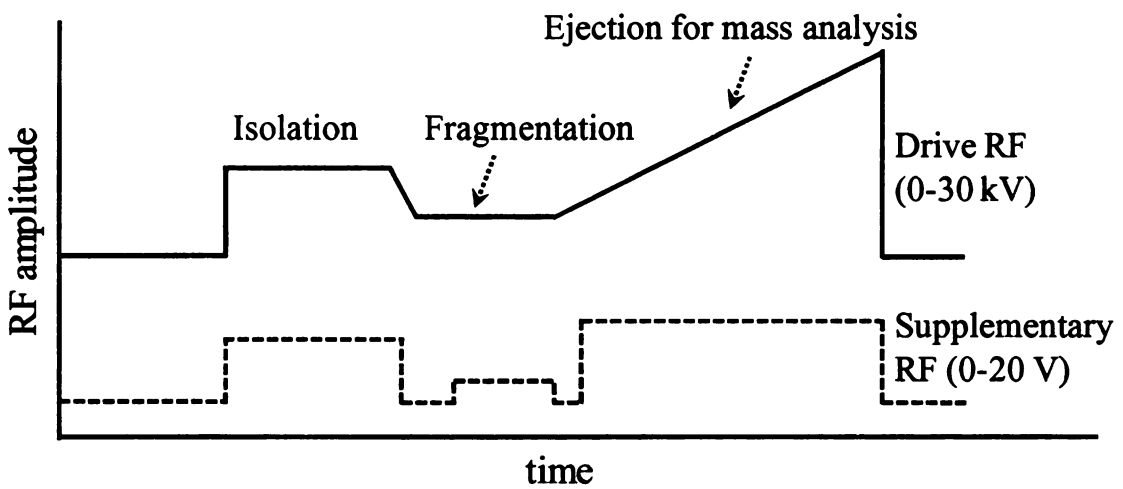

Figure 2.7 Operation modes of quadrupole ion trap as a function of the drive RF and supplementary RF amplitudes in an MS/MS example (adapted from[75]).

MS^n experiments may be performed by repeating the ion isolation and reaction event steps following the initial MS/MS process, but prior to mass analysis.

2.5.3.5 Triple Quadrupole Mass Spectrometry Analysis of Underivatized and Derivatized Aminophospholipids

All samples were centrifuged, then loaded into Whatman Multichem 96-well plates (Fisher Scientific, Pittsburgh, PA) and sealed with Teflon Ultra-Thin Sealing Tape (Analytical Sales and Services, Pompton Plains, NJ). Lipid extracts were introduced to a triple quadrupole mass spectrometer (Thermo Scientific model TSQ Quantum Ultra, San Jose, CA) via a chip-based nano-electrospray ionization (nESI) source (Advion NanoMate, Ithaca, NY) operating in infusion mode using an ESI HD_A chip, a spray voltage of 1.4 kV, a gas pressure of 0.3 psi and an air gap of 2 μL. The ion transfer tube of the mass spectrometer was maintained at 150 °C. All MS and MS/MS spectra were acquired automatically for 20 to 60 minutes at a rate of 500 m/z sec^{-1} by methods created using Xcalibur software (Thermo, San Jose, CA).[57] In MS mode, the Q1 peak width was maintained at 0.5 Da. For neutral loss and precursor ion MS/MS scans, the peak widths of both Q1 and Q3 were maintained at 0.5 Da. For product ion scan mode MS/MS experiments, Q3 was operated with peak widths of 1.0 Da. The Q2 collision gas pressure was set at 0.5 mtorr. Collision energies were individually optimized for each neutral loss, precursor ion scan mode MS/MS experiment of interest using commercially available lipid standards. Characterization of the fatty acid constituents of identified lipids was achieved by CID-MS/MS product ion scans at the specific m/z values of the $[M-H]^-$ or $[M+Ac]^-$ precursor ions of identified lipids observed in negative ion mode.[76]

2.5.3.6 Quadrupole Ion Trap Mass Spectrometry Analysis of Underivatized and Derivatized Aminophospholipids

A quadrupole ion trap mass spectrometer (Thermo, model LCQ Deca, San Jose, CA), equipped with nanoelectrospray ionization was used for further structure elucidation of derivatized lipids. Samples were filtered, centrifuged and introduced into the mass spectrometer using a syringe pump at a flow rate of 0.5 μL / min. The capillary voltage was set to 2.5 kV and capillary temperature was 150 °C. Other parameters were obtained as a result of auto tune optimization for different lipid samples. CID-MS/MS and MS^n experiments were performed using helium as the collision gas, at an activation q value of 0.25 and an activation time of 30 ms.

2.5.6 Data Processing and Sequence Conditions

Data acquisition time was determined so that equal numbers of scans were collected for each scan event either for the detection of underivatized or derivatized lipids. In lipid identification part, for example product ion scan, the number of scans acquired was within 50-150. For quantitative analysis we increased such number to up to 700.

In the lipid identification process, the mass to charge of each derivatized standard lipid was calculated by add 130 Da to the molecular mass of the underivatized lipid in positive ion mode. In negative ion mode the mass to charge of derivatized PS lipids were determined by subtract 2 from the mass to charge of each derivatized species in positive ion mode. However, since PE lipids formed acetate adduct in negative ion mode, so the mass of acetate should be added to the deprotonated derivatized PE species. Since most of the experiments were performed in triplicate, only the reproducible ions were treated as real peaks and CID-MS/MS product ion scan in both positive and negative ion mode

were used to structure elucidate not only the known lipid species but also the unknown ions.

Data analysis process was as followed. The spectra were generated as profiles. The small peak width of Q1 and Q3 was optimized to enhance the resolution so that peak height instead of peak area was reported to represent the intensity. Normalizing the spectra over the data acquisition time and generating the averaged spectra of 50-800 scans. 5-point Gaussian distribution function was applied to smooth the peaks. The intensity of each peak was reported with three significant figures.

One-way ANOVA (Graph Pad Prism version5, GraphPad Software, Inc. La Jolla, CA) followed by Turkey as a post-test was used to evaluate difference ($p<0.05$) between pooled out control and DM and TM animal groups for individual lipid molecular species. For more detailed data processing information, please refer to 3.4.6 of chapter three which will discuss standard lipid analysis and 4.3.2 of chapter four which will focus on liver lipid extract profiling.

CHAPTER THREE

DEVELOPMENT OF A NOVEL MASS SPECTROMETRY BASED CHEMICAL DERIVATIZATION METHODOLOGY FOR THE ENHANCED STRUCTURE ELUCIDATION OF AMINOPHOSPHOLIPIDS

3.1 'Fixed Charge' Sulfonium Ion Derivatization Reagents for Enhanced Mass Spectrometry and Tandem Mass Spectrometry Analysis of Biomolecules

This chapter presents a novel methodology for the MS/MS based identification of PE and PS aminophospholipids, by labeling with a 'fixed charge' sulfonium ion containing derivatization reagent, DMBNHS. The Reid laboratory has described a novel chemical derivatization strategy for peptide identification, characterization and structure elucidation involving 'fixed charged' sulfonium ion derivatization.[77-81] The introduction of this fixed charge tomethionine side chain to form sulfonium ions, followed by CID-MS/MS, results in the exclusive loss of a neutral dialkylsulfide group by selective cleavage at a site adjacent to the fixed charge and in formation of a characteristic product ions. [77-81] Such facile cleavage was proved to be an energetically favored process.[78] Compared with other fixed charged derivatization methods, for example those involving the introduction of a quaternary ammonium ion, the sulfonium ion residue is a better leaving group and therefore requires lower energy in the CID-MS/MS experiment.[78] Further structural interrogation of the modified peptide within complex mixture was achieve by MS3 in a quadrupole ion trap mass spectrometer

or by energy resolved "pseudo" MS3 in a triple quadrupole mass spectrometer. More recently the Reid Laboratory synthesized a novel 'fixed charge' sulfonium ion containing amino-group specific modification reagent-DMBNHS to couple with automated CID-MS/MS for mapping protein surface residue accessibility.[79] Such NHS ester containing reagent can readily modify amine group of the lysine residues and selectively identify modifications within each peptide by CID-MS/MS via the exclusive neutral loss of dimethylsulfide. The whole idea of stable amine tagging, facile neutral loss and further CID-MS/MS fragmentation for structure elucidation potential can be used to realize selective aminophospholipid identification from within complex.

The previously described TNBSA and Fmoc aminophospholipid labeling reagents have limitations with regards to generating quantitative information, as required for the work described in Chapter 4. They either fail to provide unbiased labeling of different lipid species, regardless of fatty acyl chain length, or are unable to achieve complete labeling. [50] As mentioned in Chapter 1, a stable-isotope-labeling strategy has recently been used to quantify aminophospholipids. [51] This N-methylpiperazine acetic acid N-hydroxysuccinimide ester labeling method is an improvement over the Fmoc-methods, but can provide limited information for reliable quantitative comparisons of lipid profiles from multiple biological samples. Moreover, the presence of interfering ions increases the difficulty to discriminate between labeled and naturally occurring lipids in very complex mixtures and requires advanced mass spectrometry methods with sufficient resolution to achieve quantitative analysis of polyunsaturated aminophospholipids.[52] This chapter will focus on the demonstration the power of 'fixed charge' sulfonium ion

containing DMBNHS tagging strategy for mass spectrometry based advance analysis of aminophospholipids.

3.2 Evaluation of the Reactivity and Specificity of Chemical Derivatization Reagents for Aminophospholipids under Organic and Aqueous Solvent Conditions

The reactivity of the different aminophospholipid labeling reagents, TNBSA, Fmoc-Cl, Fmoc-NHS and DMBNHS, were evaluated in both aqueous and organic solutions.

3.2.1 Organic Solvent Conditions

A summary of the organic solvent labeling reactivity observed for the standard PE and PS lipids is shown in Table 3.1. The labeling efficiency of the traditional reagent, TNBSA, for both PE and PS lipids was only 5% upon two hours of incubation. In contrast, the Fmoc-containing reagents reacted rapidly with the PE lipids in weakly alkaline media so that complete labeling of was achieved within 5 minutes. However, the Fmoc-containing reagents showed different reactivities when used to label PS lipids. Since chloride is a better leaving group than NHS, the Fmoc-Cl labeling reaction is much faster than the Fmoc-NHS labeling reaction (complete Fmoc-Cl derivatization of PS was completed within 10 minutes while the Fmoc-NHS derivatization required two hours and

a higher temperature). On the other hand, the specificity of Fmoc-Cl was worse than Fmoc-NHS, due to its high reactivity. Fmoc-Cl modified PS species undergo a self-catalytic methyl esterification reaction in organic solvents containing methanol.[80] This side reaction is unavoidable since methanol is a necessary component of the mass spectrometry analysis buffer solution. In contrast, when compared to these previously used reagents, the amine-specific sulfonium ion containing modification reagent DMBNHS demonstrated high reactivity and specificity for both PE and PS lipids, with the reaction proceeding to completion after 2 minutes.

Table 3.1 Summary of the reactivity of different aminophospholipid labeling reagents under aqueous and organic solvent conditions.

	TNBSA	Fmoc-Cl	Fmoc-NHS	DMBNHS
PE (organic)	2 hours, 5%	5 min, 100%	5 min, 100%	2 min, 100%
PS (organic)	2 hours, ≤ 5%	5 min, side reaction	2 hours, 90%, 37°C	2 min, 100%
PE (aq)	≤ 5% unstable	10 min, 100%	10 min, 100%	2 hours, 70%
PS (aq)	≤ 5% unstable	2 hours, side reaction100%	2 hours, 100%	2 hours, 40%

3.2.2 Aqueous Solvent Conditions

A summary of the aqueous solvent labeling reactivity observed for the standard PE and PS lipids is also shown in Table 3.1. Due to the solubility issue of lipid species in water, the rate of reaction of lipid species with labeling reagents is lower in an aqueous environment than in organic solvents. Although TNBSA was described as a hydrophilic modifying reagent which reacts readily in aqueous solution [49], the modification was found to be unstable (with only 5% labeling efficiency) and not specific. More complex adducts were generated along with those formed by reaction of primary amino groups within the lipids. Further, silica gel plate separation needs to be performed in order to isolate unmodified lipids from modified lipids. [49] This complicated preparation process may alter the initial lipid extraction profile from biological samples. Compared to TNBSA, use of the Fmoc-containing reactions was more specific, but the side reaction involving methyl esterification of PS lipids when using the Fmoc-Cl reagent was again observed. In contrast, the DMBNHS reagent resulted in relatively high labeling efficiency (70% for PE species and 40% for PS species) and specificity in water as they did in the organic solvent environment. Although complete labeling was hard to achieve under the current conditions, the final aim of the aqueous labeling reaction is to tag aminophospholipids on the outer layer of cell membranes, without affecting the inner cell membrane lipids. Given that the structure of the outer leaflet of the membrane has the head groups of different lipids organized towards the extracellular or extravesicular environment, the exposure of the amino moieties of lipid head groups allows them to be more readily tagged by the labeling reagents than in the extracellular aqueous environment. Thus, we expect that higher labeling efficiency and reactivity could be achieved when this method is applied to real cells or vesicles.

The previously described TNBSA and Fmoc labeling reagents have limitations with regards to generating quantitative information. They either fail to provide unbiased labeling of different lipid species regardless of fatty acyl chain length or are unable to achieve complete labeling. As mentioned in Chapter 1, a stable-isotope-labeling strategy has recently been used to quantify aminophospholipids. This N-methylpiperazine acetic acid N-hydroxysuccinimide ester labeling method is an improvement over the prior methods, but still provides limited information for reliable quantitative comparisons of lipid profiles from multiple biological samples. The high collision energy that is needed causes poor ion yield/transmission and loss of signal to noise. Moreover, the presence of interfering ions increases the difficulty to discriminate between labeled and naturally occurring lipids in very complex mixtures and requires advanced mass spectrometry methods with sufficient resolution to achieve quantitative analysis of polyunsaturated aminophospholipids.

The use of a sulfonium ion containing isotope labeled derivatization reagent as an alternative (see Chapter 4) favors the quantitative analysis of aminophospholipids. From a reaction process point of view, only a low molar excess of labeling reagent is needed and the weakly basic reaction environment enables the rapid modification and maintenance of original lipid profiles.

3.3 Negative Ion Mode Mass Spectrometry Analysis of Fmoc-Cl and Fmoc-NHS Derivatized Aminophospholipids

Due to their relative lack of reactivity, as well as the inability to readily incorporate isotope labels for later quantitative analysis, the TNBSA reagents were not examined further in this study. However, a further assessment of the ESI-MS sensitivity and MS/MS fragmentation behavior of the Fmoc-labeled PE and PS aminophospholipids was carried out, as described below.

3.3.1 Negative Ion Mode ESI-MS Analysis of Underivatized and Fmoc-Derivatized Deprotonated Aminophospholipids

When a standard lipid mixture (containing four PE species and two PS species with different fatty acid chain lengths and number of double bonds) was incubated with either Fmoc-Cl (Figure 3.1) or Fmoc-NHS (Figure 3.2) using the optimized organic solvent reaction conditions described in Chapter 2, the negative ion ESI mass spectra demonstrated altered ion profiles compared to the mass spectra from the underivatized lipids. After derivatization, an Fmoc moiety covalently bound to the head-group amines of both the PE and PS species resulted in a mass shift of 222 Da. It should be pointed out that ions corresponding to the Fmoc-derivatized lipids containing short acyl chains showed a slightly higher instrument response than those containing long acyl chains. This may due to differential in-source fragmentation or facile loss of the Fmoc moiety from Fmoc-derivatized lipids.[50] A significant difference was observed between the Fmoc-Cl and Fmoc-NHS reactions for the PS lipids. Fmoc-Cl derivatized PS lipids showed the expected 222 Da mass shift. However, additional ions corresponding to a further shift of 14 Da due to methyl esterification of the carboxylic acid within the serine headgroup

were observed (Figure 3.1, panel B). These additional ions were not observed by reaction with the Fmoc-NHS reagent (Figure 3.2, panel B).

Although PE lipids are typically detected with the greatest MS sensitivity as their protonated ions in positive ion mode, Fmoc derivatization decreases the proton affinity of the amino head group and thereby increases the ability to observe a deprotonated PE ion in negative ion mode. In comparison with the underivatized PE species by using peak intensities, an approximately 10-fold improvement in the negative ion mode ESI-MS sensitivity was achieved by using the Fmoc-containing reagent derivatization reactions (Figure 3.3). Unlike the PE species however, PS lipids are more acidic and are therefore typically analyzed with the greatest sensitivity in negative ion mode. Therefore, an overall loss of sensitivity was observed for the Fmoc-labelled PS lipids. This was further exacerbated for the Fmoc-Cl derivatized PS lipids, due to the self-catalyzed esterification by-product. Notice that the MS spectrum of Fmoc-Cl derivatization was acquired at high resolution (Figure 3.1) while that for the Fmoc-NHS derivatization was acquired at low resolution (Figure 3.2), so the MS spectra of the underivatized lipid mixtures were normalized to realize a direct comparison between them.

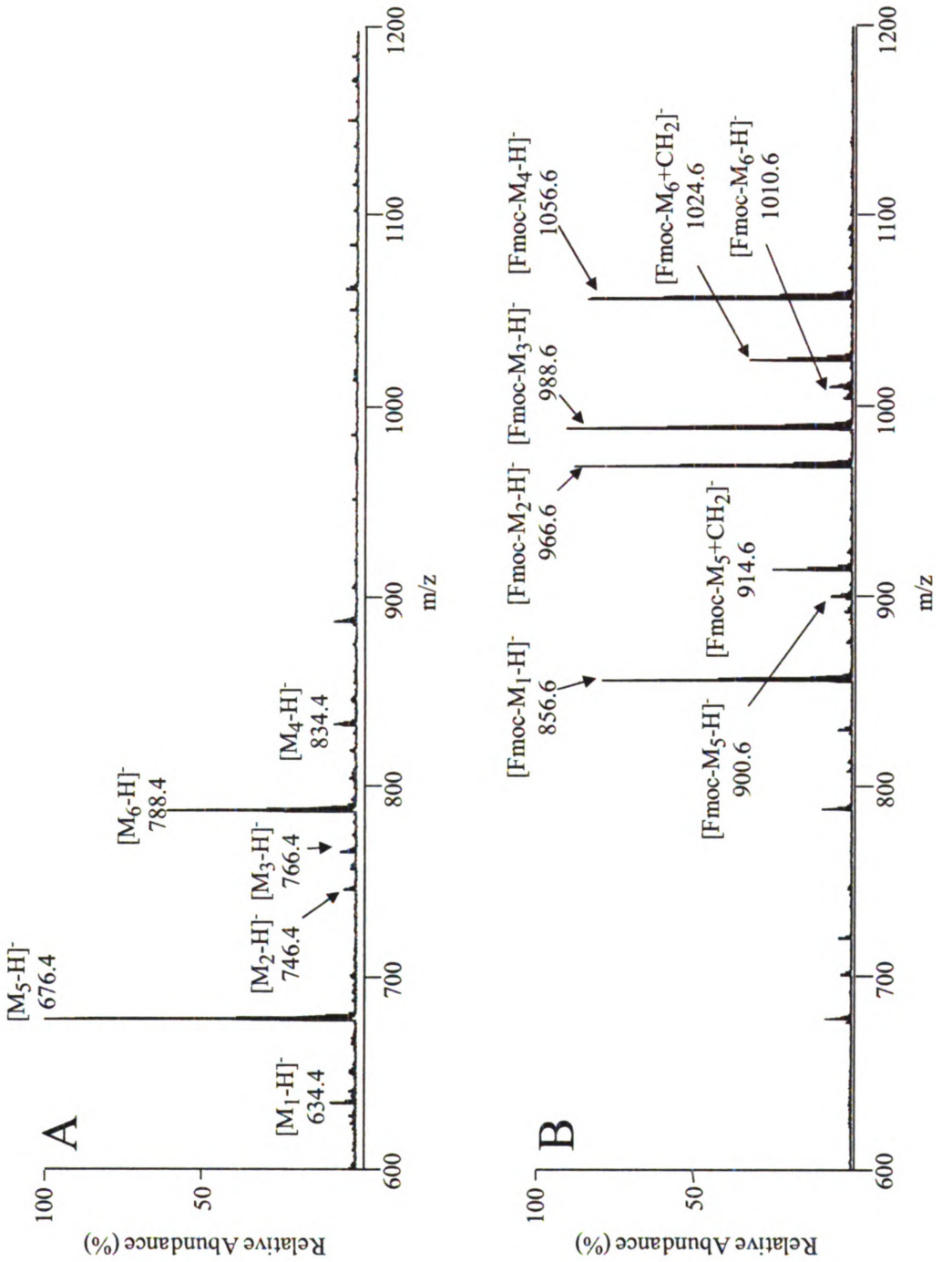

Figure 3.1 Negative ion mode nESI triple quadrupole MS analysis of underivatized (panel A) and Fmoc-Cl derivatized (panel B) PE and PS aminophospholipids. M_1 = PE (14:0/14:0), M_2 = PE (18:0/18:0), M_3 = PE (18:0/20:4), M_4 = PE (22:6/22:6), M_5 = PS (14:0/14:0), M_6 = PS (18:0/18:1).

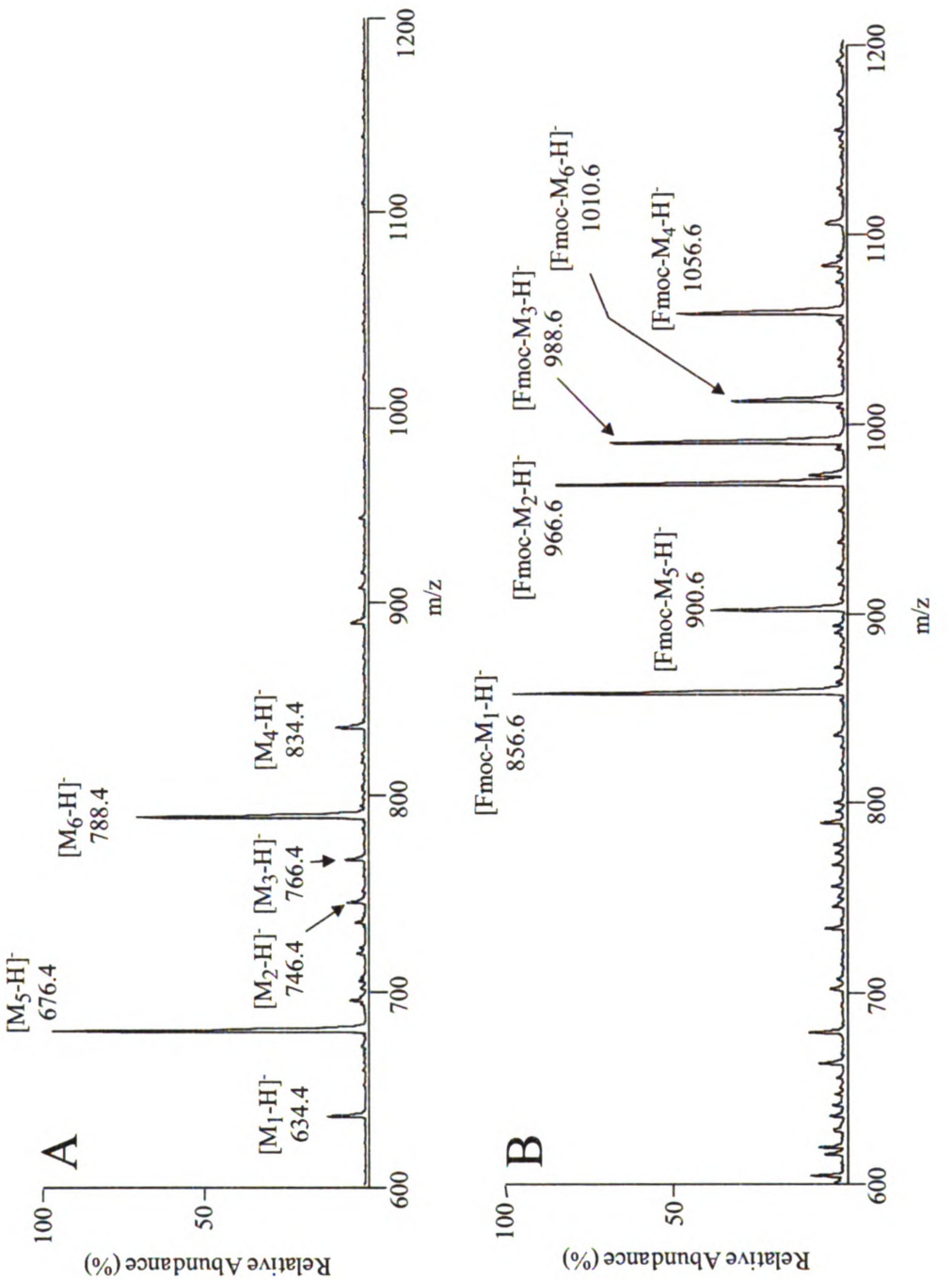

Figure 3.2 Negative ion mode nESI triple quadrupole MS analysis of underivatized (panel A) and Fmoc-NHS derivatized (panel B) PE and PS aminophospholipids. M_1 = PE $_{(14:0/14:0)}$, M_2 = PE $_{(18:0/18:0)}$, M_3 = PE $_{(18:0/20:4)}$, M_4 = PE $_{(22:6/22:6)}$, M_5 = PS $_{(14:0/14:0)}$, M_6 = PS $_{(18:0/18:1)}$.

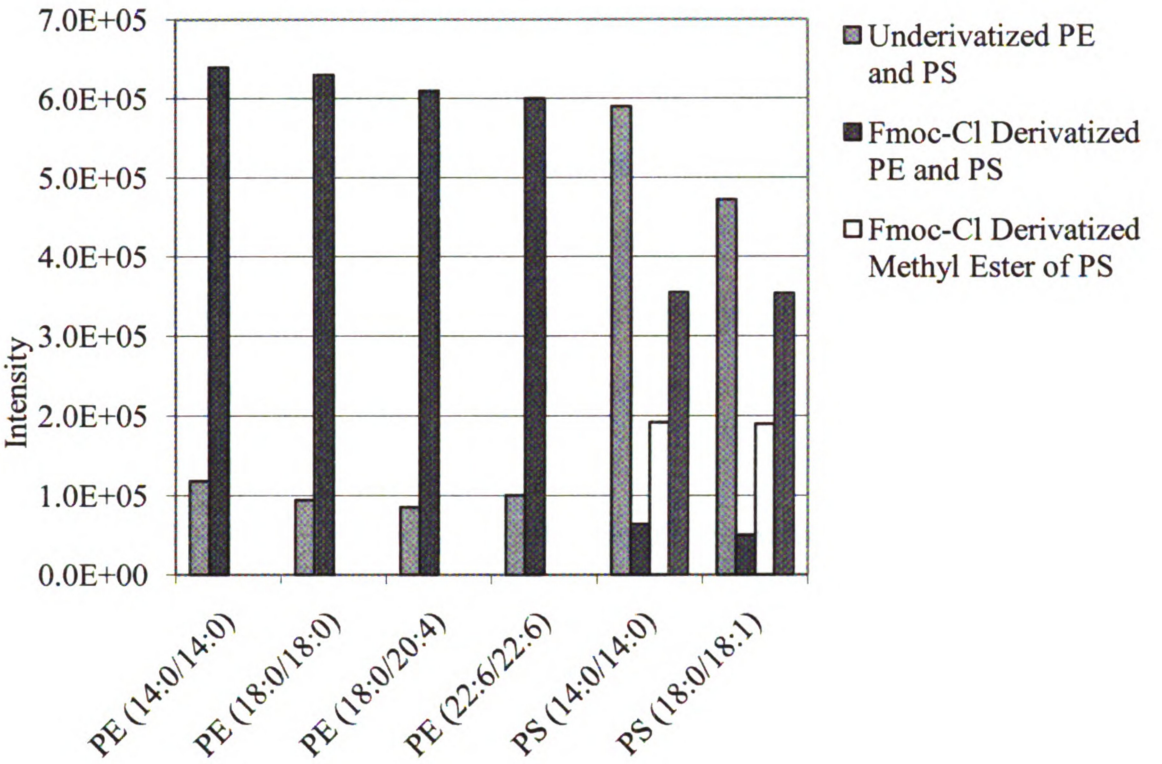

Figure 3.3 Negative ion mode ESI-MS sensitivity of underivatized, Fmoc-Cl and Fmoc NHS derivatized PE and PS aminophospholipids. Comparison was generated based on the intensity of monoisotopic $[M-H]^-$ peak or the methylester ions.

3.3.2 Negative Ion Mode CID-MS/MS Analysis of Underivatized Deprotonated Aminophospholipids

In negative ion mode CID-MS/MS, the $[M-H]^-$ product ion spectra of underivatized PE species mainly gives fatty acyl composition information in the form of fatty acid anions which are douminant product ions. (Figure 3.4A) Cleavage of the carbon-oxygen bonds of both sn1 and sn2 positions result in two main fragmentation pathways and generate two major product ions which correspond to the two fatty acyl chains (Scheme 3.1). Since cleavage at the sn2 position (pathway C2 in Scheme 3.1)

produces a 5-membered-ring neutral species, while cleavage at the sn1 position (pathway C1 in Scheme 3.1) generates a 6-membered-ring neutral species, C2 cleavage is kinetically favored [42], so the sn2 fatty acyl carboxylate is observed at higher relative abundance. For example, in Figure 3.3 the relative intensity of the m/z 281 ion corresponding to the 18:1 fatty acyl carboxylate from the C2 fragmentation is approx. 2 fold higher than that of the m/z 283 ion corresponding to the 18:0 fatty acyl carboxylate from C1 fragmentation.

The CID-MS/MS fragmentation behavior of underivatized PS species in negative ion mode is more complicated than for the PE species (Figure 3.4B, Scheme 3.2). Besides fatty acyl chain cleavage, neutral loss of 87 Da from the head group is observed, along with product ions corresponding to lysoPS species and dehydrated lyso PS species as a result of facile loss of neutral fatty acid and ketene groups, respectively.

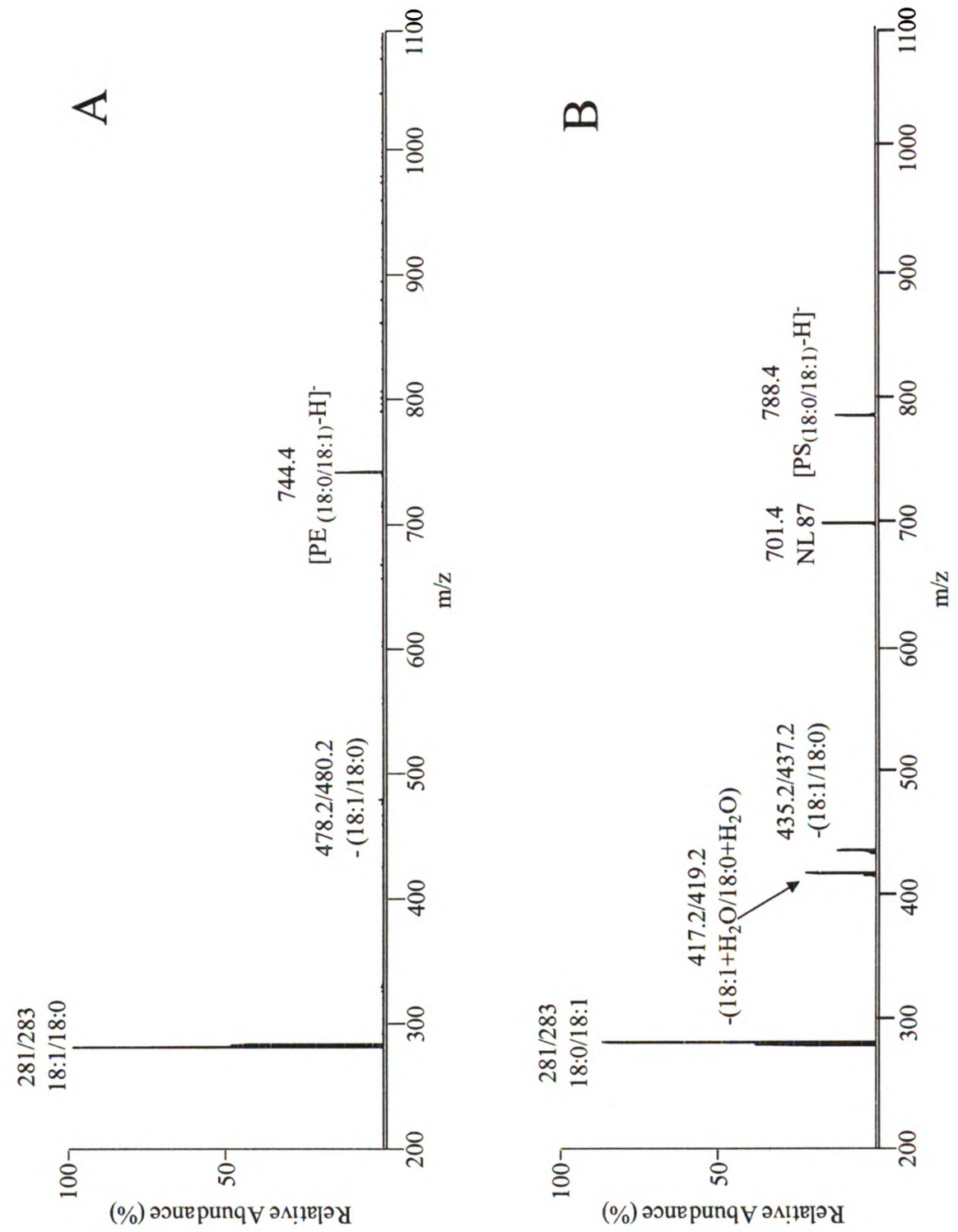

Figure 3.4 Negative ion mode nESI triple quadrupole CID MS/MS product ion spectra of the $[M-H]^-$ precursor ions of PE $_{(18:0/18:1)}$ (panel A) and PS $_{(18:0/18:1)}$ (panel B) aminophospholipids.

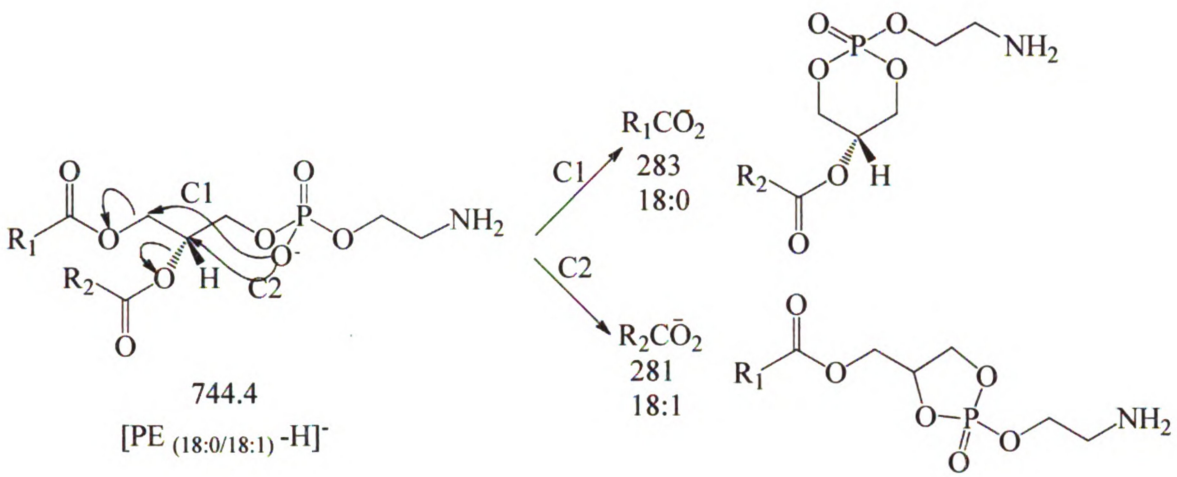

Scheme 3.1 Proposed negative ion mode CID-MS/MS fragmentation mechanisms for an underivatized deprotonated PE $_{(18:0/18:1)}$ aminophospholipid [42].

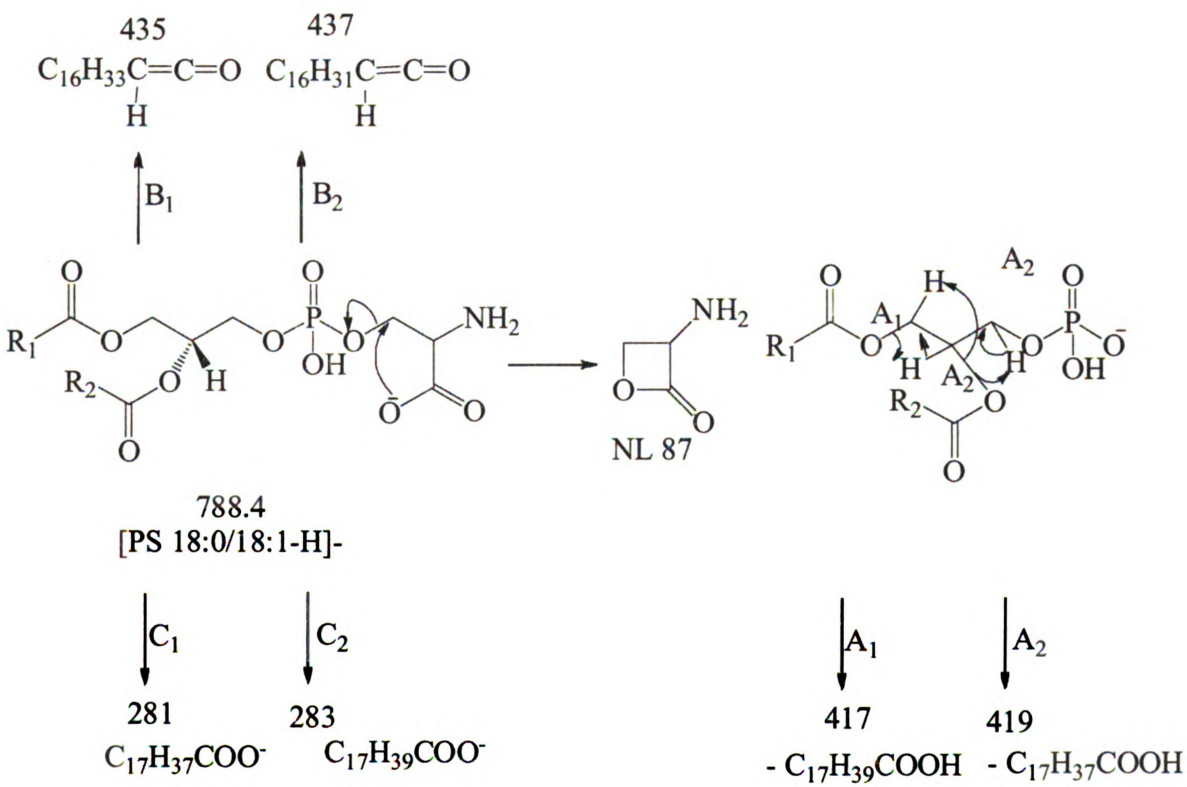

Scheme 3.2 Proposed negative ion mode CID-MS/MS fragmentation mechanisms for an underivatized deprotonated PS $_{(18:0/18:1)}$ aminophospholipid [44].

3.3.3 Negative Ion Mode CID-MS/MS Analysis of Fmoc-Derivatized Deprotonated Aminophospholipids

CID-MS/MS product ion spectra of the deprotonated Fmoc-PE and Fmoc-PS species displayed two types of fragments (Figure 3.5). The first corresponds to the neutral loss of 222.2 Da (the Fmoc moiety) from the selected precursor ion, resulting in formation of a deprotonated PE or PS product ion (Schemes 3.3 and 3.4). The second types of product ions are the same as those formed from the underivatized PE and PS lipids as described above. Thus, the fragmentation patterns of Fmoc-PE and Fmoc-PS are very similar to underivatized PE and PS lipids, albeit preceeded by the NL of 222.2 Da.

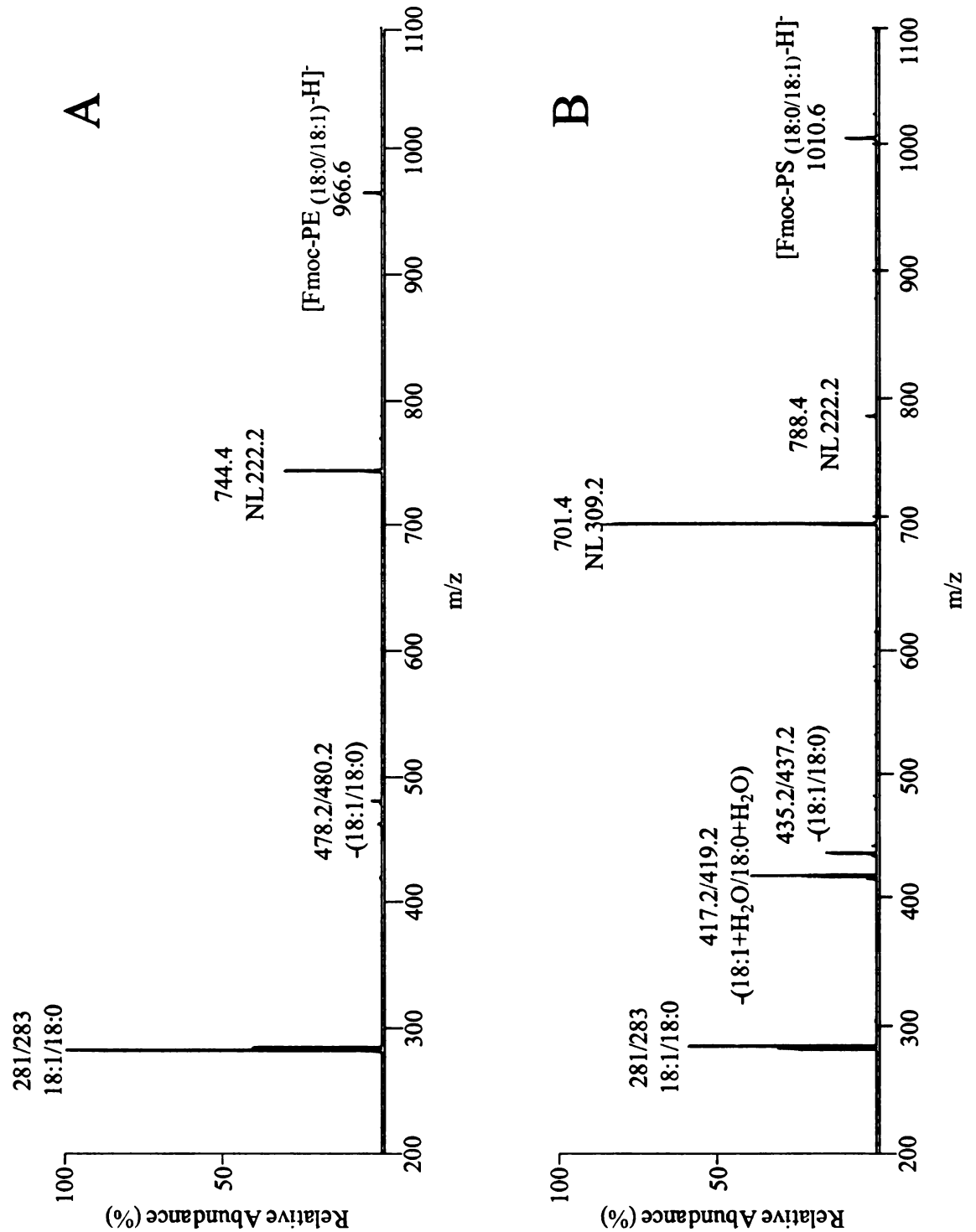

Figure 3.5 Negative ion mode nESI triple quadrupole CID MS/MS product ion spectra of the deprotonated precursor ions of Fmoc-NHS derivatized PE $_{(18:0/18:1)}$ and PS $_{(18:0/18:1)}$ aminophospholipids.

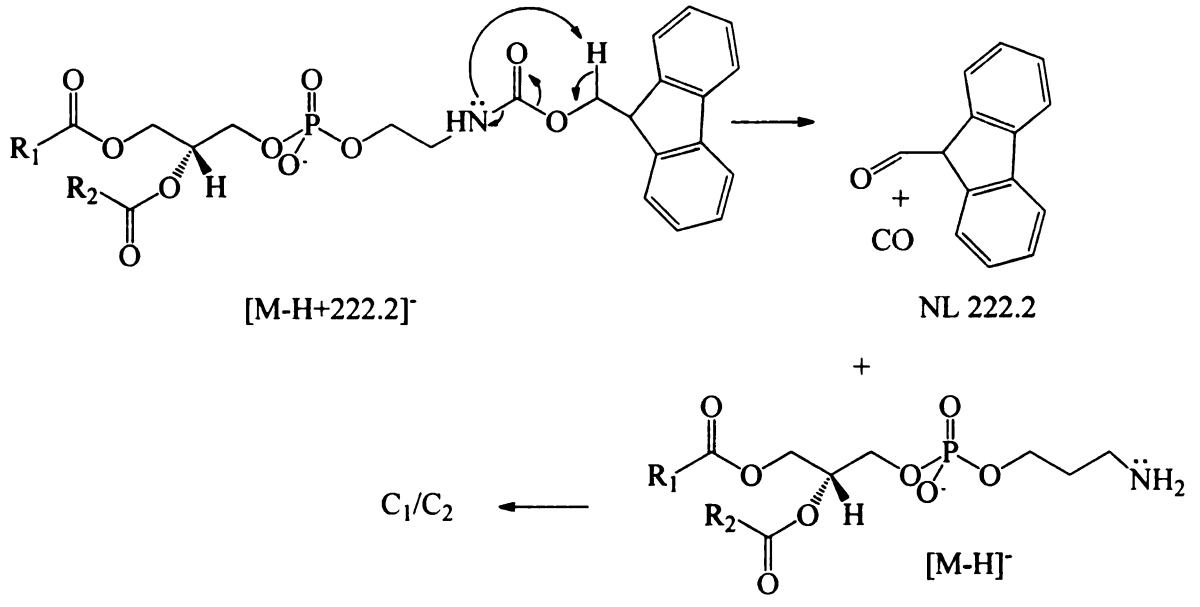

Scheme 3.3 Proposed negative ion mode fragmentation mechanisms for Fmoc-NHS derivatized PE lipids.

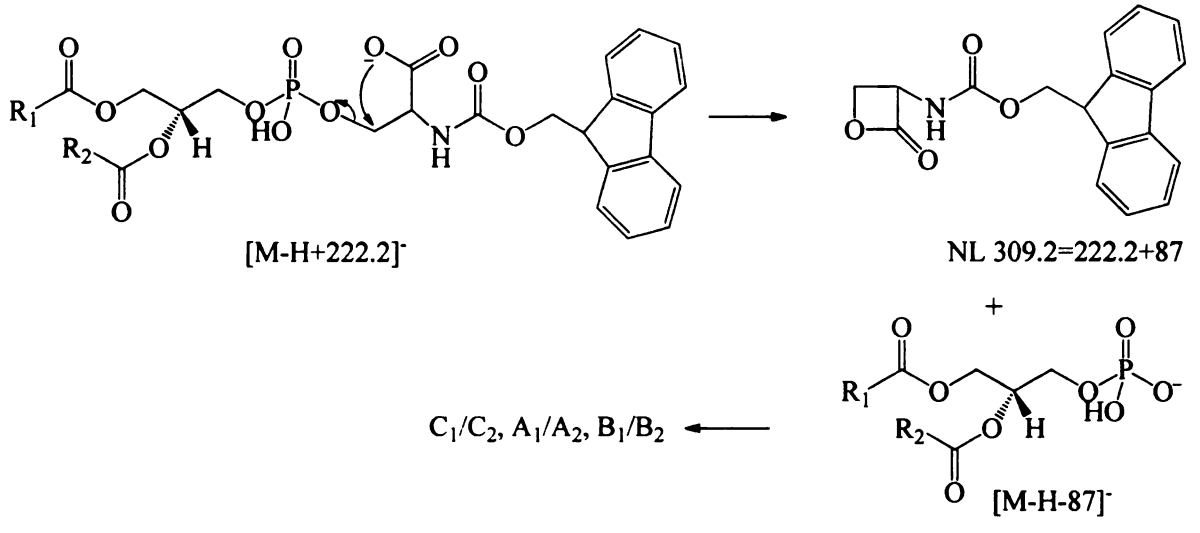

Scheme 3.4 Proposed negative ion mode fragmentation mechanism for Fmoc-NHS derivatized PS lipids.

3.4 Positive Ion Mode Mass Spectrometry Analysis of DMBNHS Derivatized Aminophospholipids

3.4.1 Positive Ion Mode ESI-MS Analysis of Underivatized and DMBNHS-Derivatized Aminophospholipids

Similar to the other reagents, an advantage of DMBNHS labelling is that such chemical derivatization shifts the m/z of the aminophospholipids out of the region where they potentially overlap with other lipid species. In positive ion mode MS, all six standard PE and PS lipids were observed to undergo a shift of 130 Da, as expected. (Figure 3.6) The instrument response of DMBNHS-derivatized short-acyl-chain lipid species was slightly higher than that of long-acyl-chain lipid species, similar to the results from the Fmoc-Cl and Fmoc-NHS derivatization reaction.

Incorporating a positively fixed charged functional group to aminophospholipids was observed to improve their positive-ion mode ESI-MS detection sensitivity by approx. 2-fold. (Figure 3.7). Importantly, this ionization enhancement was universal for both PE and PS species. Also, DMB-PE and DMB-PS were the only products that are generated due to the specificity of the labeling process.

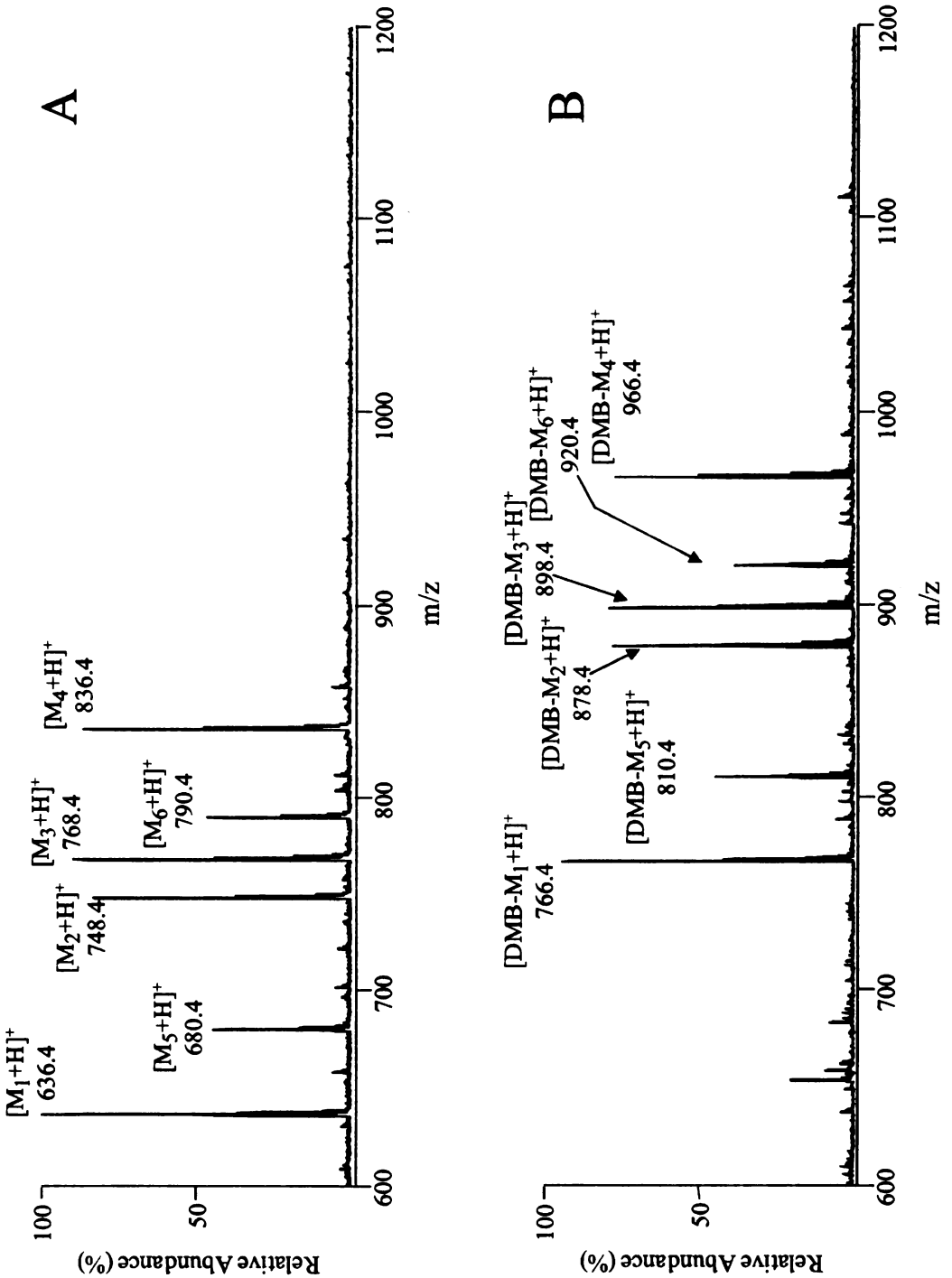

Figure 3.6 Positive ion mode nESI triple quadrupole MS analysis of underivatized (panel A) and DMBNHS derivatized (panel B) PE and PS aminophospholipids. M_1 = PE (14:0/14:0), M_2 = PE (18:0/18:0), M_3 = PE (18:0/20:4), M_4 = PE (22:6/22:6), M_5 = PS (14:0/14:0), M_6 = PS (18:0/18:1).

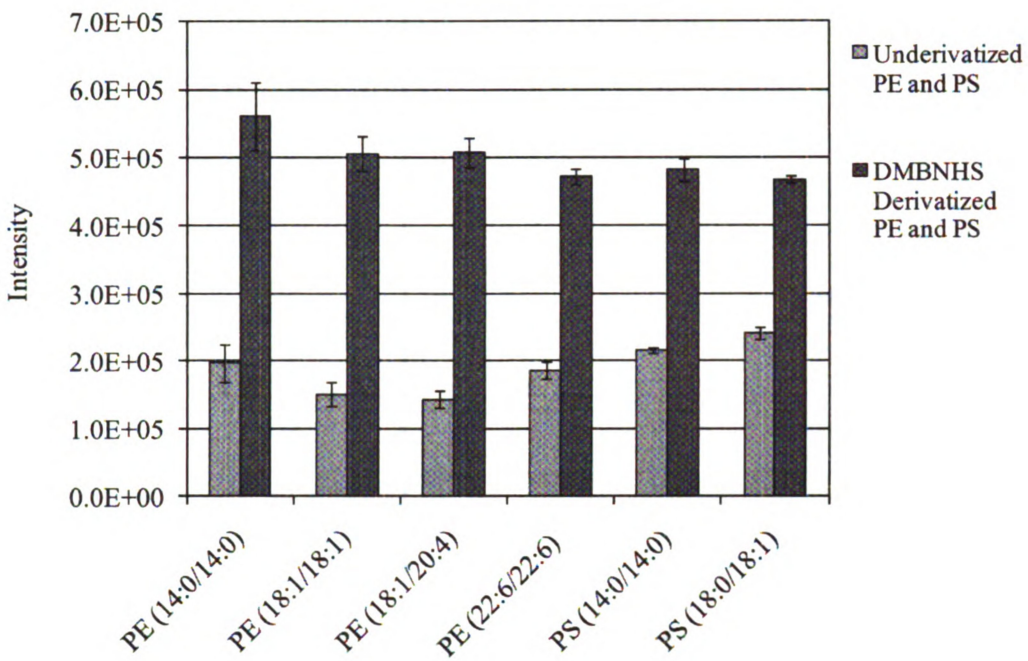

Figure 3.7 Summary of the positive ion mode ESI-MS sensitivity of underivatized and DMBNHS derivatized PE and PS aminophospholipids.

3.4.2 Positive Ion Mode CID-MS/MS Analysis of Underivatized Protonated Aminophospholipids

In positive ion mode CID-MS/MS, the protonated precursor ions from underivatized PE and PS lipids undergo exclusive dissociation at 10-35eV collision energy via the simple neutral loss of phosphoethanolamine (141 Da) (Scheme 3.5) or phosphoserine (185 Da) (Scheme 3.6) from their respective head groups (Figure 3.8A and B, respectively).

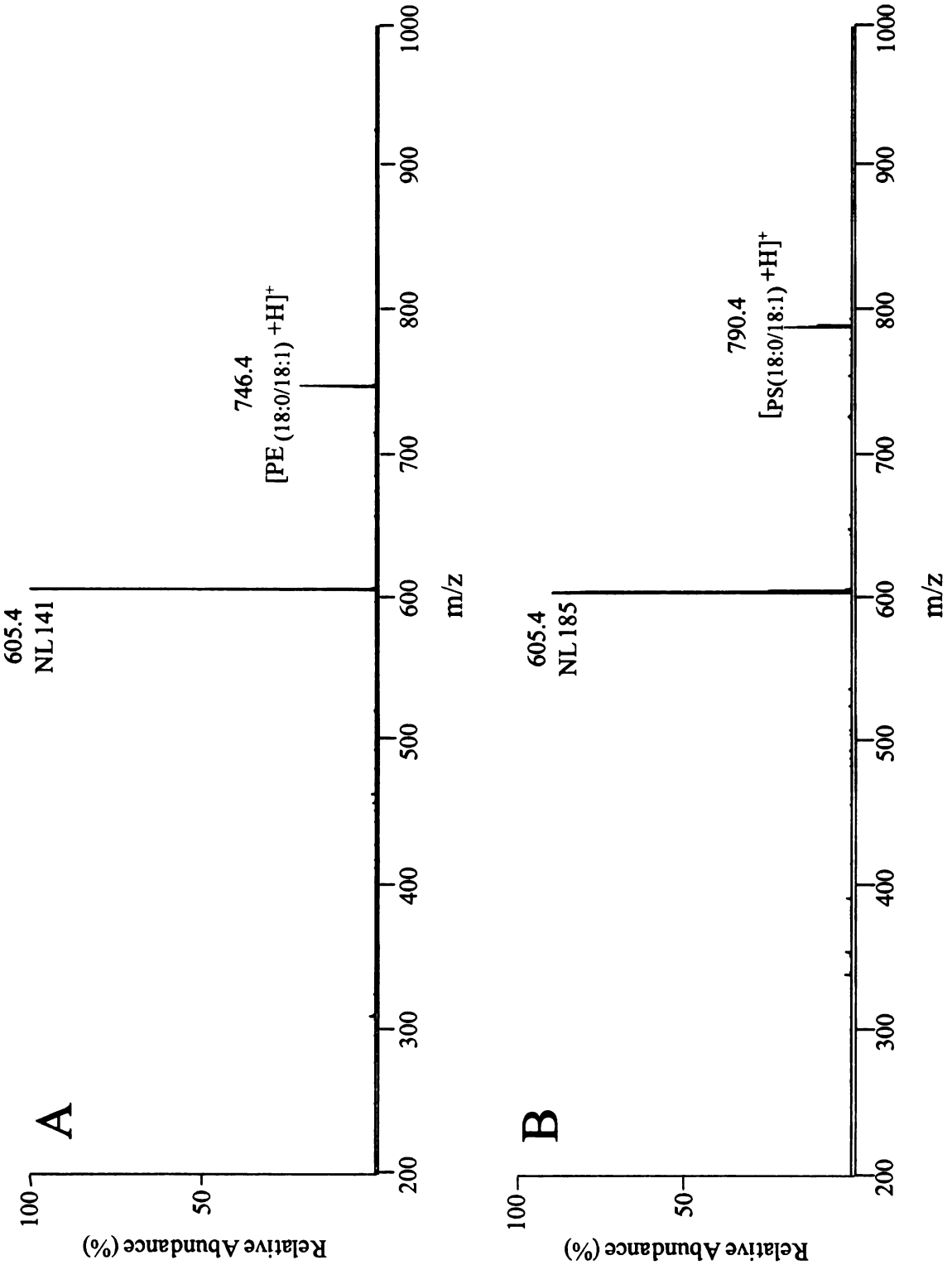

Figure 3.8 Positive ion mode nESI triple quadrupole CID MS/MS product ion spectra of the protonated precursor ions of PE $_{(18:0/18:1)}$ and PS $_{(18:0/18:1)}$ aminophospholipids.

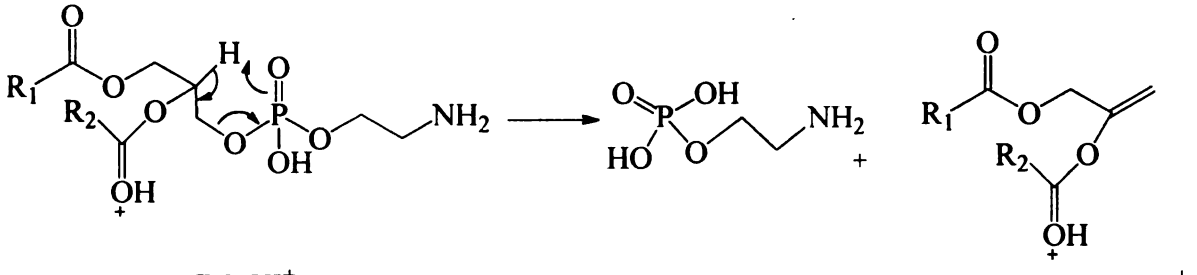

$[M+H]^+$
746.4

NL 141

$[M+H-141]^+$
605.4

Scheme 3.5 Proposed positive ion mode CID-MS/MS fragmentation mechanism for underivatized protonated $PE_{(18:0/18:1)}$ [81].

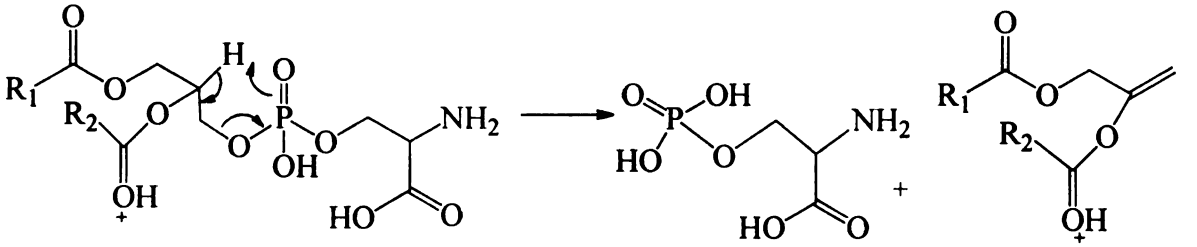

$[M+H]^+$
790.4

NL 185

$[M+H-185]^+$
605.4

Scheme 3.6 Proposed positive ion mode CID-MS/MS fragmentation mechanism for underivatized protonated $PS_{(18:0/18:1)}$ [81].

3.4.3 Positive Ion Mode CID-MS/MS Analysis of DMBNHS-Derivatized Aminophospholipids

The sulfonium ion moiety of DMBNHS not only enhances the ionization efficiency of aminophospholipids but also serves as a facile leaving group to enable the neutral loss of dimethylsulfide (62 Da) upon CID-MS/MS. The loss of 62 Da is a

common primary fragmentation channel for both PE and PS aminophopholipids under both triple quadrupole and ion trap CID-MS/MS conditions (see Figure 3.9 and Figure 3.10, respectively). Other product ions correspond to the sequential loss of an additional 209 Da for the PE lipids (for a total neutral loss of 271 Da) and the sequential loss of an additional 253 Da for the PS lipids (for a total neutral loss of 318 Da) (see Figure 3.9 (triple quadrupole CID-MS/MS) and Figure 3.11 (ion trap CID-MS^3), respectively), via cleavage between the sn3 carbon and the oxygen of the phosphate group. This secondary cleavage is analogous to the losses of 141 and 185 Da from the underivatized PE and PS lipids, as described above in Figure 3.8. Product ions at m/z 210 and 254 were also observed in the spectra of the PE and PS lipids, respectively. Proposed mechanisms for the formation of each of these ions are shown in Schemes 3.7 and 3.8. Due to the expected higher proton affinity of the PE head group derived product formed via the sequential neutral loss of 209 Da from the $[M-62]^+$ ion, compared to that for the PS derived head group formed from the neutral loss of 253 Da from its respective $[M-62]^+$ ion, the relative abundance of the PE specific m/z 210 product ion (formed via an intermolecular proton transfer reaction as shown in Scheme 3.7) is higher than that of the PS specific m/z 254 product ion.

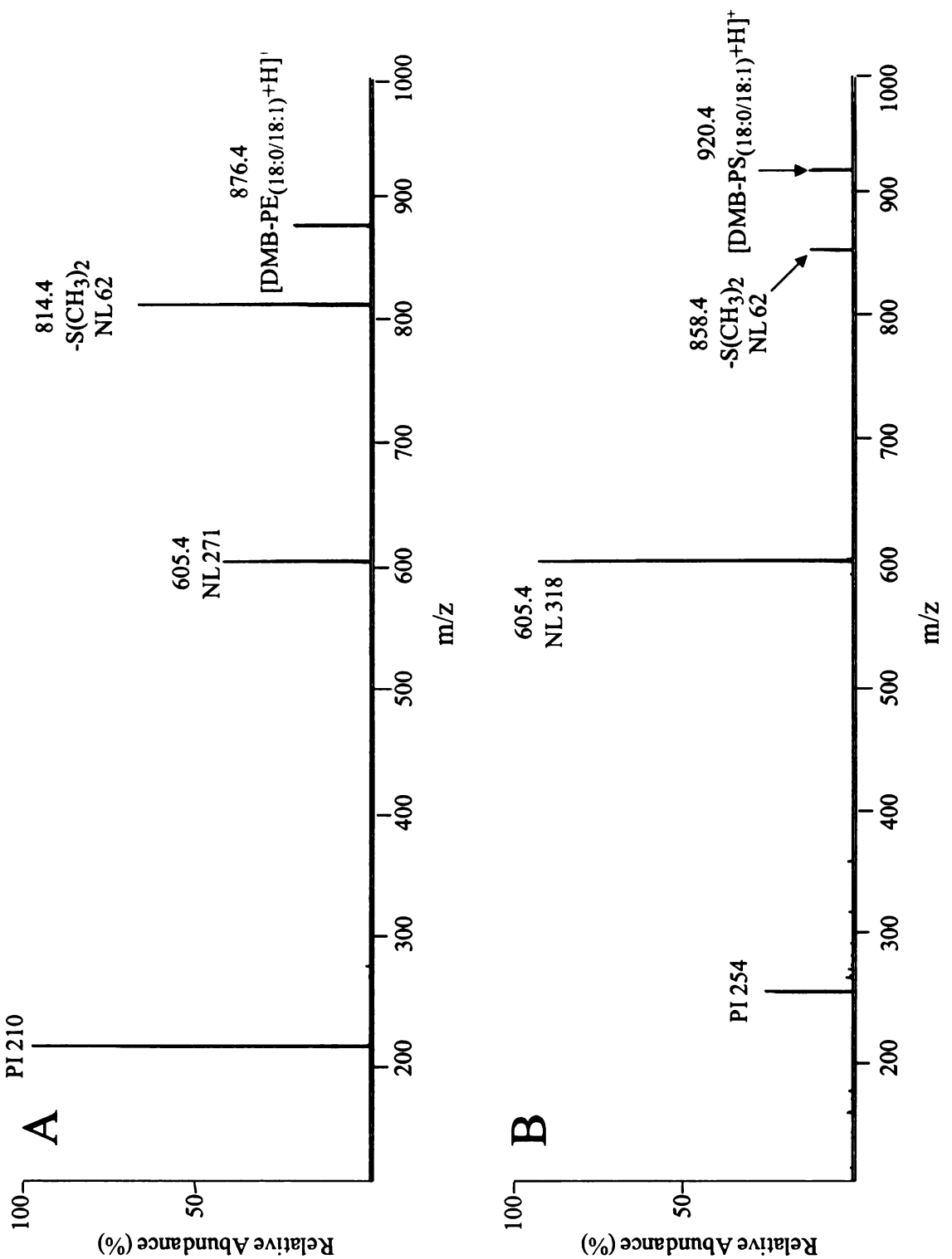

Figure 3.9 Positive ion mode nESI triple quadrupole CID MS/MS product ion spectra of DMBNHS derivatized PE $_{(18:0/18:1)}$ (panel A) and PS $_{(18:0/18:1)}$ (panel B).

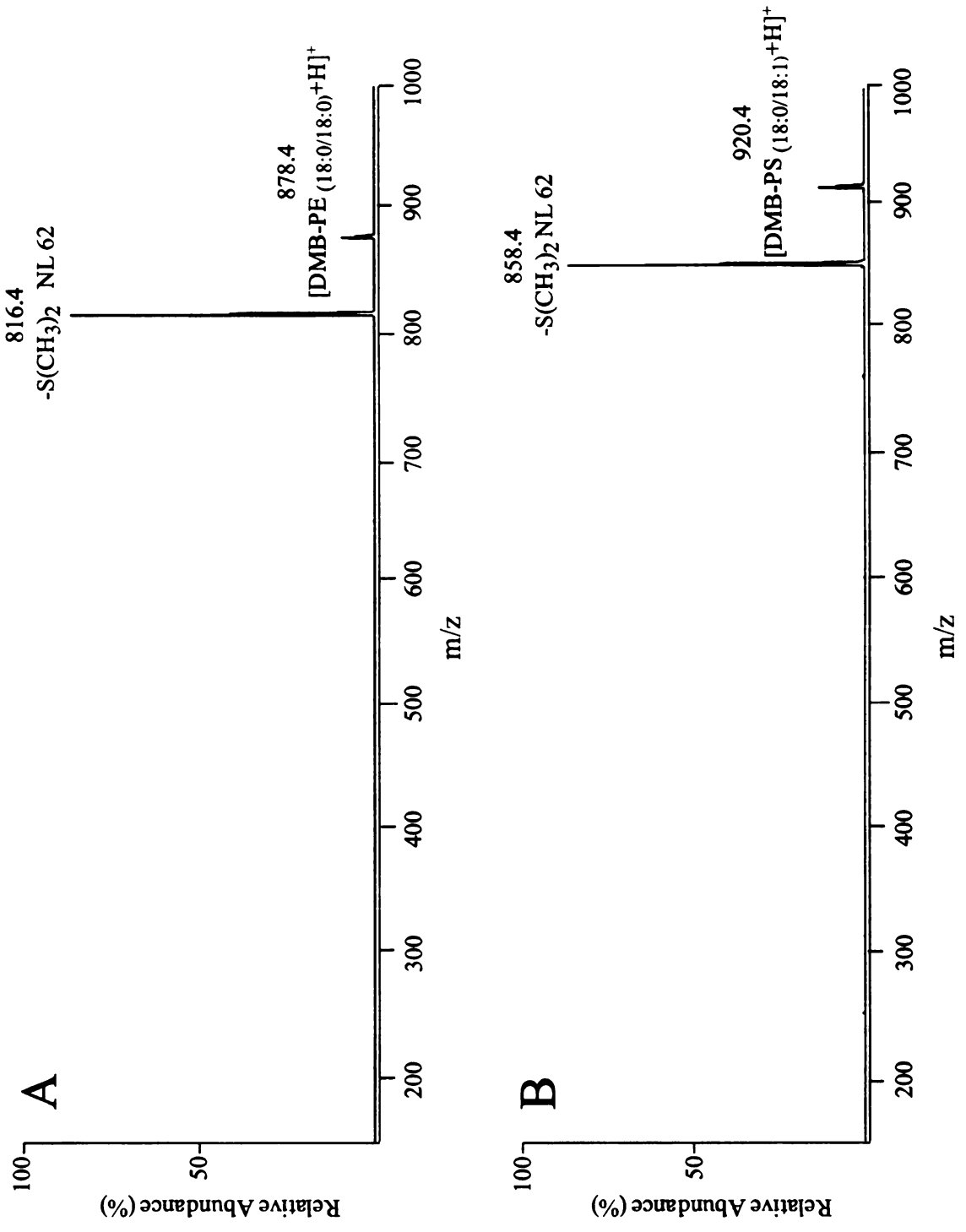

Figure 3.10 Positive ion mode nESI LCQ ion trap CID MS/MS product ion spectra of DMBNHS derivatized PE $_{(18:0/18:1)}$ (panel A) and PS $_{(18:0/18:1)}$ (panel B).

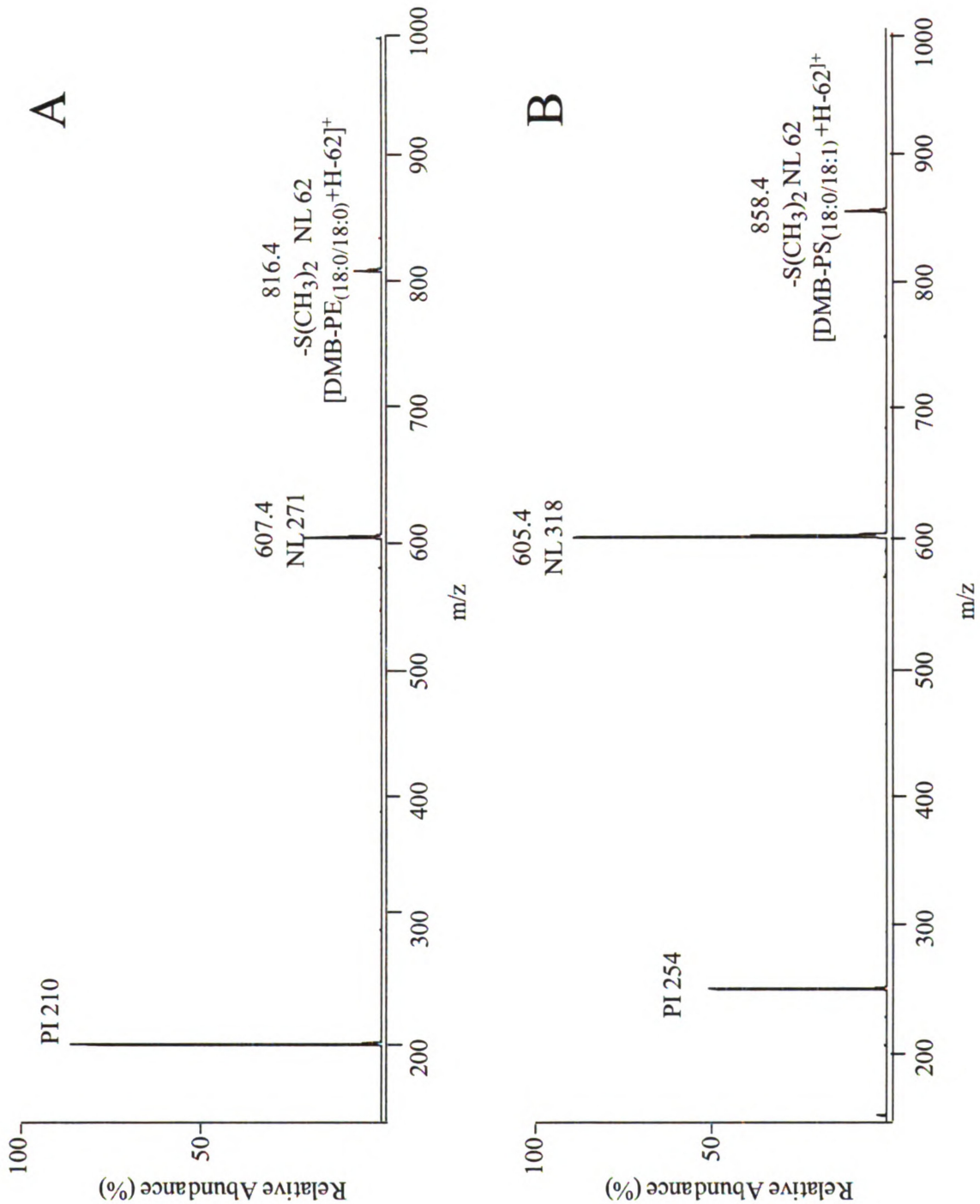

Figure 3.11 Positive ion mode nESI LCQ ion trap CID MS^3 product ion spectra of the NL 62 product ions of $PE_{(18:0/18:0)}$ (panel A) and $PS_{(18:0/18:1)}$ (panel B) lipids from Figure 3.10.

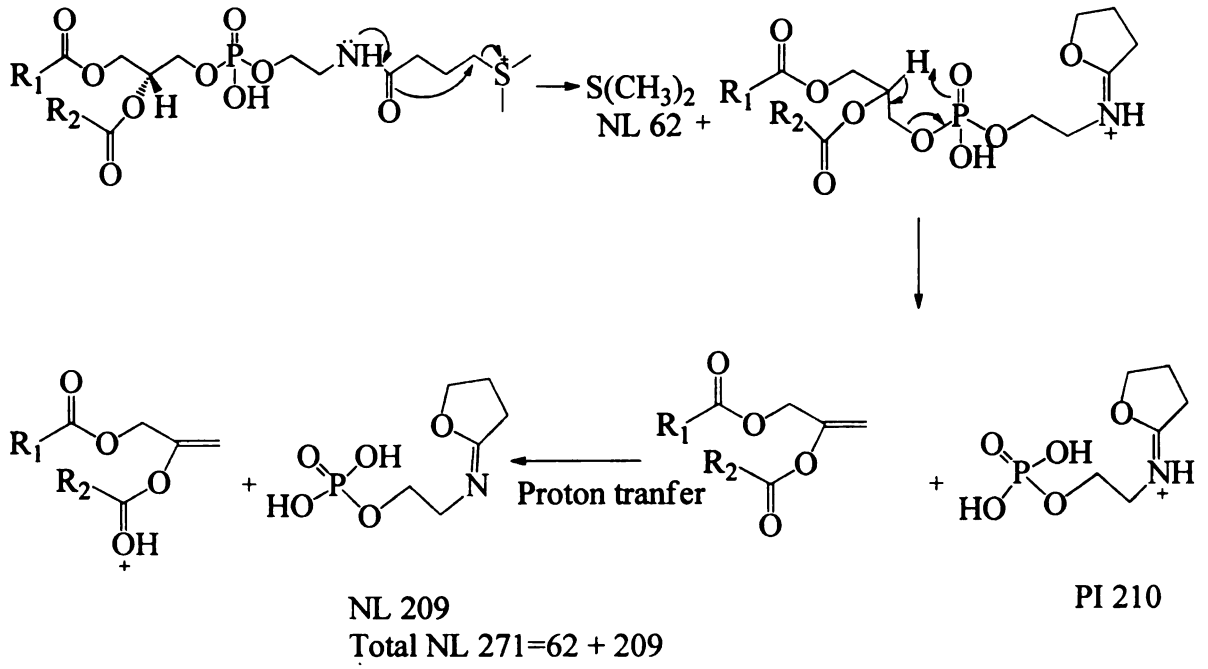

Scheme 3.7 Proposed positive ion mode CID-MS/MS fragmentation mechanism for DMBNHS derivatized PE aminophospholipids.

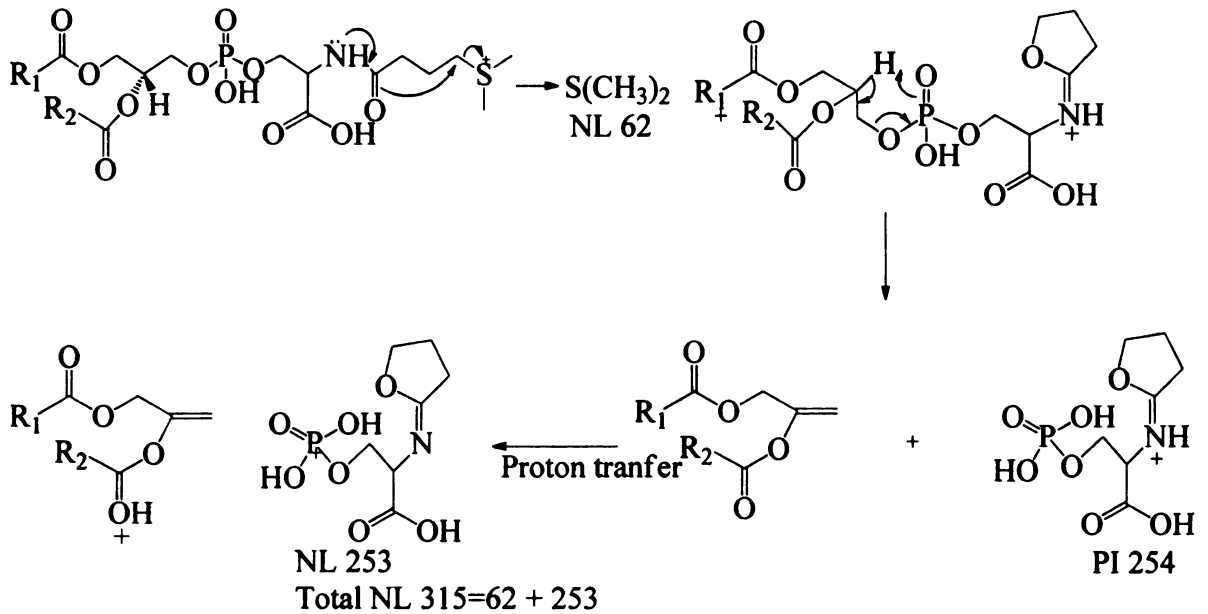

Scheme 3.8 Proposed positive ion mode CID-MS/MS fragmentation mechanism for DMBNHS derivatized PS aminophospholipids.

3.4.4 Collision Energy Optimization for MS/MS detection of DMBNHS Derivatized Aminophospholipids in the Triple Quadrupole Mass Spectrometer

The triple quadrupole product ion scan CID-MS/MS spectra for the PE and PS lipids in Figure 3.9 shows five possible detection channels for these species. A neutral loss scan mode experiment to monitor for the loss of 62 Da would allow detection of DMBNHS-derivatized PE and PS lipids in a single experiment, while neutral loss scans for 271 Da and 218 Da would allow the detection of DMBNHS-derivatized PE and PS lipids, respectively, in separate experiments. Similarly, precursor ion scan mode experiments to monitor for m/z 210 or m/z 254 would allow the separate detection of DMBNHS-derivatized PE and PS lipids.

In order to determine the optimal collision energies and maximum product ion abundances for each of these fragmentation channels, a collision energy resolved breakdown curve was generated for each standard aminophospholipid by monitoring the relative intensities of the different product ions while altering the collisional energy. As the abundance of the PE and PS lipid precursor ions decreased, the abundances of their corresponding product ions were observed to rise, with similar trends for both categories of lipid (see Figure 3.12, panel A and panel B). The primary common neutral loss of 62 u reaches a maximum at relatively low collision energy (between 17 to 20 eV). As the intensity of this primary neutral loss decreases, the intensity of the sequential neutral loss products of 271 Da or 315 Da and the product ions at m/z 210 Da or 254 Da steadily

increased. The optimized collision energy was around 35 eV for the NL 271, around 33 eV for the NL 315, around 32 eV for the 210 Da product ion, and around 28 eV for the 254 Da product ion. By comparing the collision energy resolved breakdown curve of DMBNHS derivatized aminophospholipids of different fatty acid chain length and number of double bonds, the optimized collision energy for each fragmentation channel was found within a narrow range. For example, the optimized collision energy of four standard PE species (with fatty acyl chains from 14:0 to 22:6) only varied between 31 and 33 eV for the precursor ion scan of m/z 210. The optimized collision energy for the neutral loss of 141 Da for underivatized PE lipids ranged from 20 eV to 30 eV. This means that the derivatization process makes the fragmentation tendency of lipids within the same class relatively universal. This narrow range of optimum collision energy also occurred in the neutral loss scan of 315 for PS lipids detection.

A

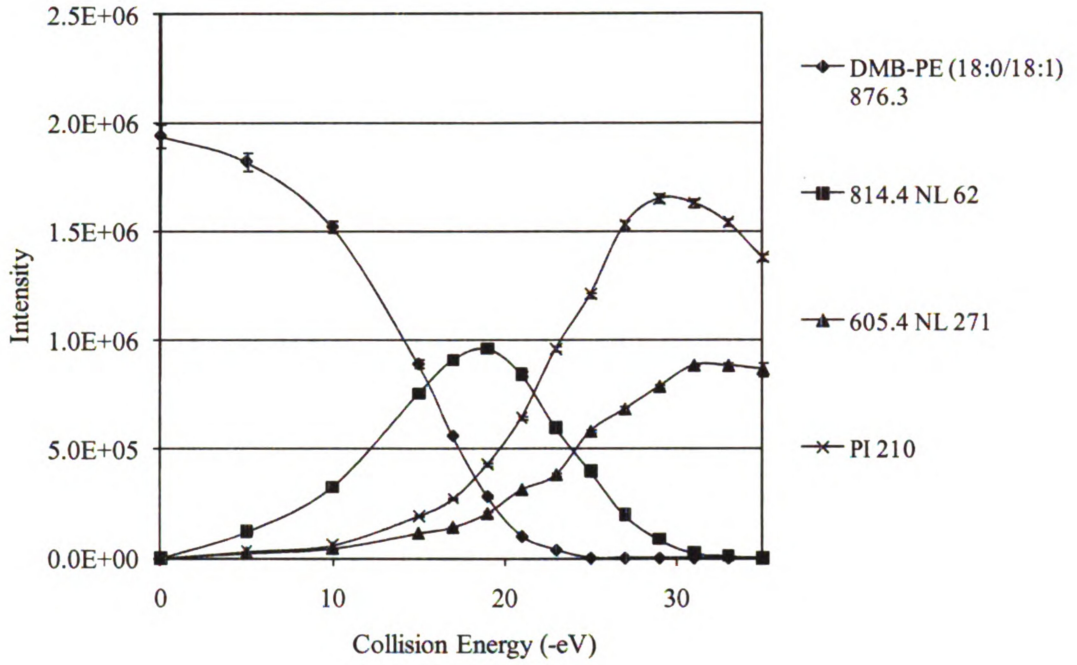

B

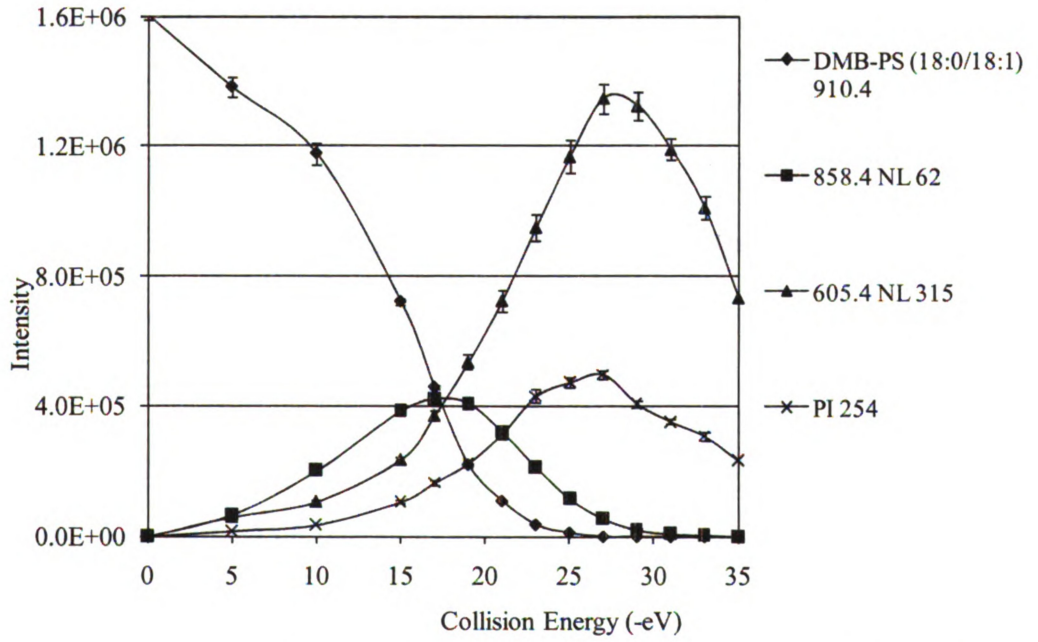

Figure 3.12 Positive ion mode triple quadrupole collision energy resolved breakdown curve of PE $_{(18:0/18:0)}$ (panel A) and PS $_{(18:0/18:1)}$ (panel B).

3.4.5 Determination of the CID-MS/MS Product Ion Detection Sensitivity of DMBNHS Derivatized Aminophsopholipids

Using each of the optimized collision energies determined above, the detection sensitivity and specificity of the neutral losses of 62 Da, 271 Da, 318 Da and the products ion at m/z 210 and m/z 254 were determined for the DMBNHS derivatized PE and PS lipids. The PE detection sensitivities were compared with the neutral loss of 141 Da used for detection of underivatized PE. Although NL 141 is the predominant fragmentation pathway for underivatized PE lipids, DMB-PE undergoes sequential fragmentations and gives rise to three detection channels. The three fragmenting steps split the pseudomolecular ion abundance into three terminal products, so the relative intensity of ions corresponding to NL 141 from the underivatized PE lipids are higher than the ions generated by NL 62, NL 217 or PR 210 from the DMBNHS-derivatized PE lipids. However, due to the 2-fold increase in MS ionization efficiency of the DMBNHS-derivatized PE lipids, as demonstrated in Figure 3.7, a comparable or overall increase (approx. two fold for the m/z 210 ion) in absolute detection sensitivity was achieved for each of the three separate fragmentation channels. An approx. three fold increase for PS detection sensitivity was observed for the neutral loss of 315 Da from the DMBNHS-derivatized PS lipids compared to that obtained by detection of the neutral loss of 185 Da from the underivatized PS lipids.

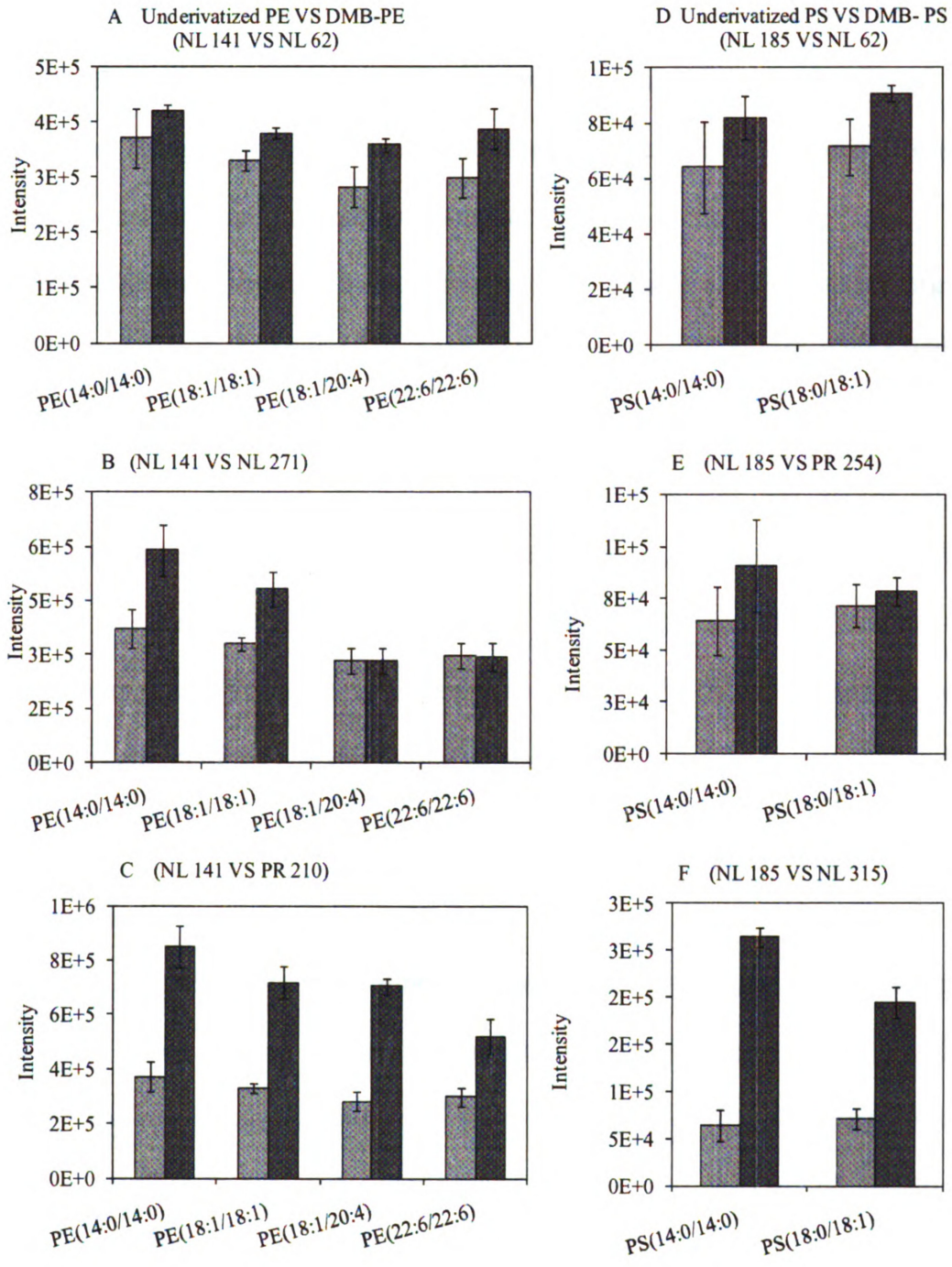

Figure 3.13 Summary of the positive ion mode MS/MS sensitivity of underivatized and DMBNHS-derivatized PE (panel A, B, C) and PS (panel D, E, F) aminophospholipids.

Following the sensitive detection of the DMBNHS-derivatized PE and PS aminophospholipids as described above, identification of their fatty acyl chain compositions (length and the number of double bonds) can be achieved by using CID MS/MS product ion scans in negative ion mode.

DMBNHS derivatized PS lipids can be observed with a net negative charge state by deprotonation of both phosphate group and carboxylic acid groups (along with with the positively charged sulfonium ion head group). However, DMBNHS derivatized PE lipids are zwitterionic neutral species and are therefore unable to lose another proton to yield $[M-H]^-$ ions. Fortunately, negatively charged precursor ions of the DMBNHS derivatized PE lipids can be formed by the formation of an anionic adduct of the sulfonium ion group. [76] Here, acetate adducts of the DMB-PE lipids were formed due to the salt condition of the analysis buffer. As an example, the acetate adduct of DMB-PE $_{(14:0,\ 14:0)}$ was observed at m/z 824.35 in the negative ion mode MS spectrum. (Figure 3.14 panel B).

The CID-MS/MS fragmentation pathway of the deprotonated DMB-PS lipids in negative ion mode resulted in an initial neutral loss of the dimethylsulfide (62 Da), similar to that seen in positive ion mode. (Figure 3.15 panel A and Scheme 9) After this initial loss, similar fragmentation pathways as those observed for the underivatized deprotonated PS lipids yielded fatty acyl chain information.

The initial fragmentation pathway of the acetate adduct DMB-PE lipids involved the neutral loss of methyl acetate (74 Da) (Figure 3.15 panel B and Scheme 10), followed by secondary cleavage of the head group and the fatty acyl chains.

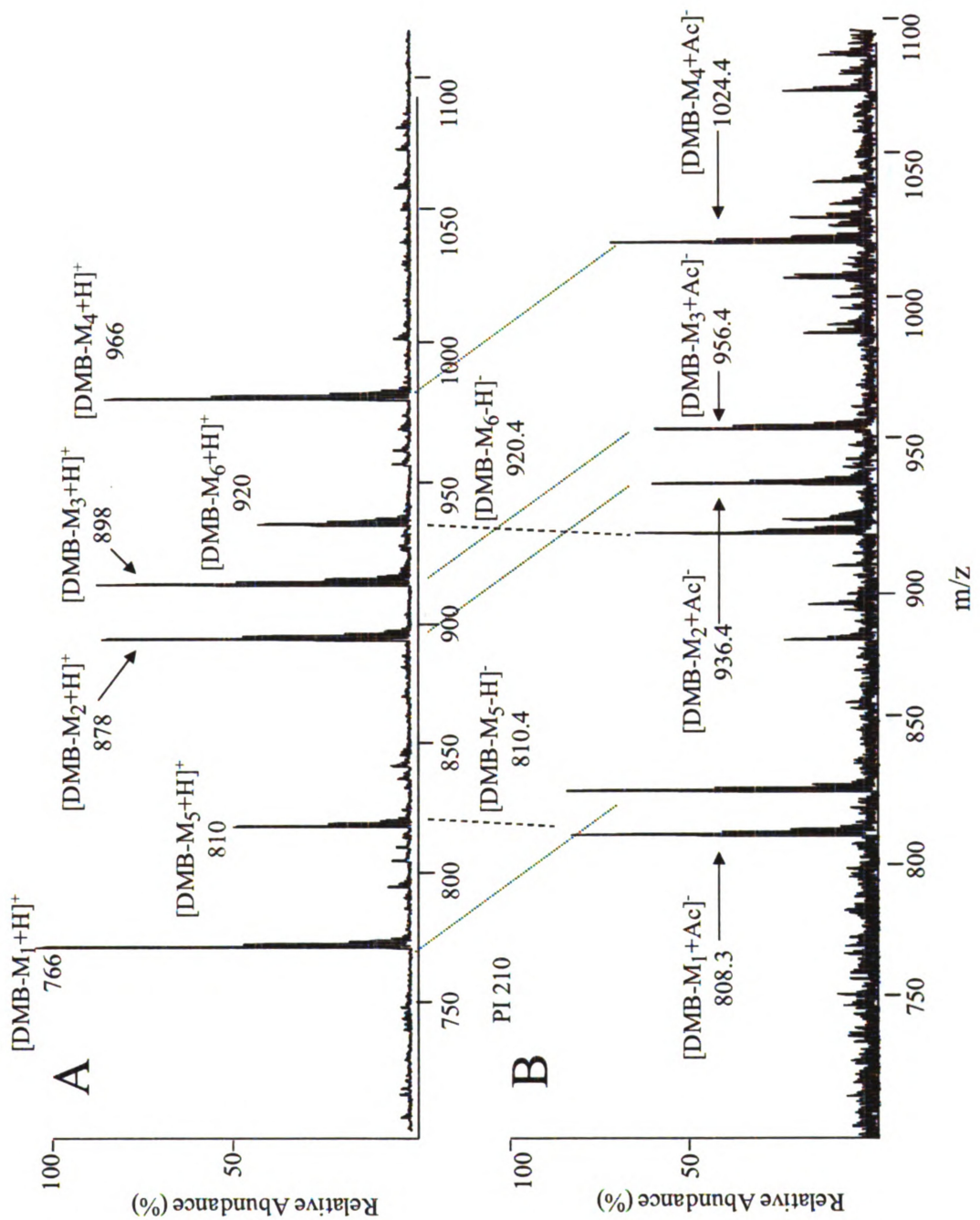

Figure 3.14 Positive ion mode (panel A) and negative ion mode (panel B) nESI triple quadrupole MS analysis of DMBNHS-derivatized PE and PS aminophospholipids. M_1 = PE $_{(14:0/14:0)}$, M_2 = PE$_{(18:0/18:0)}$, M_3 = PE $_{(18:0/20:4)}$, M_4 = PE $_{(22:6/22:6)}$, M_5 = PS $_{(14:0/14:0)}$, M_6 = PS $_{(18:0/18:1)}$.

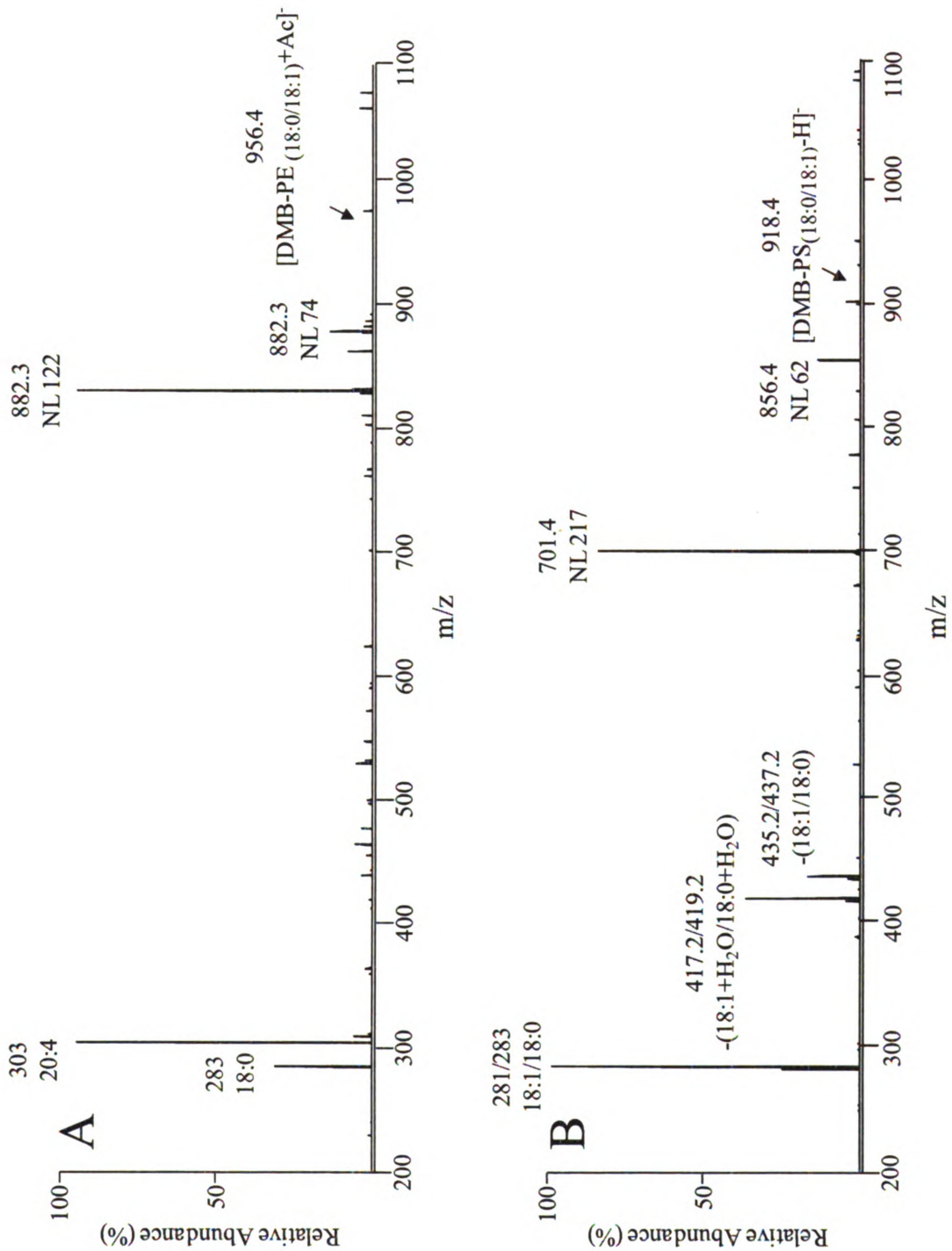

Figure 3.15 Negative ion mode nESI triple quadrupole CID MS/MS product ion spectra of DMBNHS derivatized PS $_{(18:0/18:1)}$ and PE $_{(18:0/20:4)}$ aminophospholipids.

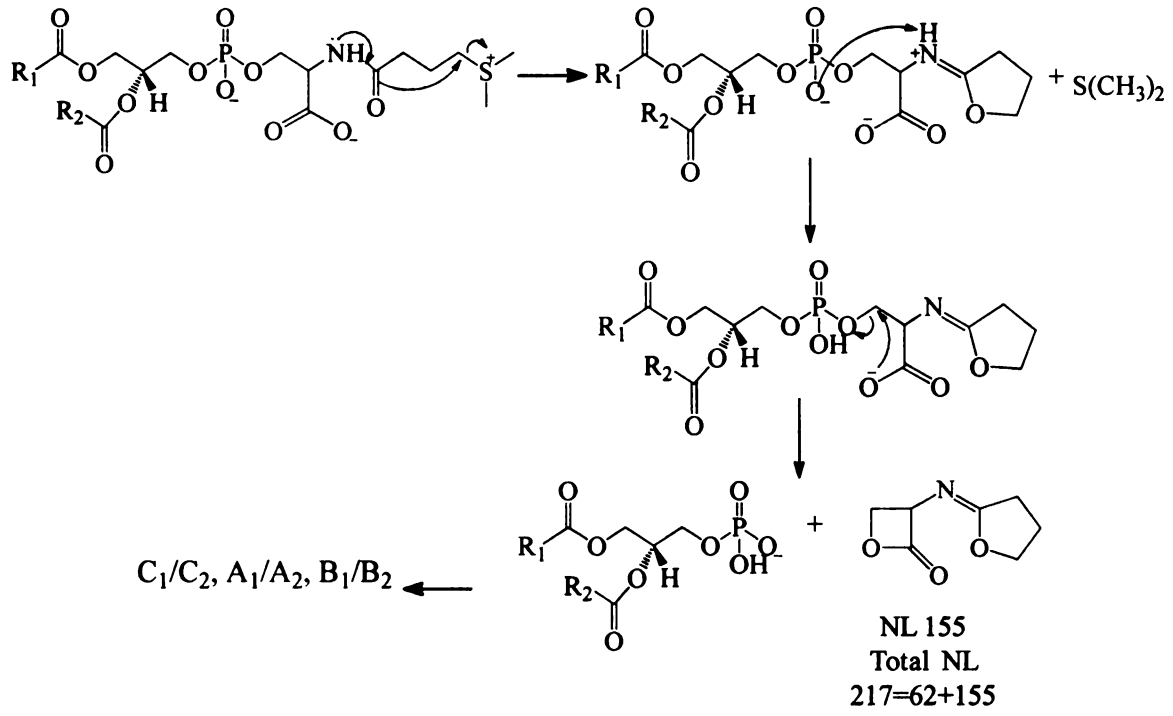

Scheme 3.9 Proposed negative ion mode CID-MS/MS fragmentation mechanism for DMBNHS derivatized PS aminophospholipids.

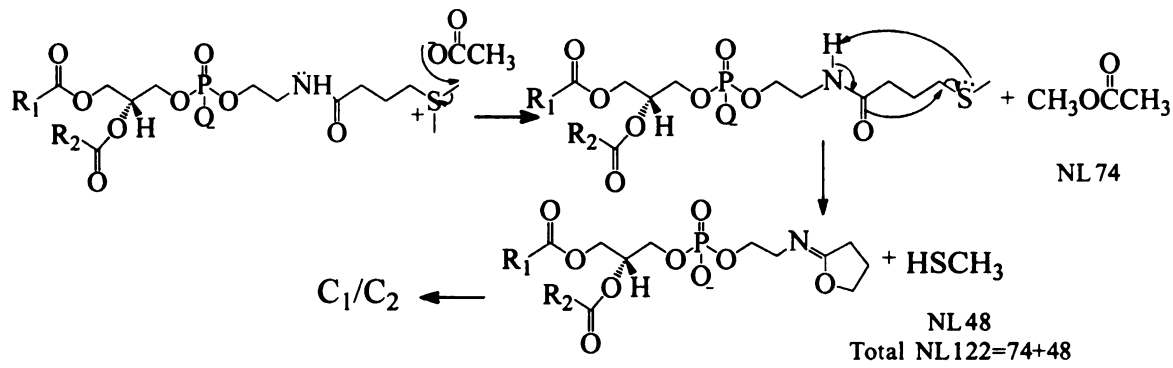

Scheme 3.10 Proposed negative ion mode CID-MS/MS fragmentation mechanism for DMBNHS derivatized PE aminophospholipids.

3.4.6 DMBNHS ('light') and D_6-DMBNHS ('heavy') Derivatization of Aminophospholipids

The minor detection bias towards low m/z lipid species with short chain length as described above, particularly in positive ion mode, is a prevalent issue for both derivatized and underivatized lipids. To solve this issue, one method is to determine the linear relationship between detection signal response and fatty acyl chain composition for lipids of known absolute concentration.[39] However, the lack of a suitable number of internal standards and the need for more sophisticated data analysis software prevents this methodology from achieving adequate precision.[48] Lipidomics was developed to be a systems biology approach to better understand contextual changes in lipid composition within an organelle, cell, or tissue as a result of challenge, stress, metabolism and disease. [27] The quantification of lipid profile changes is crucial for determining the roles of lipids in cell function and disease. Analysis of the abundance of product ions formed from 'normal' and 'diseased' populations of aminophospholipids derivatized with 'light' and 'heavy' isotopically labeled DMBNHS reagents, (to be described in Chapter 4) allows quantitation of the changes of aminophospholipid profiles between different samples.

When the isotopic pair of labeled compounds is electrosprayed from identical solution conditions, this isotopic labeling strategy can potentially improve the precision of relative quantification by minimizing or negating errors associated with run-to-run or even scan-to-scan irreproducibility. A second benefit of utilizing a derivatization reagent is that it can 'extract' specific lipid categories of interest by targeting a certain functional

group. The chemical bonding properties of the DMBNHS and D_6-DMBNHS reagents are almost identical and therefore their modification reactivities were found to be compatible (Figure 3.16). In this experiment, standard lipid mixtures which contains six aminophospholipids with equal moles were derivatized by DMBNHS and D_6-DMBNHS respectively. After labeling reaction, the 'light' and 'heavy' tagged standard lipids were mixed with 1to1 ratio. Positive ion mode CID-MS/MS PI210 experiment was performed and data was collected from 75 scans. Then quantitative analysis of 'light' and 'heavy' labeled lipid standard was achieve following a triplicate derivatization-mass spectrometry analysis process. The average ratio of six DMBNHS derivatized aminophospholipids over D_6-DMBNHS derivatized aminophospholipids is 1.01 ± 0.03. The average ratios of 'light' labeled over 'heavy' labeled individual species are 1.01 ± 0.03, 0.97 ± 0.01, 0.96 ± 0.01, 0.98 ± 0.01, 1.03 ± 0.01, 1.04 ± 0.02 from M_1 to M_6 in the spectrum of Figure 3.16. The total average ratio of six 'light' and 'heavy' derivatized species in triplicate experiments is 1.00 ± 0.03. Such analysis illustrated that the chemical derivatization efficiencies of DMBNHS and D6-DMBNHS are identical. The biased detection of 'light' and 'heavy' derivatized aminophospholipids was negligible. The application of these reagents to the differential quantitative analysis of 'normal' and 'diseased' populations of aminophospholipids will be described in Chapter 4 below.

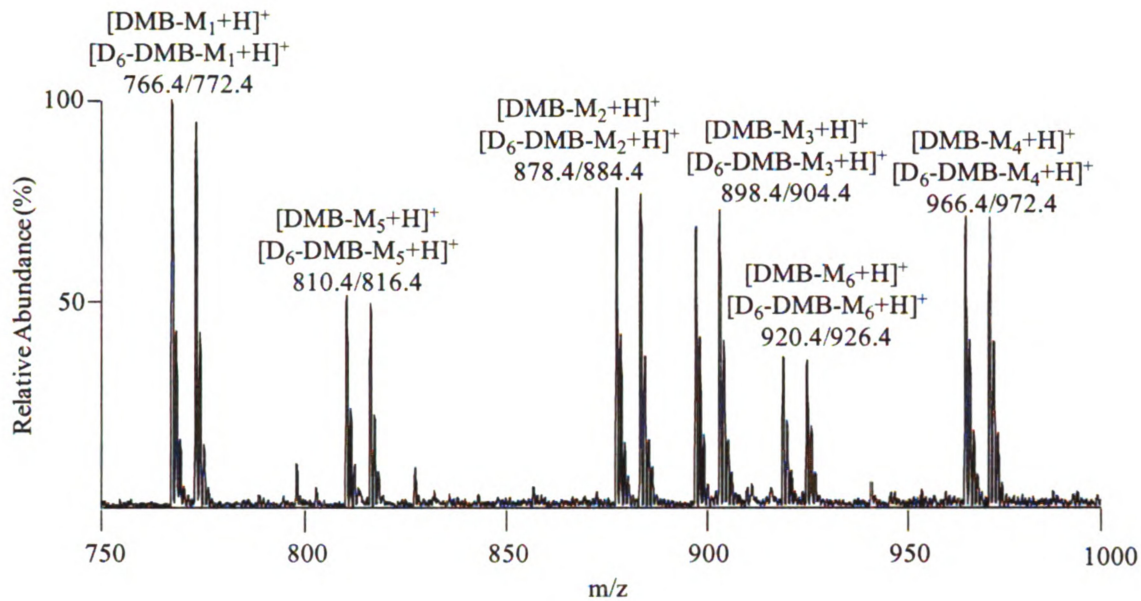

Figure 3.16 Positive ion mode nESI triple quadrupole MS analysis of DMBNHS and D_6-DMBNHS derivatized PE and PS aminophospholipids. M_1 = PE $_{(14:0/14:0)}$, M_2 = PE $_{(18:0/18:0)}$, M_3 = PE $_{(18:0/20:4)}$, M_4 = PE $_{(22:6/22:6)}$, M_5 = PS $_{(14:0/14:0)}$, M_6 = PS $_{(18:0/18:1)}$.

CHAPTER FOUR

RELATIVE QUANTIFICATION OF AMINOPHOSPHOLIPIDS FROM BIOLOGICAL SAMPLES BY ISOTOPE DERIVATIZATION-TANDEM MASS SPECTROMETRY

4.1 Introduction

Sulfonium ion chemistry was previously been proved to be a useful tool to target the goal of quantitative analysis. [77,82] Not only did the sulfonium ion derivatized analytes perform specific cleavage to generate characteristic product ion, more importantly the incorporation of "light" and "heavy" isotopically encoded labels into the derivatives facilitate the application of this derivatization strategy to quantitative analysis.[77] A recent study from the Reid laboratory reported a fast and robust 'Fixed charge' DMBNHS chemical derivatization strategy to quantify protein surface relative solvent accessibility. [53] In chapter 3, the result of standard aminophospholipid derivatization by using this reagent demonstrated its utility in the area of lipidomics. To apply the DMBNHS derivatization strategy to quantitative biological sample lipid profile analysis, an isotope tagged heavy version of DMBNHS reagent was synthesized via incorporation of six deuteriums into two methyl groups to provide isotopic analogues of the DMBNHS. Its high reactivity and specificity, improved ionization character and structure elucidation ability indicate the power of DMBNHS for aminophospholipid identification. In the meanwhile, heavy and light versions of this regent generate unique

'reporter neutral loss' of dialkylsulfide or deuterated dialkylsulfide from sulfonium derivatives. Other studies have developed isotopic derivatization strategies for direct quantification of several classes of lipids including fatty acids and phospholipids. [51,48] However multiple-step reaction was required to tag fatty acids and high collision energy was need to detect the characteristic fragment of isotope-labeled phospholipids.[51, 48] This study will demonstrate the ability of isotope-incorporated DMBNHS single-step derivatization strategy to fulfill the quantitative analysis of aminophopholipids in real samples.

4.2 Aminophospholipid Analysis of Conventional Shotgun and DMBNHS-Derivatization-Based Lipidomics

4.2.1 ESI-MS Analysis of Underivatized and DMBNHS Derivatized Mouse Liver Lipid Extracts

Previous studies discussed phospholipid profiling of mouse liver tissues by mass spectrometry.[60, 61] MS analysis of abundant phospholipids especially PC lipids indicated alterations of liver lipid extract of double mutant mice compared to that of control mice.[60, 61] It also demonstrated similarities between control mice and triple mutant mice liver lipid profiles. [61] Significant differences of high abundant PE aminophospholipids were also be illustrated between control mice liver tissue and double mutant (DM) mice liver tissue by using conventional mass spectrometry analysis. Quantititive profiles of low abundance PS species between control, DM and TM liver

samples were unable to be generated due to the detection limitation and sensitivity issue of the instrument. Our novel isotope labeling strategy leads to the generation of relative quantification assay of all aminophospholipids.

Positive ion mode ESI-MS analysis following the triple quadrupole mass spectrometry analysis procedure of chapter 2 of a 1:1600 diluted control mouse pooled liver lipid extract displayed many abundant peaks within mass range 650-950 Da (Figure. 4.1A). Lipid class specific precursor ion and neutral loss scan mode MS/MS experiments identified that most of these peaks correspond to phosphocholine lipids (e.g., internal standard PC $_{(14:0/14:0)}$ at m/z 678.4, endogenous PC $_{(16:0/18:2)}$ at m/z 758.4 and PC $_{(16:0/22:6)}$ at m/z 806.4). Some of the abundant aminophospholipids were also detected (e.g. internal standard PE $_{(14:0/14:0)}$ at m/z 636.4, PE $_{(16:0/20:4)}$ at 764.4). Since most underivatized PE and PS molecular species are minor components of the total lipid profile, they either are below the detection limit or overlap with high intensity PC ion peaks in the MS spectrum.

When DMBNHS derivatization reaction was applied to the identical control mouse pooled liver lipid extract, and then an aliquot with the same dilution was analyzed by ESI-MS, the ions of each modified aminophospholipid shifted to the higher mass range with about two fold increase of relative intensity (compare Figure. 4.1A and 4.1B). For example, the internal standard PE $_{(14:0/14:0)}$ shifted from m/z 636.4 to m/z 766.4, while an endogenous PE $_{(16:0/22:6)}$ lipid which overlapped with abundant PC ion at m/z 766.4 in the conventional MS spectrum shifted to m/z 896.4 and therefore could be detected unambiguously. Even trace amount aminophospholipid species PS $_{(18:0/22:6)}$ which initially overlapped with PC $_{(18:0/22:5)}$ at m/z 836.4 increased its m/z value to 966.4 as was shown in the MS spectrum of derivatized liver extract.

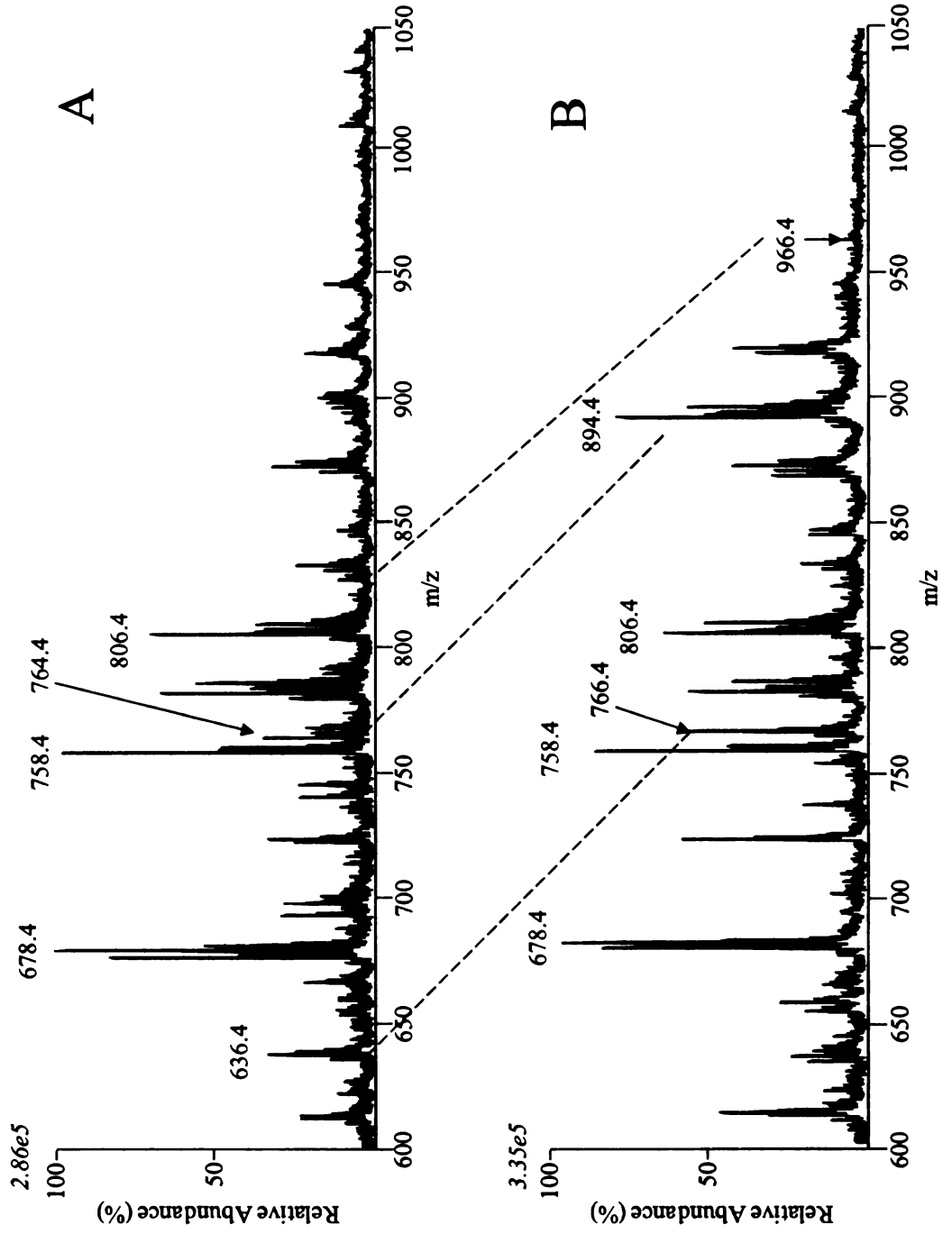

Figure 4.1 Positive ion mode ESI-MS analysis of control mouse liver lipid extract. (A) underivatized liver sample, (B) DMBNHS derivatized liver sample. A selected region of the mass spectrum from m/z 600-1050, containing the major PC lipids and underivatized PE lipids or derivatized PE lipids respectively are shown.

4.2.2 ESI-MS/MS Analysis of Underivatized and DMBNHS Derivatized Mouse Liver Lipid Extract

A PE lipid class specific neutral loss (NL) scan mode CID-MS/MS experiment was performed to profile the PE lipid distribution in the underivatized control mouse liver extract by monitoring for the characteristic loss of phosphoethanolamine of 141 Da. Analysis of PE lipids in the DMBNHS-derivatized control mouse liver extract was performed by using a CID-MS/MS precursor ion (PI) scan at m/z 210, a NL scan of 62 Da and a NL scan of 271. As mentioned in the MS analysis, the underivatized and derivatized lipid samples were from the same tissue source. To demonstrate unbiased derivatization efficiency of the whole cluster of PE species we expect NL 141 for unmodified PE analysis and PI 210, NL 62, NL 271 to display identical lipid distributions regardless of the labeling process. Noticed that NL 62 which is a exclusive neutral loss for all derivatized aminophospholipids, this scan mode not only fingerprinted PE lipids but also 'extracted' other amino-containing lipids, including PS.(see Figure 4.2 panel C) By using the optimized collision energy for gas-phase fragmentation which was discussed in chapter 3, we achieved unbiased ionization, fragmentation, detection and comprehensive profiling of derivatized PE species. The pseudomolecular ions of derivatized PE lipids shifted to higher mass range by 130 Da while maintaining the original ratios between species. (Figure 4.2). Moreover, the cleavages of derivatized lipids enhanced analytic sensitivity by 2 to 3 times which is consistent with CID-MS/MS result of standard aminophospholipid analysis discussed in chapter 3. As a result it increased the dynamic range to allow the identification of low-abundance species.

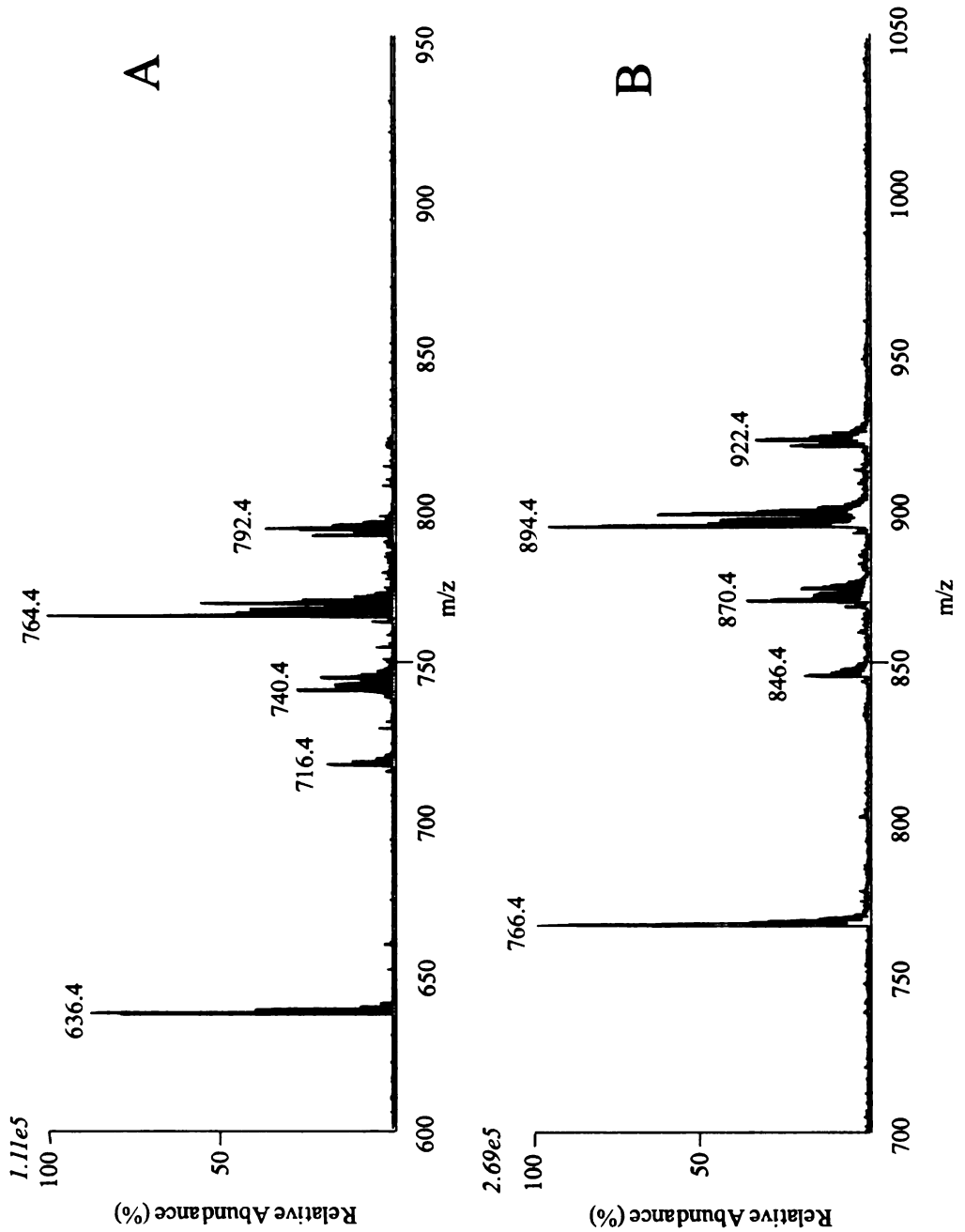

Figure 4.2 Positive ion mode CID-MS/MS analysis of underivatized (panel A) and DMBNHS derivatized (panel B, C, D) PE species from liver lipid extract. (A) Conventional NL 141 scan for the detection of underivatized PE species; (B) PI 210 (C) NL 62 (D) NL 271 scans for the detection of DMBNHS derivatized PE lipids.

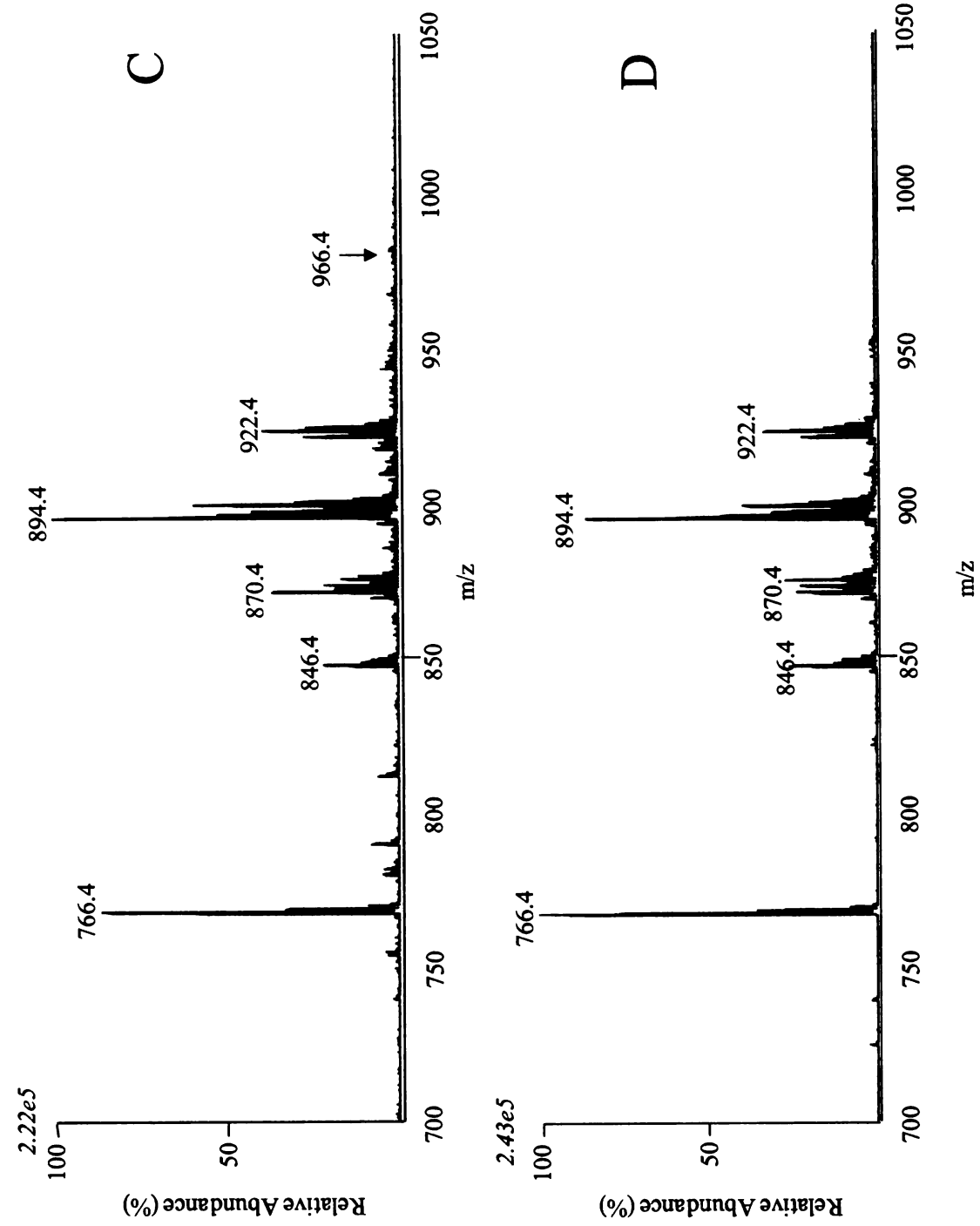

Figure 4.2 (Cont.)

A subclass of low-abundant aminophospholipids – PS lipids exhibit better ionization behavior after derivatization. The characteristic MS/MS analysis of unmodified PS lipids in positive ion mode is accomplished by NL 185 scan. Product ion spectrum of DMBNHS derivatized PS lipid also shows 3 representative fragments. Correspondingly, NL 62, NL 315 and PI 254 can be used for PS profiling. However the carboxylic acid structure of the serine residue determined that the major fragmentation is NL 315. (see chapter 3) Comparing to NL 185, NL 315 monitor the loss of DMB-tagged phosphoserine head group (see Figure 4.3). This neutral loss scan mode experiment generated spectrum of derivatized PS molecular species with 3 fold higher peak intensity and improved coverage of low-abundant PS lipids.

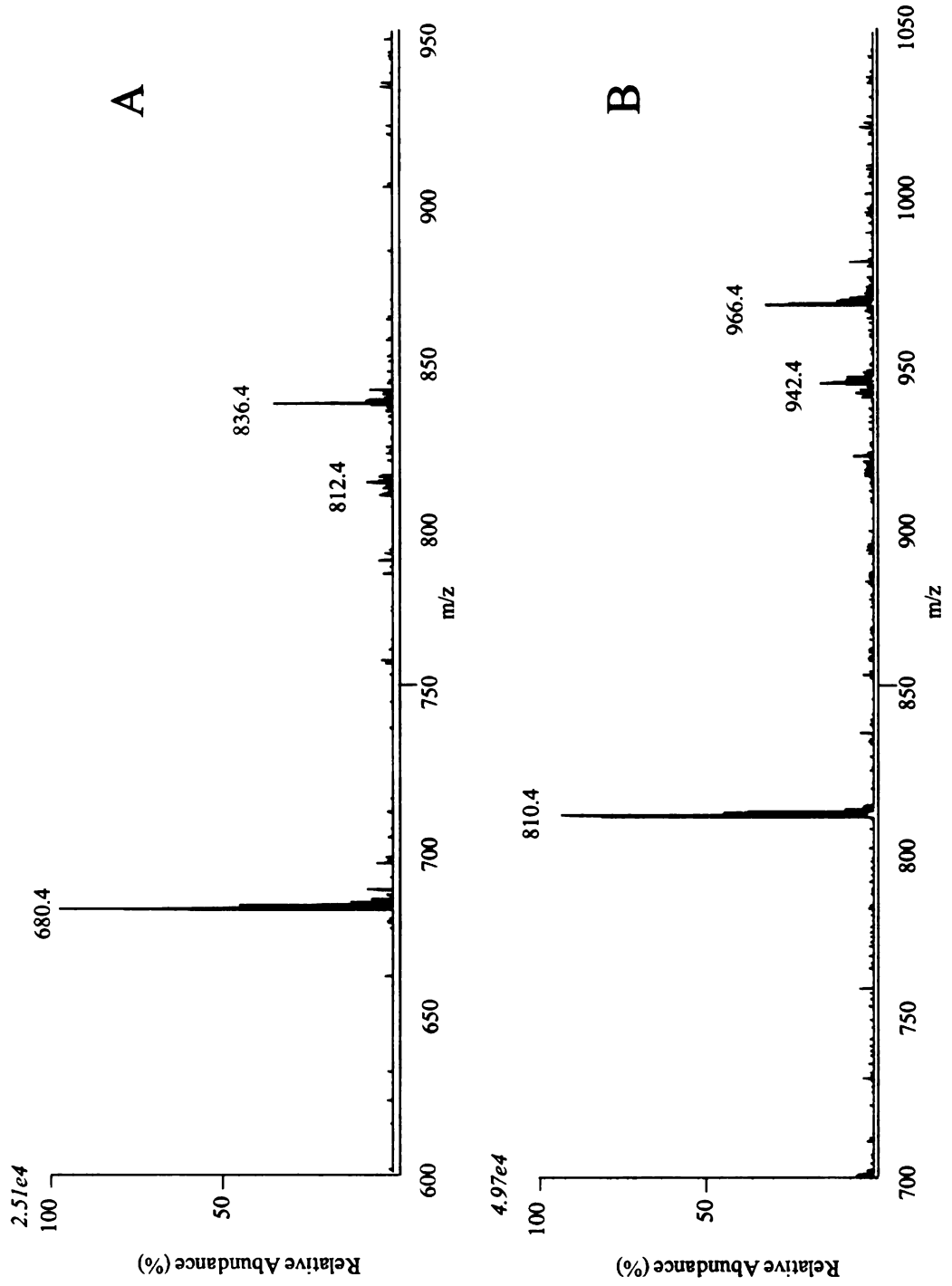

Figure 4.3 Positive ion mode CID-MS/MS analysis of underivatized (panel A) and DMBNHS derivatized (panel B) PS species from liver lipid extract. (A) Conventional NL 185 scan for the detection of underivatized PS species; (B) NL 315 for the detection of DMBNHS derivatized PS lipids.

4.3 Aminophospholipid Quantification with Isotopic-Derivatization Reagents

4.3.1 Quantification Reagent Selection and Scan Mode Selection

To accomplish the goal of comprehensive relative quantification of aminophospholipids, proper MS/MS scan mode was chosen to demonstrate sensitivity by direct comparison. Table 4.1 listed three self-synthesized isotopic versions of DMBNHS reagents. Their analogue MS/MS experiment scan events corresponding to the same cleavage site of the derivatized PE or PS lipids were shown in parallel. Based on the result of MS/MS experiments by employing these 3 different scan events, (see Figure 4.2 panel B, C, D) NL 210 gives the highest intensity of ion peaks which means during collision-induced dissociation the major fragmentation of DMB-PE is a common neutral loss of 210 Da. NL 210 can realize simultaneous single-scan detection of normal version DMBNHS and D_6-Heavy-DMBNHS derivatized PE species. DMBNHS and D_6-Heavy-DMBNHS tagged aminophospholipids give isotope-dependent reporter neutral loss of 315 and 321 respectively that could be used to provide relative quantification information for individual PS members of two sample sets.

Table 4.1 Isotope dependent precursor ion and neutral loss scan mode CID-MS/MS experiments employed for class specific quantitative identification of DMBNHS derivatized aminophospholipids.

isotopic version / lipid class	DMBNHS	D_6-DMBNHS
PE / lyso PE / Plasmenyl PE	NL 62	NL 68
	PI 210	PI 210
	NL 271	NL 277
PS / lyso PS/ Plasmenyl PS	NL 62	NL 68
	PI 254	PI 254
	NL 315	NL 321

4.3.2 Strategy for the Relative Quantitation of DMBNHS-Derivatized Aminophospholipids

The strategy employed here to quantitatively profile the DMBNHS-derivatized aminophospholipids is shown in Figure 4.4. Pooled lipid extracts from control, DM or TM liver tissue samples are reacted with DMBNHS or D_6-DMBNHS. After completion of derivatization reaction, control and DM or control and TM samples are mixed and analyzed by ESI-MS, and neutral loss and precursor ion scan mode CID-MS/MS. In each of the MS/MS scans, the relative intensity of premixed spiked-in internal standard indicates the labeling efficiency and mix precision of the two channel reaction. By ratiometrically comparing the intensities of the light- and heavy- derivatized internal

standard with equal final concentration, the peak intensity of each spectrum accordingly. Considering that light- and heavy- labeled aminophospholipids have slightly different isotope distribution also that the complex mixture potentially still have overlaps between the pseudomolecular peak of a given aminophospholipid with the $[M+H+2]^+$ isotope peak of another aminophospholipid species with one less double bond, isotopic correction was calculated by Isopro to minimize the effects of ^{13}C, ^{2}H and peak overlapping. More specifically, in the quantitative analysis of liver sample extracts, the Isopro suggested isotope distribution and experimental generated isotope distribution of lipids with different fatty acid chain length and number of double bonds were compared. A linear relationship was generated for the isotope distribution as a function of mass to charge value. Then for each species subtracted such calculated isotopic peak intensity from the real intensity to determine whether a new species was overlapped with the isotopic peak of the initial species. Most of the cases were an overlap between lipids with mass to charge differences of 2 corresponding to 1 double bond variance. After isotope correction, normalization was the next step based on the intensity difference of internal standard. Such difference came from personal sample handling processes including mix ratio inaccuracy and spike in variance. The intensities of 4 of the most abundant isotopic peaks of the internal standards (derivatized PE $_{(14:0/14:0)}$ and PS $_{(14:0/14:0)}$) were summed together for the analysis. The accepted ratio range of D_6-DMBNHS labeled over DMBNHS labeled internal standerds was 0.95 to 1.05. The intensity of the whole D_6-DMBNHS derivatized lipid profile was multiplied by a number which was inversely proportional to the determined ratio of D_6-DMBNHS over DMBNHS derivatized internal

standards. After repeated such experiment 5 times, data were averaged and standard deviation of each species were determined.

One-way ANOVA (Graph Pad Prism version5, GraphPad Software, Inc. La Jolla, CA) followed by Tukey as a post-test was used to determine statistically significant ($p<0.05$) changes in the abundances of individual lipid species between the pooled control and DM or the pooled control and TM samples.

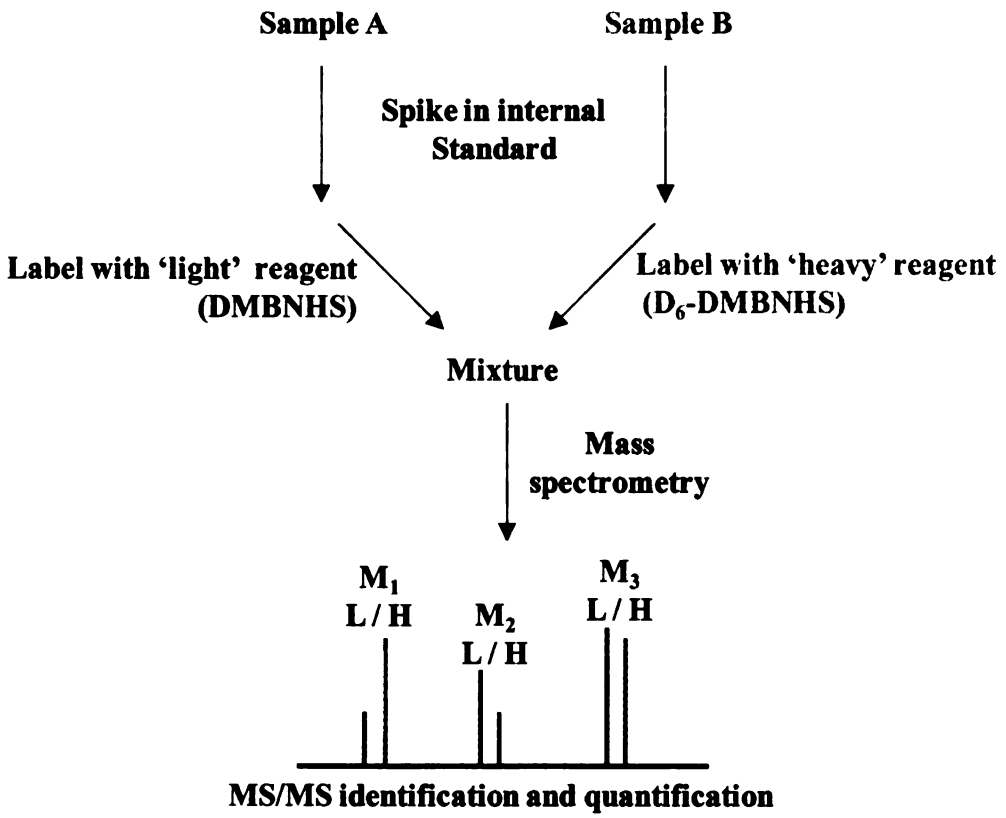

Figure 4.4 Aminophospholipid quantification by isotopic derivatization and tandem mass spectrometry analysis.

4.4 Relative Quantification of DMBNHS-Derivatized Aminophospholipids from Control, Double Mutant and Triple Mutant Mouse Liver Tissue Lipid Extracts

To demonstrate the advantages of isotopic derivatization based quantification, we applied the established DMBNHS labeling strategy to the aminophospholipid analysis of control and disease state mice liver sample. Lipid extracts of five control mice liver tissue were pooled and reacted with DMBNHS as described in the Experimental Section. Lipid extracts of five DM mice liver tissue and five TM mice liver tissue samples were separately pooled and individually reacted with the D_6-DMBNHS reagent. The product solutions from control mice were mixed with either that from DM mice or TM mice in a ratio of 1:1. These mixtures were introduced to the mass spectrometer via a chip-based nano-electrospray ionization (nESI) source followed by automated CID-MS/MS PI 210 and NL 315 scans in positive ion mode to quantify PE and PS lipids.

Representative mass spectra, obtained by using NL 210 in positive ion mode to quantify and compare PE lipids in control mice liver, DM mice liver and TM mice liver are shown in Figure 4.5. Each PE species from control mice liver and mutation mice liver appeared in the precursor ion 210 spectra as double ion peaks with 6 Da difference. Comparing Figure 4.5 panel A and B, the derivatization and sample handing efficiency is identical for control, DM and TM liver sample, which is demonstrated by the equivalent intensity of light and heavy labeled internal standard PE $_{(14:0/14:0)}$ at m/z 766.4 and 772.4 respectively. An apparent decrease of omega 6 fatty acid containing PE $_{(16:0/20:4)}$ at m/z 870.4 or 876.4 and an increase of omega 3 fatty acid containing PE $_{(16:0/22:6)}$ at m/z

894.4 or 900.4 were observed in DM mouse liver samples compared with control group. (See Figure 4.5 panel A) On the other hand, the same omega 6 and omega 6 fatty acid containing PE lipid distribution in TM samples reversed to normal level compatable to control samples. (See Figure 4.5 panel B) At the same time NL 315/321 scans were used to simultaneously profile the light- and heavy derivatized PS species from control mice and transgenic mice liver samples. (Figure 4.6) Similar ratiometric comparison of the NL 315 and NL 321 scans allowed relative quantitation of the PS lipids. Interestingly an apparent increase of omega 9 fatty acid containing PS $_{(18:0/18:1)}$ at m/z 892.4 or 898.4 was indicated in DM mouse liver samples compared with control group. (Compare Figure 4.6 panel A and panel B) An apparent decrease of this specific PS species in TM mice compare with DM mice was also discovered. This result is consistent with previous HPLC analysis of total fatty acid which reported the deficiency of 18:1 omega 9 fatty acid in TM mice compared with DM mice [61]. Quantification of differences between control and diseased samples by CID-MS/MS typically involves a comparison of peak intensity/area of an ion of interest, analyzed in separate runs. Hereby, taking the ratio of isotopic peak intensities within a single run or even a single MS/MS scan improves the precision of relative quantification.

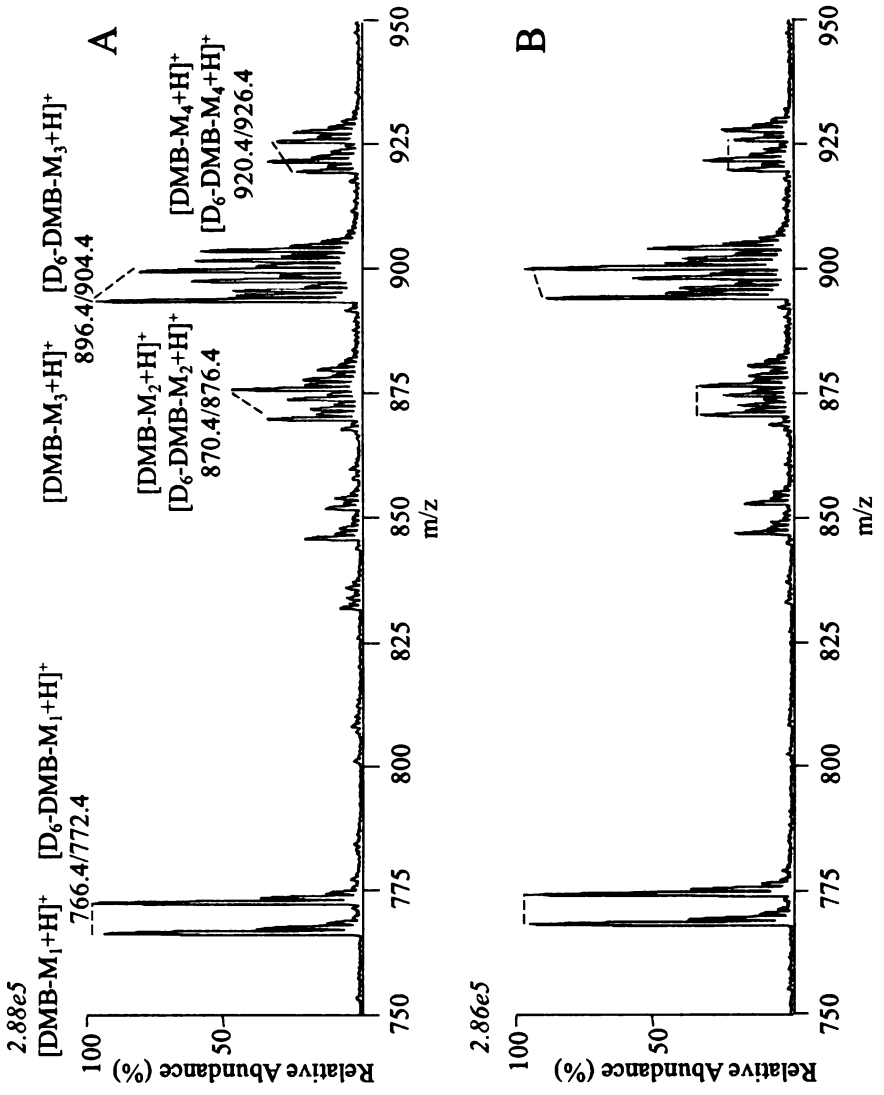

Figure 4.5 Representative Positive ion mode ESI-MS/MS PI 210 analysis of DMBNHS and D_6-DMBNHS derivatized PE lipids isolated from control, DM and TM transgenic mouse liver samples. (A) DMBNHS (light reagent) derivatized control liver PE lipids VS. D_6-DMBNHS (heavy reagent) derivatized DM liver PE lipids. (B) DMBNHS (light reagent) derivatized control liver PE lipids VS. D_6-DMBNHS (heavy reagent) derivatized TM liver PE lipids. Dotted line indicate a pair of light and heavy isotope labeled lipid ion peaks with 6 Da m/z difference. M_1: respectively spiked in internal standard PE $_{(14:0/14:0)}$, endogenous M_2 : PE $_{(16:0/20:4)}$, M_3 : PE $_{(16:0/22:6)}$, M_4 : PE $_{(18:1/22:6)}$.

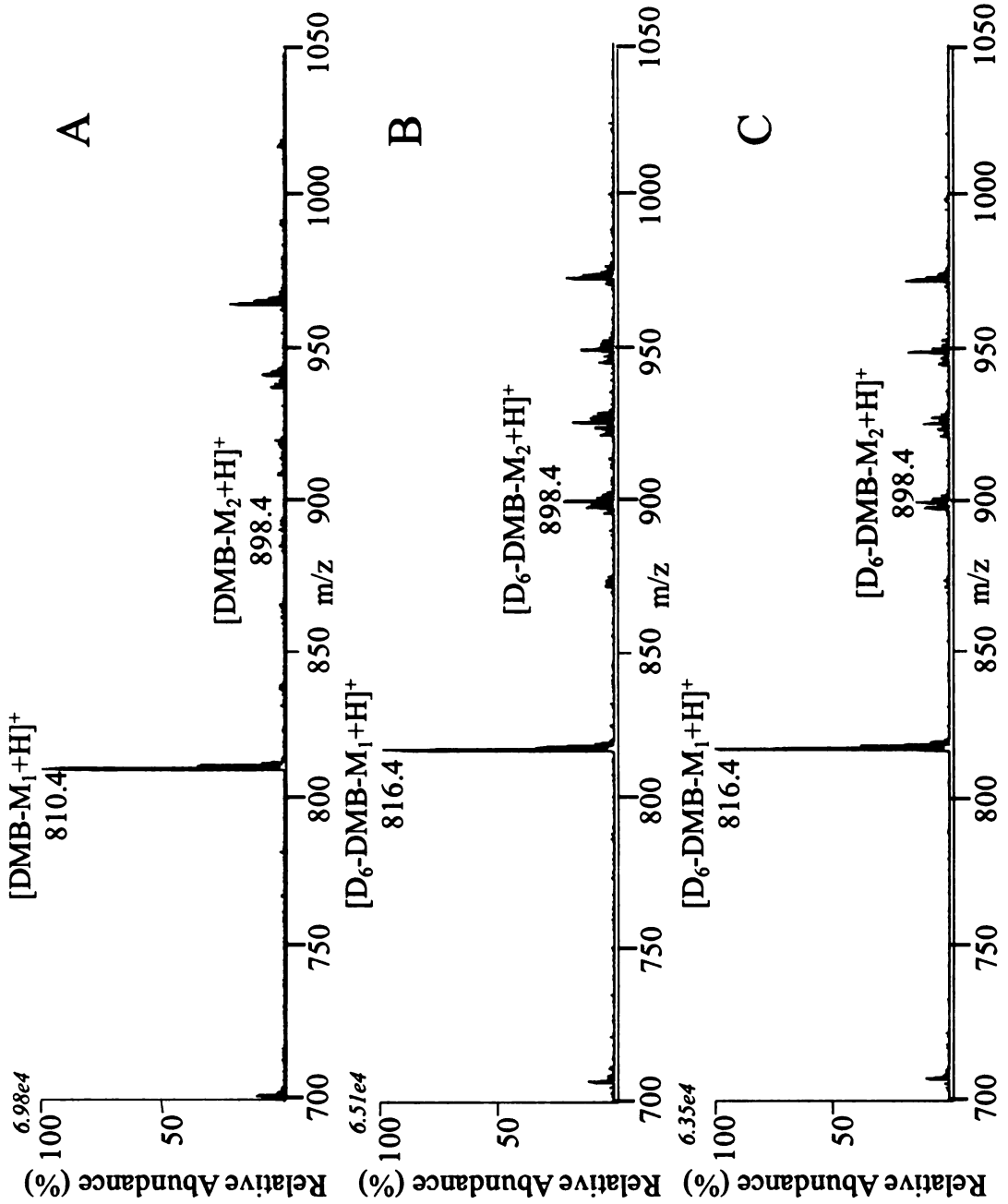

Figure 4.6 Representative positive ion mode ESI-MS/MS NL 315/321 analysis of DMBNHS and D_6-DMBNHS derivatized PS lipids isolated from control, DM and TM transgenic mouse liver samples. (A) DMBNHS-derivatized control liver PS lipids NL 315 scan spectrum. (B) D_6-DMBNHS-derivatized DM liver PS lipids NL 321 scan spectrum (C) D_6-DMBNHS-derivatized TM liver PS lipids NL 321 scan spectrum.

Generally 6 u m/z difference is shown compare spectrum A with spectra B and C. M_1: respectively spiked in internal standard PS $_{(14:0/14:0)}$, M_2 : endogeneous PS $_{(18:0/18:1)}$.

To evaluate whether the apparent changes of PE species distribution of Figure 4.5 and Figure 4.6 are significant, statistical analysis was performed as described in section 4.3.2 and the result was shown in Figure 4.7. The quantification of PE species distribution reconstruction is especially consistent with our previously published data using conventional analysis methods (i.e. significant decrease of PE $_{(16:0/20:4)}$ and significant increase of PE $_{(16:0/22:6)}$ in DM mice). Comparing Figure 4.7 A below with Figure 5 from previously published paper [61], the trend in the relative abundance changes observed for each aminophospholipid is identical in both the conventional and derivatized lipid analysis methods. However, in the conventional analysis, only 15 PE lipids were analyzed by using CID-MS/MS. All the detected PE species belongs to diacylglycerol PE category since the conventional analysis monitored the cleavage of the phosphoethanolamine head group (141 Da) which is a exclusive neutral loss of only diacyl-PE lipids.[51] As a result, in conventional underivatized PE studies there is no single common transition that permits all PE species to be detected. [51] In contrast, the novel DMBNHS isotope derivatization strategy increased the number of PE species been detected to 23. Not only 3 more diacylglycerol PE species were quantitatively analyzed, 4 low-abundant lysoPE species and one plasmalogen PE lipid were also accessed. Because there is a common fragment ion (m/z 210) at medium collision energy. Not only a dramatic increase number of low-abundant diacyl-PE lipids is quantitatively covered by this isotope-labeling method, lysoPE species and plasmalogen PE species are also

mapped. The single scan of PI 210 appeared to be a common detection channel for all three subclasses of PE aminophospholipids making this automatic tandem mass single run analysis a more comprehensive quantification tool of amino-containing phospholipids. This result potentially means that deacylation (diacyl-PE cleavages to form lysoPE) process under certain biological stimulation could be monitored by this DMBNHS derivatization coupled CID-MS/MS analysis. [83]

At the same time, statistic data of conventional PE analysis provided that only 6 out of 15 PE molecular species were shown to exhibit significant differences between control liver sample and DM liver samples, and 3 out of 15 PE molecular species showed significant differences between DM and TM liver samples as well as similarities between control and TM liver samples. In contrast, use of the DMBNHS derivatization strategy increased the number of PE lipid species that demonstrated statistically significant changes in abundance. In this study, 21 out of 23 PE lipids were proved to have significant difference in their distribution when comparing control liver lipid profile and DM liver lipid profile, within these 21 analytes, 12 molecular species also been illustrated to have significant difference in the DM and TM liver sample comparison and have similar distribution in control and TM liver samples. (Figure 4.7 panel A)

It should be indicated that the statistic discussion of conventional PE analysis and DMBNHS derivatization based PE analysis focused on different aspects. In conventional study 5 individual samples of each groups (control, DM and TM) were compared, the sample size to represent the whole population helped to demonstrate any differences between groups. However, in this specific study, pooled sample which is a ratiometric mixture of the same 5 individual samples as conventional study was replicated 5 times, so

the comparison in this study may not represent the variance between groups. But it is still a solid evaluation of the alternation of aminophospholipid profiles between the pooled out samples.

Due to the relatively low abundance of PS species in liver tissue, direct analysis of PS lipids by conventional NL 185 showed poor quantification capacity, however out developed isotopic-derivatization coupled tandem mass experiment determined 14 out 17 PS analytes with alter distribution compare control and DM mouse liver lipid extracts. Although the comparison of PS lipid profiles was not achieved in a single CID-MS/MS scan (as PI 210 for PE lipids), the relative quantification of PS distribution is still within a single run collection data of NL 315/321 scans simultaneously. This aminophospholipid quantization result demonstrated that the derivatization strategy carries powerful quantitative analysis advantages which favor an assay comparison between control and disease- state sample lipid profile. The result also convinced the metabolic alteration of liposome in liver tissue from mice containing double mutations induced liver neoplasis and an interesting 'back up' of lipid profile when the third mutation-FAT-1 was introduced to the triple mutation mice model. The pathological changes of TM mouse liver tissue is proved to be similar to control mouse liver tissue.

This study will also allow fundamental insights into the pathogenicity of liver cancer which has a lipid component in its epidemiology.[84] The molecular level understanding of the contribution of aminophospholipids to hepatocarcinogenesis will help to allow the development of novel approaches to prevention, diagnosis and cure.

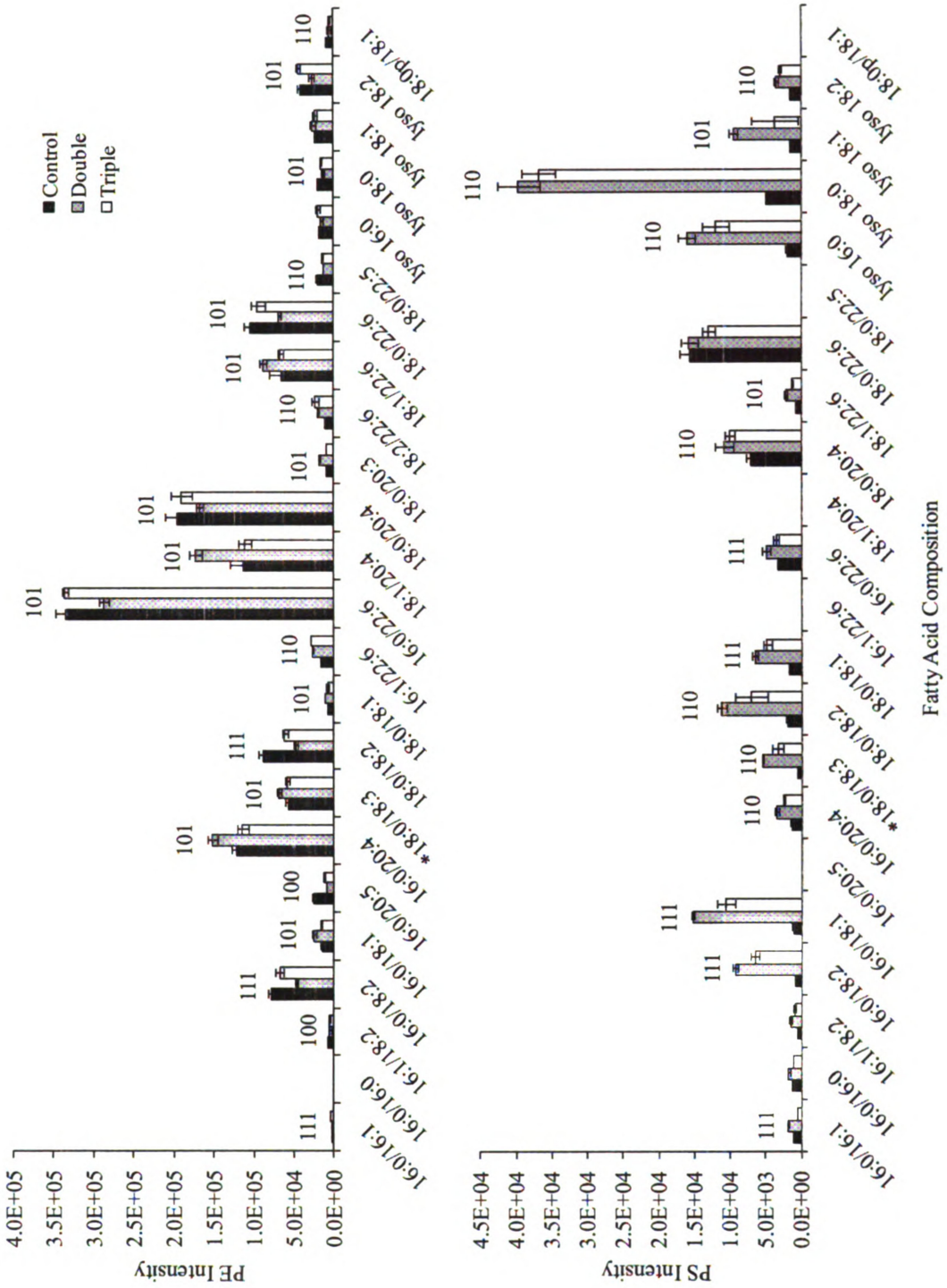

Figure 4.7 Quantitative ESI-MS/MS analysis of (A) PE and (B) PS lipids from pooled out lipids tissue extracts of 40 weak control(n=5), DM (n=5) and TM (n=5) mice. *The PE $_{(18:0/18:3)}$ lipid PE contained an abundant PE $_{(16:0/20:3)}$ lipid species. The PE

$_{(16:0/20:5)}$ lipid was also found to contain an abundant PE $_{(16:1/20:4)}$ lipid species. The 3-digit key used to indicate significant differences between groups is: first digit, control and DM groups, second digit, control and TM groups, third digit DM and TM groups. (1 significant, 0 insignificant)

REFERENCES

1. Fahy, E.; Subramaniam, S.; Murphy, R. C.; Nishijima, M.; Raetz, C. R. H.; Shimizu, T.; Spener, F.; van Meer, G.; Wakelam, M. J. O.; Dennis, E. A., Update of the LIPID MAPS comprehensive classification system for lipids. *J. Lipid Res.* **2009,** *50*, S9-S14.

2. Phillips, R.; Ursell, T.; Wiggins, P.; Sens, P., Emerging roles for lipids in shaping membrane-protein function. *Nature* **2009,** *459* (7245), 379-385.

3. van Meer, G.; Voelker, D. R.; Feigenson, G. W., Membrane lipids: where they are and how they behave. *Nat. Rev. Mol. Cell Biol.* **2008,** *9* (2), 112-124.

4. Resh, M. D., Fatty acylation of proteins: new insights into membrane targeting of myristoylated and palmitoylated proteins. *Biochim. Biophys. Acta-Mol. Cell Res.* **1999,** *1451* (1), 1-16.

5. Casey, P. J., Protein lipidation in cell signaling. *Science* **1995,** *268* (5208), 221-225.

6. Lee, A. G., How lipids affect the activities of integral membrane proteins. *Biochim. Biophys. Acta-Biomembr.* **2004,** *1666* (1-2), 62-87.

7. Pichler, H.; Riezman, H., Where sterols are required for endocytosis. *Biochim. Biophys. Acta-Biomembr.* **2004,** *1666* (1-2), 51-61.

8. Fahy, E.; Subramaniam, S.; Brown, H. A.; Glass, C. K.; Merrill, A. H.; Murphy, R. C.; Raetz, C. R. H.; Russell, D. W.; Seyama, Y.; Shaw, W.; Shimizu, T.; Spener, F.; van Meer, G.; VanNieuwenhze, M. S.; White, S. H.; Witztum, J. L.; Dennis, E. A., A comprehensive classification system for lipids. *J. Lipid Res.* **2005,** *46* (5), 839-861.

9. Labrouche, S.; Freyburger, G.; Gin, H.; Boisseau, M. R.; Cassagne, C., Changes in phospholipid composition of blood cell membranes (erythrocyte, platelet, and polymorphonuclear) in different types of diabetes - Clinical and biological correlations. *Metab.-Clin. Exp.* **1996,** *45* (1), 57-62.

10. Funk, C. D., Prostaglandins and leukotrienes: Advances in eicosanoid biology. *Science* **2001,** *294* (5548), 1871-1875.

11. Coleman, R. A.; Lee, D. P., Enzymes of triacylglycerol synthesis and their regulation. *Prog. Lipid Res.* **2004,** *43* (2), 134-176.

12. Hannun, Y. A.; Bell, R. M., Functions of sphingolipids and sphingolipid breakdown products in cellular-regulation. *Science* **1989,** *243* (4890), 500-507.

13. Spiegel, S.; Merrill, A. H., Sphingolipid metabolism and cell growth regulation. *Faseb J.* **1996,** *10* (12), 1388-1397.
14. Brown, D. A.; London, E., Structure and function of sphingolipid- and cholesterol-rich membrane rafts. *J. Biol. Chem.* **2000,** *275* (23), 17221-17224.

15. McMahon, H. T.; Gallop, J. L., Membrane curvature and mechanisms of dynamic cell membrane remodelling. *Nature* **2005,** *438* (7068), 590-596.

16. Zambrano, F.; Fleischer, S.; Fleischer, B., Lipid-composition of golgi apparatus of rat-kidney and liver in comparison with other subcellular organelles. *Biochimica Et Biophysica Acta* **1975,** *380* (3), 357-369.

17. Devaux, P. F.; Morris, R., Transmembrane asymmetry and lateral domains in biological membranes. *Traffic* **2004,** *5* (4), 241-246.

18. Daleke, D. L., Regulation of transbilayer plasma membrane phospholipid asymmetry. *J. Lipid Res.* **2003,** *44* (2), 233-242.

19. Fadeel, B.; Xue, D., The ins and outs of phospholipid asymmetry in the plasma membrane: roles in health and disease. *Crit. Rev. Biochem. Mol. Biol.* **2009,** *44* (5), 264-277.

20. Daleke, D. L.; Lyles, J. V., Identification and purification of aminophospholipid flippases. *BBA-Mol. Cell. Biol. Lipids* **2000,** *1486* (1), 108-127.

21. Pomorski, T.; Menon, A. K., Lipid flippases and their biological functions. *Cell. Mol. Life Sci.* **2006,** *63* (24), 2908-2921.

22. Daleke, D. L., Phospholipid flippases. *J. Biol. Chem.* **2007,** *282* (2), 821-825.

23. Zhang, W. H.; Tsan, R.; Schroit, A. J.; Fidler, I. J., Apoptotic cells initiate endothelial cell sprouting via electrostatic signaling. *Cancer Res.* **2005,** *65* (24), 11529-11535.

24. Yeung, T.; Gilbert, G. E.; Shi, J.; Silvius, J.; Kapus, A.; Grinstein, S., Membrane phosphatidylserine regulates surface charge and protein localization. *Science* **2008,** *319* (5860), 210-213.

25. Fadeel, B.; Xue, D.; Kagan, V., Programmed cell clearance: Molecular regulation of the elimination of apoptotic cell corpses and its role in the resolution of inflammation. *Biochem. Biophys. Res. Commun.* **2010,** *396* (1), 7-10.

26. Chaurio, R. A.; Janko, C.; Munoz, L. E.; Frey, B.; Herrmann, M.; Gaipl, U. S., Phospholipids: Key Players in Apoptosis and Immune Regulation. *Molecules* **2009,** *14* (12), 4892-4914.

27. Brown, H. A., Methods In Enzymology Volume 432, Lipidomics and Bioactive Lipids: Mass-Spectrometry-Based Lipid Analysis, PREFACE. In *Methods in Enzymology; Lipidomics and Bioactive Lipids: Mass-Spectrometry-Based Analysis*, Elsevier Academic Press Inc: San Diego, 2008; Vol. 432, pp XVII-XVII.

28. Speelmans, G.; Staffhorst, R.; deKruijff, B., The anionic phospholipid-mediated membrane interaction of the anti-cancer drug doxorubicin is enhanced by phosphatidylethanolamine compared to other zwitterionic phospholipids. *Biochemistry* **1997,** *36* (28), 8657-8662.

29. Ran, S.; Thorpe, P. E., Phosphatidylserine is a marker of tumor vasculature and a potential target for cancer imaging and therapy. *Int. J. Radiat. Oncol. Biol. Phys.* **2002,** *54* (5), 1479-1484.

30. Wang, X. J.; Li, N.; Liu, B.; Sun, H. Y.; Chen, T. Y.; Li, H. Z.; Qiu, J. M.; Zhang, L. H.; Wan, T.; Cao, X. T., A novel human phosphatidylethanolamine-binding protein resists tumor necrosis factor alpha-induced apoptosis by inhibiting mitogen-activated protein kinase pathway activation and phosphatidylethanolamine externalization. *J. Biol. Chem.* **2004,** *279* (44), 45855-45864.

31. Fattal, E.; Couvreur, P.; Dubernet, C., "Smart" delivery of antisense oligonucleotides by anionic pH-sensitive liposomes. *Adv. Drug Deliv. Rev.* **2004,** *56* (7), 931-946.

32. Skipski, V. P.; Barclay, M.; Peterson, R. F., Quantitative analysis of phospholipids by thin-layer chromatography. *Biochem. J.* **1964,** *90* (2), 374-&.

33. Chalvard.A; Rudnicki, E., Determination of lipid phosphorus in nanomolar range. *Anal. Biochem.* **1970,** *36* (1), 225-&.

34. Fay, L.; Richli, U., Location of double-bonds in polyunsaturated fatty-acids by gas-chromatography mass-spectrometry after 4,4-dimethyloxazoline derivatization. *Journal of Chromatography* **1991,** *541* (1-2), 89-98.

35. Lehmann, W. D.; Kessler, M., Characterization and quantification of human-plasma lipids from crude lipid extracts by field desorption mass-spectrometry. *Biomedical Mass Spectrometry* **1983,** *10* (3), 220-226.

36. Lehmann, W. D.; Kessler, M., Fatty-acid profiling of phospholipids by field desorption and fast atom bombardment mass-spectrometry. *Chem. Phys. Lipids* **1983,** *32* (2), 123-135.

37. Chilton, F. H.; Murphy, R. C., Fast-atom-bombardment analysis of arachidonic acid-containing phosphatidylcholine molecular-species. *Biomedical and Environmental Mass Spectrometry* **1986,** *13* (2), 71-76.

38. Brugger, B.; Erben, G.; Sandhoff, R.; Wieland, F. T.; Lehmann, W. D., Quantitative analysis of biological membrane lipids at the low picomole level by nano-electrospray ionization tandem mass spectrometry. *Proc. Natl. Acad. Sci. U. S. A.* **1997,** *94* (6), 2339-2344.

39. Ejsing, C. S.; Sampaio, J. L.; Surendranath, V.; Duchoslav, E.; Ekroos, K.; Klemm, R. W.; Simons, K.; Shevchenko, A., Global analysis of the yeast lipidome by quantitative shotgun mass spectrometry. *Proc. Natl. Acad. Sci. U. S. A.* **2009,** *106* (7), 2136-2141.

40. Fujiwaki, T.; Yamaguchi, S.; Sukegawa, K.; Taketomi, T., Application of delayed extraction matrix-assisted laser desorption ionization time-of-flight mass spectrometry for analysis of sphingolipids in tissues from sphingolipidosis patients. *J. Chromatogr. B* **1999,** *731* (1), 45-52.

41. Han, X. L.; Gross, R. W., Structural determination of picomole amounts of phospholipids via electrospray ionization tandem mass spectrometry. *J. Am. Soc. Mass Spectrom.* **1995,** *6* (12), 1202-1210.

42. Hsu, F. F.; Turk, J., Charge-remote and charge-driven fragmentation processes in diacyl glycerophosphoethanolamine upon low-energy collisional activation: A mechanistic proposal. *J. Am. Soc. Mass Spectrom.* **2000,** *11* (10), 892-899.

43. Berry, K. A. Z.; Murphy, R. C., Electrospray ionization tandem mass spectrometry of glycerophosphoethanolamine plasmalogen phospholipids. *J. Am. Soc. Mass Spectrom.* **2004,** *15* (10), 1499-1508.

44. Hsu, F. F.; Turk, J., Studies on phosphatidylserine by tandem quadrupole and multiple stage quadrupole ion-trap mass spectrometry with electrospray ionization: Structural characterization and the fragmentation processes. *J. Am. Soc. Mass Spectrom.* **2005,** *16* (9), 1510-1522.

45. Little, J. L.; Wempe, M. F.; Buchanan, C. M., Liquid chromatography-mass spectrometry/mass spectrometry method development for drug metabolism studies: Examining lipid matrix ionization effects in plasma. *Journal of Chromatography B-Analytical Technologies in the Biomedical and Life Sciences* **2006,** *833* (2), 219-230.

46. Koivusalo, M.; Haimi, P.; Heikinheimo, L.; Kostiainen, R.; Somerharju, P., Quantitative determination of phospholipid compositions by ESI-MS: effects of acyl chain length, unsaturation, and lipid concentration on instrument response. *J. Lipid Res.* **2001,** *42* (4), 663-672.

47. Quirke, J. M. E.; Adams, C. L.; Vanberkel, G. J., Chemical derivatization for electrospray-ionization mass-spectrometry .1. alkyl-halides, alcohols, phenols, thiols, and amines. *Anal. Chem.* **1994,** *66* (8), 1302-1315.

48. Lamos, S. M.; Shortreed, M. R.; Frey, B. L.; Belshaw, P. J.; Smith, L. M., Relative quantification of carboxylic acid metabolites by liquid chromatography - Mass spectrometry using isotopic variants of cholamine. *Anal. Chem.* **2007,** *79* (14), 5143-5149.

49. Hullin, F.; Bossant, M. J.; Salem, N., Aminophospholipid molecular-species asymmetry in the human erythrocyte plasma-membrane. *Biochimica Et Biophysica Acta* **1991,** *1061* (1), 15-25.

50. Han, X. L.; Yang, K.; Cheng, H.; Fikes, K. N.; Gross, R. W., Shotgun lipidomics of phosphoethanolamine-containing lipids in biological samples after one-step in situ derivatization. *J. Lipid Res.* **2005,** *46* (7), 1548-1560.

51. Berry, K. A. Z.; Murphy, R. C., Analysis of cell membrane aminophospholipids as isotope-tagged derivatives. *J. Lipid Res.* **2005,** *46* (5), 1038-1046.

52. Berry, K. A. Z.; Murphy, R. C., Analysis of polyunsaturated aminophospholipid molecular species using isotope-tagged derivatives and tandem mass spectrometry/mass spectrometry/mass spectrometry. *Anal. Biochem.* **2006,** *349* (1), 118-128.

53. Zhou X., Lu Y., Wang W., Borhan B., Reid G. E., ' Fixed Charge' Chemical derivatization and Data Dependant Multistage Tandem Mass Spectrometry for Mapping Protein Surface Residue Accessibility. *J. Am. Soc. Mass Spectrom.* **2010,** *21* (8), 1339-1351.

54. Williams, K. A.; Doi, J. T.; Musker, W. K., Neighboring-group participation in organic redox reactions .10. the kinetic and mechanistic effects of imidazole and benzimidazole nitrogen on thioether oxidations. *J. Org. Chem.* **1985,** *50* (1), 4-10.

55. Jessing, M.; Brandt, M.; Jensen, K. J.; Christensen, J. B.; Boas, U., Thiophene backbone amide linkers, a new class of easily prepared and highly acid-labile linkers for solid-phase synthesis. *J. Org. Chem.* **2006,** *71* (18), 6734-6741.

56. Crouch, N. P.; Adlington, R. M.; Baldwin, J. E.; Lee, M. H.; MacKinnon, C. H.; Paul, D. R., Stereochemical course of the conversion of alpha-ketoisocaproate to beta-hydroxyisovalerate by soluble, recombinant mammalian 4-hydroxyphenylpyruvate dioxygenase. *Tetrahedron* **1997,** *53* (31), 10827-10840.

57. Lydic. T., Busik. J. V., Reid, G. E., Analysis of Retina and Erythrocyte Glycerophospholiipid Alterations in a Rat Model of Type 1 Diabetes. *Journal of the Society for Laboratory Automation and Screening* **2009,** *14* (6), 383-399.

58. Calvisi, D. F.; Thorgeirsson, S. S., Molecular mechanisms of hepatocarcinogenesis in transgenic mouse models of liver cancer. *Toxicol. Pathol.* **2005,** *33* (1), 181-184.

59. Murakami, H.; Sanderson, N. D.; Nagy, P.; Marino, P. A.; Merlino, G.; Thorgeirsson, S. S., Transgenic mouse model for synergistic effects of nuclear oncogenes and growth-factors in tumorigenesis - interaction of c-myc and transforming growth factor-alpha in hepatic oncogenesis. *Cancer Res.* **1993,** *53* (8), 1719-1723.

60. Griffitts, J.; Tesiram, Y.; Reid, G. E.; Saunders, D.; Floyd, R. A.; Towner, R. A., In vivo MRS assessment of altered fatty acyl unsaturation in liver tumor formation of a TGF alpha/c-myc transgenic mouse model. *J. Lipid Res.* **2009,** *50* (4), 611-622.

61. Griffitts, J.; Saunders, D.; Reid, G. E.; Salih, A.; Liu, S.; Todd, L. A.; Busik, J. V.; Kang, J. X.; Towner, R. A., Non-mammalian fat-1 gene prevents neoplasia when introduced to a mouse hepatocarcinogenesis model: Omega-3 fatty acids prevent liver neoplasia. *Biochemical and Biophysical Acta* **2010,** *1801* (10), 1133-1144.

62. Kang, J. X., Fat-1 transgenic mice: A new model for omega-3 research. *Prostaglandins Leukot. Essent. Fatty Acids* **2007,** *77* (5-6), 263-267.

63. Folch, J.; Lees, M.; Stanley, G. H. S., A simple method for the isolation and purification of total lipides from animal tissues. *J. Biol. Chem.* **1957,** *226* (1), 497-509.

64. Chen, P. S.; Toribara, T. Y.; Warner, H., Microdetermination of phosphorus. *Anal. Chem.* **1956,** *28* (11), 1756-1758.

65. Lin, Y. Y.; Smith, L. L., Chemical ionization mass-spectrometry of steroids and other lipids. *Mass Spectrom. Rev.* **1984,** *3* (3), 319-355.

66. Schiller, J.; Arnhold, J.; Benard, S.; Muller, M.; Reichl, S.; Arnold, K., Lipid analysis by matrix-assisted laser desorption and ionization mass spectrometry: A methodological approach. *Anal. Biochem.* **1999,** *267* (1), 46-56.

67. Fenn, J. B.; Mann, M.; Meng, C. K.; Wong, S. F.; Whitehouse, C. M., Electrospray ionization for mass-spectrometry of large biomolecules. *Science* **1989,** *246* (4926), 64-71.

68. Malcolm Dole, L. L. M., R. L. Hines, R. C. Mobley, L.D. Ferguson, M. B. Alice, Molecular Beams of Macroions. *J. Chem. Phys.* **1968,** *49* (5), 2240-2250.

69. Iribarne, J. V.; Thomson, B. A., Evaporation of small ions from charged droplets. *J. Chem. Phys.* **1976,** *64* (6), 2287-2294.

70. Schmidt, A.; Karas, M.; Dulcks, T., Effect of different solution flow rates on analyte ion signals in nano-ESI MS, or: When does ESI turn into nano-ESI? *J. Am. Soc. Mass Spectrom.* **2003,** *14* (5), 492-500.

71. Constans, A., Better mass spec results off-line - Advion BioSciences' NanoMate 100 speeds up ESI-based mass spectrometry. *Scientist* **2003,** *17* (7), 49-49.

72. McLuckey, S. A.; Wells, J. M., Mass analysis at the advent of the 21st century. *Chem. Rev.* **2001,** *101* (2), 571-606.

73. Hoffmann E.; Vincent, S., *Mass Spectrometry: Principles and Applications Third Edition*. 2007; p 91-93.

74. March, R. E., An introduction to quadrupole ion trap mass spectrometry. *J. Mass Spectrom.* **1997,** *32* (4), 351-369.

75. Glish, G.; Vachet, R., Quadrupole Ion Trap Mass Spectrometry. In *ASMS lecture notes*, 2007; Vol. June 2-3.

76. Zhang, X.; Reid, G. E., Multistage tandem mass spectrometry of anionic phosphatidylcholine lipid adducts reveals novel dissociation pathways. *Int. J. Mass Spectrom.* **2006,** *252* (3), 242-255.

77. Reid, G. E.; Roberts, K. D.; Simpson, R. J.; O'Hair, R. A. J., Selective identification and quantitative analysis of methionine containing peptides by charge derivatization and tandem mass spectrometry. *J. Am. Soc. Mass Spectrom.* **2005,** *16* (7), 1131-1150.

78. Amunugama, M.; Roberts, K. D.; Reid, G. E., Mechanisms for the selective gas-phase fragmentation reactions of methionine side chain fixed charge sulfonium ion containing peptides. *J. Am. Soc. Mass Spectrom.* **2006,** *17* (12), 1631-1642.

80. Du, J. T.; Li, Y. M.; Chen, Z. Z.; Luo, S. Z.; Zhao, Y. F., The self-catalytic esterification reaction of O-phosphoryl serine derivative. *Chin. Chem. Lett.* **2005,** *16* (7), 856-858.

81. Pulfer, M.; Murphy, R. C., Electrospray mass spectrometry of phospholipids. *Mass Spectrom. Rev.* **2003,** *22* (5), 332-364.

82. Froelich, J. M.; Kaplinghat, S.; Reid, G. E., Automated neutral loss and data dependent energy resolved "pseudo MS3" for the targeted identification, characterization and quantitative analysis of methionine-containing peptides. *Eur. J. Mass Spectrom.* **2008,** *14* (4), 219-229.

83. Tessner, T. G.; Greene, D. G.; Wykle, R. L., Selective deacylation of arachidonate-containing ethanolamine-linked phosphoglycerides in stimulated human neutrophils. *J. Biol. Chem.* **1990,** *265* (34), 21032-21038.

84. Gerrit van Meer, D. R. V., Gerold W. Feigenson, Membrane Lipids: where they are and how they behave. *Nanure reviews* **2008,** *9*, 112-124.